LBL-34386
UC-213

Current-Potential Characteristics of Electrochemical Systems

Vincent S. Battaglia
Ph.D. Thesis

Department of Chemical Engineering
University of California

and

Materials Sciences Division
Lawrence Berkeley Laboratory
University of California
Berkeley, California 94720

July 20, 1993

This work was supported by the Assistant Secretary for Conservation and Renewable Energy, Office of Transportation Technologies, Electric and Hybrid Propulsion Division of the U. S. Department of Energy under Contract No. DE-AC03-76SF00098.

MASTER

Abstract

Current-Potential Characteristics of Electrochemical Systems

by

Vincent Santo Battaglia

Doctor of Philosophy in Chemical Engineering

University of California, Berkeley

Professor John S. Newman, Chair

This dissertation contains investigations in three distinct areas. Chapters 1 and 2 provide an analysis of the effects of electromagnetic phenomena during the initial stages of cell discharge. Chapter 1 includes the solution to Maxwell's equations for the penetration of the axial component of an electric field into an infinitely long cylindrical conductor. This work investigates two time regimes: the "short time" and the "diffusive time". During the short time the current increases at a rate proportional to the time, and during the diffusive time it increases at a rate proportional to the square root of time. Also included in this chapter are mathematical expressions that describe the manner in which the electric field penetrates a conductive medium during the two time regimes. Chapter 2 contains the analysis of the conductor included in a radial circuit. The time constant for the discharge of the circuit is depicted as a function of the size of the system and the important physical parameters. Also included are analytic approximations of the time constant and a comparison to the lumped parameter approximation of

inductance.

Chapter 3 provides a complete description of the equations that describe the growth of an oxide film. A finite difference program was written to solve the equations. The system investigated is the iron/iron oxide in a basic, aqueous solution. Figures are presented which provide a comparison of the simulations to the experimental data provided in the literature. Discussion of the quality of the fit is also provided. Ultimately, we found that at low voltages iron dissolves preferentially to form ferrous ions and at higher voltages reacts to form ferrous oxide.

Chapters 4 and 5 include the experimental attempts of replacing formaldehyde with an innocuous reducing agent for electroless deposition. In chapter 4, current-*versus*-voltage curves are provided for a sodium thiosulfate bath in the presence of a copper disk electrode. Also provided are the cathodic polarization curves of a copper/EDTA bath in the presence of a copper electrode. Explanations for the poor performance of thiosulfate as a reducing agent for copper are included. Chapter 5 contains the experimental results of work done with sodium hypophosphite as a reducing agent. Mixed-potential-*versus*-time curves for solutions containing various combinations of copper sulfate, nickel cloride, and hypophosphite in the presence of a palladium disk electrode provide an indication of the reducing power of the solutions. It appears that the hypophosphite is preferentially oxidized on nickel and its oxidation is inhibited on copper.

Table of Contents

Title Page i

Approval Page ii

Abstract 1

Table of Contents iii

Preface vi

Acknowledgements ix

Chapter 1: Magnetic Field Effects in High-Power Batteries 1

I: The Penetration of an Electric Field into a Cylindrical Conductor

Foreword 1
Introduction 1
The Electromagnetic System 4
Full Solution 9
Diffusion Solution 11
Inner Solution 15
Current 18
Summary 22
List of Symbols 23
References 24

Chapter 2: Magnetic Field Effects in High-Power Batteries 27

II. Time Constant of a Radial Circuit Terminated by a Cylindrical Cell with Inductance

Foreword 27
Introduction 27
Analytic Approach 29

Transmission-Line Analysis 29
Case 1: Outer Conductors of Infinite Conductivity 34
Initial Conditions 35
Boundary Conditions 35
Solution 38
Time Constants 38
Case 2: Outer Conductors of Finite Conductivity 41
Solution 44
Time Constants 44
Discussion 48
Conclusions 49
List of Symbols 50
References 51

Chapter 3: The Modeling of a Growing Oxide Film 53

Foreword 53
Introduction 53
General System Description 57
Equations 61
Mole Flux Balance 61
Summing Equations 64
Poisson's Equation 65
Velocity 66
Boundary Conditions 68
Mole Balance 69
Potential 74
Velocity 75
Initial Conditions 76
Reactions 77
Electric Fields on Homogeneous Reactions 77
Thermodynamic Consistency of Heterogeneous Reactions 79
Solving Computationally 81
Coordinate Transformation 81
Equations in Finite Difference 82
Iron/Iron Oxide System 83
Summary of Earlier Work as Provided by Vetter 84
Model 85
System Parameters 89
Results and Discussion 94
Equilibrium 95
Comparison with Experimental Data 97
Underpotential Deposition 108
Summary 113
List of Symbols 115
References 118
Appendix 123
Program 123
Main Program: iren 126
Data File: iren.dat 172

Chapter 4: The Oxidation of Thiosulfate on Copper for Electroless Deposition 174

Foreword 174
Introduction 174
Experimental 180
Results 182
Reduction of Copper Sulfate in the Presence of EDTA 182
Oxidation of Sodium Thiosulfate 185
Results of Combining Thiosulfate and Copper in the Presence of Copper 188
Discussion 192
Conclusions 193
References 194

Chapter 5: Electroless Deposition of Copper by Hypophosphite and Nickel Solutions 197

Foreword 197
Introduction 197
Experimental 198
Results and Discussion 199
Nickel Chloride Solutions with Sparing Amounts of Copper Sulfate 199
Discussion 202
Copper Sulfate Solutions with Sparing Amounts of Nickel Sulfate 204
Discussion 206
Further Discussions 207
Conclusions 207
References 208

Preface

This dissertation consists of three distinct subjects covered over five chapters. The first investigation is on the effect the magnetic field, or inductance, has on the charging of a system. Chapter one illustrates the manner in which an electric field penetrates an infinite cylindrical conductor that short circuits two perfect plates. That analysis provides part of the solution to finding the time constant of a complete circuit that is instantaneously subject to a constant potential source. In chapter 2, a cylindrical conductor is included in a radial circuit. Solution to a transmission-line equation provides the time constant of the system as a function of the various physical parameters. The second subject considered is the modeling of a growing oxide film. Chapter 3 provides a physical description of the system and the equations governing the transport in the oxide. This analysis is then applied to the iron/iron oxide system. Results generated from a computer program are compared with experimental evidence reported in the literature. The third area of research is electroless deposition of copper. This work was exploratory. The goal was to find a workable yet less hazardous replacement for the widely used reducing agent formaldehyde. The end result maintains that under the present conditions neither sodium thiosulphate nor sodium hypophosphate is the answer. A significant and sustained amount of copper deposition was never achieved. Chapter 4 contains the polarization curves of the copper deposition and thiosulphate oxidation. Chapter 5 contains the

results of using hypophosphite with various amounts of nickel.

This thesis can also be considered a monograph of the three primary techniques that are available to the engineer for systems analysis: an analytical approach, used in the magnetic field work; a computational approach, applied in the oxide film work; and an experimental approach, undertaken in the electroless deposition work. To perform a complete analysis of the magnetic field effects we solved Maxwell's equations of electromagnetism using a perturbation analysis. This method divided the problem into a short time and long time analysis. To obtain the time constant of the circuit configuration, concepts in Laplace transforms, Duhamel's superposition, and residue theory were applied. Upon developing the equations for describing oxide film growth, a computer program was prepared. The program was written in a general manner such that any number of species, phases, and homogeneous and heterogeneous reactions could be considered. Preparing such a model required a general algorithm for combining mole balance equations such that any reactions that were considered to be at equilibrium were eliminated from all but one mole balance equation. That equation was then replaced by an equilibrium expression. The substitution of Poisson's equation for the electroneutrality equation introduced the complexities associated with rapid variations in concentration and potential distributions near interfaces. These variations, which can severely hinder convergence, were minimized by a number of programming techniques. The exploratory work in electroless deposition has not only allowed an enhance-

ment of my experimental skills, but has exposed me to the methodology involved in starting any project from ground zero.

This work has, accordingly, provided a vehicle for exploring a wide breath of physical phenomena and has been a valuable learning experience in the methods of problem solving. I am appreciative of the experience.

V. S. Battaglia

Acknowledgements

This space is set aside for the author to express thanks to those who made contributions towards his achieving the goal of becoming a Ph.D. This space has no format or guidelines; I am on my own.

As anyone will attest, I am no genius. I made it to this point by a lot of hard work and by being fortunate enough to be surrounded by *many* good people who had my best interests at heart. It is impossible to thank all of them, but I can thank those who provided the most significant assistance.

Growing up in Baltimore, I did not sit around dreaming of the day when I would become a Chemical Engineering Ph.D. As a matter of fact, I thought very little about my future. The one thing I did do was to listen to my parents say "Stay in school and everything will work itself out." Although they were probably not the first parents to utter these words. they were the people who said them to me. They are the source of my continuing success and I love them.

Some people play major factors in another's life and know little of the outcome. Two people are indirectly, directly responsible for my ending up at Berkeley and should be acknowledged: my junior high school guidance counselor, who got me out of her poor school and into the college preparatory curriculum at the Baltimore Polytechnic Institute; and Professor William Schwarz, who told me to go to the best graduate school that would accept me. Thank you for your guidance. The direct influence on my decision to come to Berkeley rests

with my father, who, while lying partially asleep in bed, had the wisdom to ask the immortal phrase "Minnesota instead of California?" Thanks dad.

Coming to Berkeley was the first time I lived away from my parents: a very scary experience. If it were not for Joseph D. Puglisi ("Joe D."), I seriously doubt that I would have survived here. He helped me not only to adjust to my new surroundings but through my Master's thesis, my Preliminary Examination, and my Qualifying Examination. Thank you is not strong enough. I thrank you, I thrunk you.

The choice of an advisor is a major decision that influences the remainder of your life. Alan West, having fought his internal instincts to not allow his room mate to also share the same lab, convinced me to work in Prof. Newman's research group. Thank you, Alan, for fighting those instincts and providing excellent advice.

Finally, this Ph.D thesis was five and a half years in the making. In those five and a half years I have experienced significant growth, both intellectually and personally. John Newman deserves most of the credit for this maturation. His patience and honesty have deeply enriched my life.

This work was supported by the Assistant Secretary for Conservation and Renewable Energy, Office of Transportation Technologies, Electric and Hybrid Propulsion Division of the U.S. Department of Energy under Contract No. DE-AC03-76SF00098.

Chapter 1

Magnetic Field Effects in High-Power Batteries

I: The Penetration of an Electric Field into a Cylindrical Conductor

Foreword

The penetration of the axial component of an electric field into a cylindrical conductor is described by an asymptotic solution method for long and short times. The development of the respective current distributions allows for a mathematical comparison of the solution schemes and indicates that the current initially increases at a rate proportional to time until a time of order ϵ/σ, subsequently at a rate proportional to the square root of time, and finally levels off exponentially to the steady-state value. Criteria for the proper omission of the displacement current are also given.

Introduction

In the 70 years since Kapitza[1] used an electrochemical system (a lead-acid bipolar battery) for delivering short pulses of high-power, the design of batteries for this purpose has drawn little attention. However, the ever increasing reliance of the business sector on computer and telecommunication systems has enticed a renewed effort in research of rapid-discharge, high, back-up power batteries. E. Willihnganz[2] studied the effect of high rates of discharge on the negative plate of a lead-acid battery. Gibbard[3] has designed and tested

a number of high-power lithium batteries and has presented an overall design criterion.[4] And LaFollette and Bennion discuss the design fundamentals of high-power, pulse-discharged lead acid batteries in terms of experiments[5] and modeling.[6] Researchers are now also asking what is the minimum time required to bring a battery to maximum power.

Inductance, used to denote the effect of a rapidly varying electric field which produces a varying magnetic field which counters with an opposing electric field, governs the rise time of the current. This phenomenon falls under the heading of electrodynamics. LaFollette and Bennion[5] mention that the rigorous way to incorporate magnetic field effects in a battery model is to solve Maxwell's equations of electromagnetism simultaneously with the equations that govern the battery performance. Due to the complicated nature of the equations of electrodynamics and the associated boundary conditions, this is something most modelers would like to avoid. LaFollette *et al.* did not include the inductance in their model after demonstrating that their system was small enough that the inductance effect occurred within the first microsecond and that they were more interested in the 10 to 1000 μs range. Methods of simplifying the equations for handling the inductance while not neglecting it entirely do exist. McKinney *et al.*[7] include a magnetic field effect of the circuit when analyzing the current from a power source by including a lumped inductance term in their circuit-theory model. Cahan *et al.*[8] performed a parametric study of the impedance of a gen-

eric power source as a function of the frequency of the signal. The power source was approximated as a modified, semi-infinite, strip-line. Inductance was included by means of a skin-effect. The skin-depth is a measure of the depth of penetration of a sinusoidal signal and is a function of the frequency and conductivity. (For a sinusoidal signal, 95 percent of the signal is limited to 3 skin-depths from the surface.) The skin-depth analysis is applicable for a sinusoidal signal; however, an analogous treatment for a stepped current has not yet been presented. Moreover, these techniques only provide for an adjustment of the total current as a function of time, they do not provide a description of the instantaneous current distribution. The current distribution can play an important role in battery design if a large battery is required for high currents and only a fraction is utili .ed.

In part I of our study, we shall demonstrate the manner in which an electric field penetrates a cylindrical conductor when the conductor is instantaneously subjected to a constant electric field at its surface. This work provides a first approximation to the instantaneous current distribution in a bipolar battery, the typical battery design chosen for delivering high power. In part II, the cylindrical conductor is included in a radial circuit. A transmission-line analysis is used in conjunction with the above treatment to determine the time constant of the complete system. The importance of addressing the complete circuit lies in the fact that the electromagnetic field distribution is not a localized entity but is a function of the

entire circuit geometry.

The Electromagnetic System

The transition of an electrical signal from one amplitude and frequency to another begins at the source of the disturbance and propagates to the rest of the electrical configuration. The new form of the signal travels at the speed of light between the electrical conductors used to direct the electrical power from the source to the intended load. During the initial stages of the transition, the charge on the conductors distributes itself such that the potential around the circuit is consistent with Ohm's law. (Further comments on the initial stages of current start-up are provided by Rosser[9] and Heald.[10])

For conductors of finite conductivity, the electric field penetrates the conductors to within a few skin depths, for an alternating signal, and throughout the conductors, for a direct signal. The rate at which the new signal can penetrate the conductors determines the rate to a periodic or steady state. Using Maxwell's equations, it is the purpose of this paper to describe the penetration of the axial electric field into an electrically conducting medium.

It is well-known that Maxwell's four coupled equations of electromagnetism reduce to two, noncoupled modified wave equations in a linear, homogeneous, conducting medium:

$$\nabla^2 E = \mu\epsilon\frac{\partial^2 E}{\partial t^2} + \mu\sigma\frac{\partial E}{\partial t}, \tag{1}$$

$$\nabla^2 B = \mu\epsilon\frac{\partial^2 B}{\partial t^2} + \mu\sigma\frac{\partial B}{\partial t}. \tag{2}$$

The solution to these equations for the transient electric field distribution in the conductors and surrounding medium for a finite geometry with a load and source is difficult to obtain. Since we are interested here in the time it takes for the penetration of the electrical signal into the power source, we shall address the specific problem of a step in an electrical signal propagating down an infinitely long coaxial cable. The radial component of the electrical signal propagates between the two conductors at the speed of light while the axial component propagates radially into the inner and outer conductors. With this configuration, the problem of determining the penetration of the electric field into the transmission line is virtually reduced to the mathematically one-dimensional problem of the penetration of an axial electric field component into an infinitely long cylindrical conductor.

From this analysis we shall assume that the bipolar battery configuration can be approximated by the properties of the central wire of the coaxial cable, the return current of the circuit being located in an outer cylindrical can. In a bipolar battery, a circular cathode and anode are separated by a circular ionically conducting separator to form a cell. A number of these cells are then stacked together and separated by cylindrical electronic conductors, such as

steel plates, to form the battery, which resembles the Volta pile. Although a cylindrical wire is a reasonable approximation of the bipolar battery geometry, it does not account for the details of the battery. The solid wire obviously lacks the multiple regions of various conductivities, surfaces of capacitance, electromotive force, and chemical reactions, and possible concentration variations found in a battery. However, as a first approximation, the infinite-wire analysis will allow us to predict the rate and the manner in which an electric field penetrates a conductor. And although this falls well short of a complete analysis, a considerable amount of information can still be inferred about the magnetic field effects.

Solutions have been derived for the electric field distribution inside and outside of an infinite wire maintained at a fixed current. A. Marcus[11] provided the field distribution of the infinite wire surrounded by an axially symmetric, perfectly conducting, outer cylinder. Sommerfeld[12] described the field distribution of a steady current in an infinite wire in free space. And D. Marcuse[13] gave the general solution to the electric field distribution of an infinite wire carrying a steady current; the particular solution being a function of the rest of the circuit configuration.

Solutions to the steady-periodic electric field distributions in media of high but finite conductivity also exist. Maxwell[14] solved for the self inductance of a periodic electric field in a cylindrical conductor. Jackson[15] showed the electric field distribution of a periodic electric field penetrating a slab.

The problem that has been solved that closest resembles the problem we address here is that of a linearly increasing current in an infinite conductor. This problem was addressed by Shakur[16] and furthered by Chervenak.[17] However, these analyses assume that the current is uniform through the conductor; Heald[2] raised some further questions of the results.

Typically, when solving the Maxwell equations in electrically conducting media, the first term on the right of equations 1 and 2, referred to as the "displacement current," is omitted.[6,7,18,19,20] In this analysis, this term is retained in what we shall call the "full solution" and in the "inner solution" and neglected in the "diffusion solution." The development of these solutions will elucidate the effect the displacement current plays in the initial stages of the field penetration and provide criteria for cases when its omission is justified, greatly simplifying the equations.

The full solution maintains all the physics and is applicable for all times; however its open form requires a large number of terms to investigate the short time regime. To probe the short time effects the problem is divided into the three regimes depicted in figure 1. Region I is the inner regime. The solution obtained for this regime highlights the effects of the initial penetration of the electric field traveling at the speed of light into the conductor. Region II is the diffusion regime. After a time of ($O\ \epsilon/\sigma$) the field penetrates parabolically into the conductor. Region III is the outer regime. This is a long time regime in which the field penetrates to

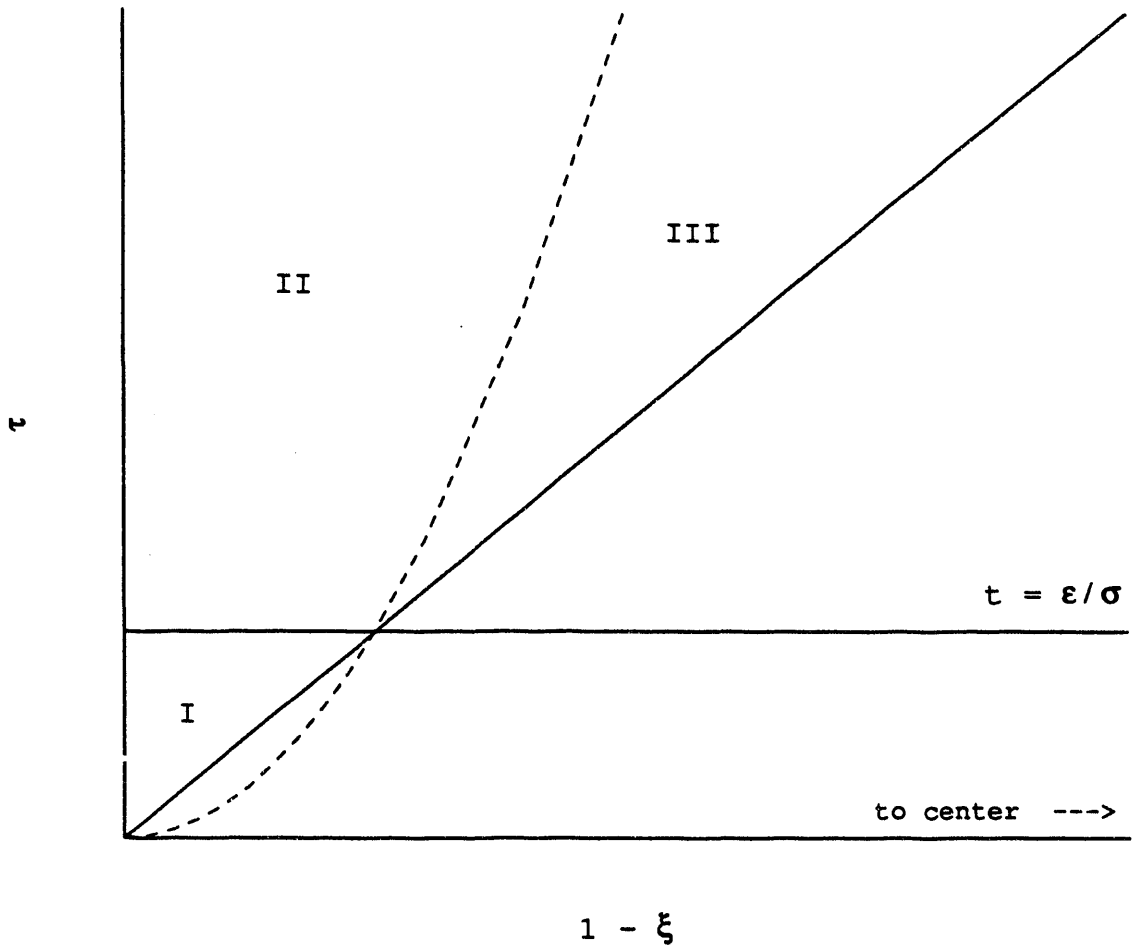

Figure 1. Solution regimes in the space-time coordinate.

the center of the conductor at the speed of light, but with an essentially negligible magnitude. We shall not refer to this regime again.

Full Solution

For the geometry described above, the characteristic length is the radius of the inner conductor, r_o. Defining the electric diffusivity of the propagating electric field as the reciprocal of the electric conductivity times the permeability, $1/\mu\sigma$, a characteristic time is developed as the radius of the wire squared divided by the electric diffusivity. Thus, substitution of the dimensionless parameters

$$\xi = r/r_o \text{ and } \tau = t/r_o^2\mu\sigma,$$

into equation 1 gives it the form

$$\frac{\partial^2 E}{\partial \xi^2} + \frac{1}{\xi}\frac{\partial E}{\partial \xi} = \delta^2 \frac{\partial^2 E}{\partial \tau^2} + \frac{\partial E}{\partial \tau}, \tag{3}$$

where $\delta = 1/\mu\sigma r_o\sqrt{\mu\epsilon}$. δ can be interpreted as the ratio of the displacement current to the conduction current. To simplify matters, we assume that initially the electric field is zero in the wire; then, at time 0, a step change in the electric field with axial component of magnitude E_o at a certain position z and r_o is imposed. This signal, as it proceeds along the coaxial line, will be felt initially only on the inner wall of the outer conductor and outer wall of the inner conductor. If the outer conductor is a perfect conductor, as

in this example, the rate of propagation of the electric field throughout the inner conductor will be the limiting effect to steady state. Thus, in this investigation we shall treat only the propagation of the field into the inner conductor. The conditions are described in mathematical terms as:

boundary conditions

E is well-behaved at $\xi = 0$;

$E = E_o$ at $\xi = 1$;

initial conditions

$E = 0$ at $\tau = 0$;

$\frac{\partial E}{\partial \tau} = 0$ at $\tau = 0$.

The Laplace transformed solution of equation 3 is

$$\frac{\bar{E}(s)}{E_o} = \frac{I_o[(\delta^2 s^2 + s)^{\frac{1}{2}}\xi]}{s\, I_o[(\delta^2 s^2 + s)^{\frac{1}{2}}]}, \tag{4}$$

where $I_p(x)$ is the modified Bessel function of the first kind, of order p. This solution can then be inverted by the method of residues.

Regardless of the solution scheme used, the radial penetration of the axial electric field component is given by*

When $2\lambda_k\delta > 1$, ω_k becomes a pure imaginary number. Equation 5 continues to apply.

$$\frac{E}{E_o} = \sum_{k=1}^{\infty} \frac{2\, J_o(\lambda_k \xi)}{\lambda_k\, J_1(\lambda_k)} \left\{ 1 - \left[\cosh(\omega_k \tau) + \frac{\sinh(\omega_k \tau)}{2\delta^2 \omega_k} \right] \exp(-\tau/2\delta^2) \right\}, \qquad (5)$$

where $\omega_k = [1-(2\lambda_k\delta)^2]^{\frac{1}{2}}/2\delta^2$, $J_p(x)$ is the Bessel function of the first kind of order p, and λ_k is the kth zero of $J_o(x)$. Although this solution is mathematically correct, it is not of a beneficial form for investigating short-time results. We say this because more and more terms of the summation are required for an accurate numerical solution at shorter and shorter times. With this in mind, we shall reapproach the problem using an asymptotic solution scheme to develop a long-time and a short-time solution. As will be shown, the long-time or diffusion solution is that which is felt throughout the conductor for times proportional to $r_o^2\mu\sigma$ (for a 10-cm-thick lead wire this is $\approx$ 60 ms), whereas, the short-time or inner solution is that which is felt just at the outer edge of the conductor at a time scale proportional to ϵ/σ (for the same lead wire this is $\approx 1\times10^{-18}$ s). This approach will allow us to describe the development of the electric field for all time regimes. Since the first term on the right of equation 3 is usually neglected, δ was chosen as the stretching parameter.

Diffusion Solution

The variables in equation 3 have been made dimensionless such that they are of O(1) in the diffusion region. It follows that, as a first approximation, the first term on the right of equation 3 can be neglected for $\delta^2 \ll 1$. The equation reduces to the form of the

transient diffusion equation in cylindrical coordinates found in the mass-transfer literature,

$$\frac{\partial^2 E}{\partial \xi^2} + \frac{1}{\xi}\frac{\partial E}{\partial \xi} = \frac{\partial E}{\partial \tau}. \tag{6}$$

This is a major simplification; the highest derivative with respect to time is omitted. However, the equation takes a more manageable form, and one that we are familiar solving. We shall address the implications of this mathematical simplification, shortly.

Equation 6 is solved by separation of variables with the boundary and first of the initial conditions listed above equation 4 to yield

$$\frac{E}{E_o} = \sum_{k=1}^{\infty} \frac{2\, J_o(\lambda_k \xi)}{\lambda_k\, J_1(\lambda_k)} \left\{1 - \exp(-\lambda_k^2 \tau)\right\}. \tag{7}$$

Equation 7 is plotted as a function of ξ for different fractions of the time constant in figure 2. The current distribution is directly related to the electric field distribution through Ohm's law, $i = \sigma E$. Other than the absence of the hyperbolic cosines and sines and ω's of the full solution, this solution does not appear to be much of an improvement over the "full solution", equation 5, since it too is of open form. Nevertheless, from this solution it is apparent that the time constant for the exponential decay of the long-time solution is

$$\tau_o = \frac{r_o^2 \mu\sigma}{\lambda_1^2}. \tag{8}$$

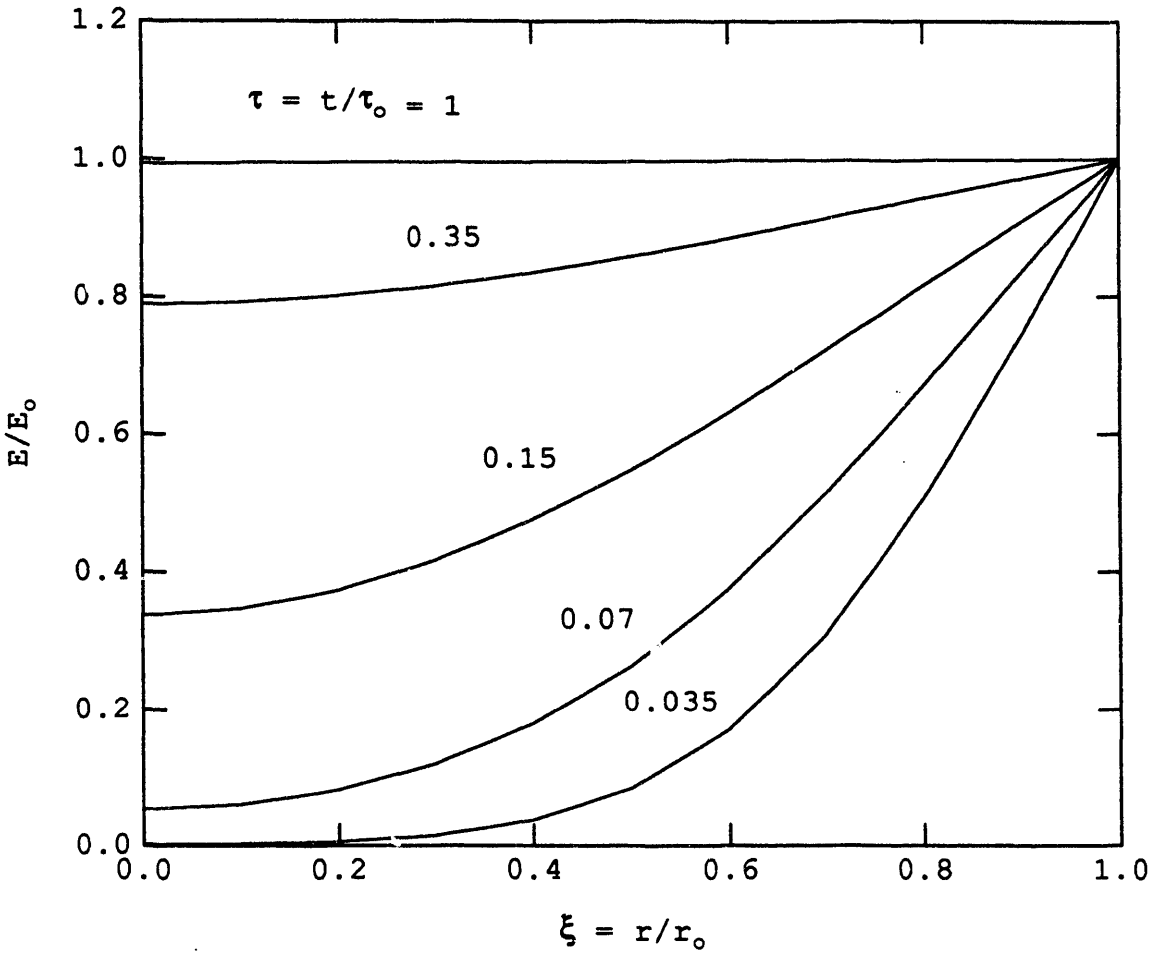

Figure 2. Axial electric field distibution divided by the magnitude of the electric field at the surface *versus* the dimensionless distance from the center of a cylindrical conductor.

This is the same time regime that is approximated by a the lumped-inductance analysis where the current approaches the steady-state current exponentially as the time over the inductive time constant L/R. Thus, L/R is equal to τ_o.

We now solve for the short-time solution of the diffusion region to determine how the field increases with time for relatively short times (and for future comparison with the long-time solution of the inner region.) Solving equation 6 by Laplace transforms,

$$\frac{\bar{E}(s)}{E_o} = \frac{I_o(s^{\frac{1}{2}}\xi)}{s\, I_o(s^{\frac{1}{2}})}, \tag{9}$$

expanding this solution for large s, and then inverting it, we obtain the short-time solution of the diffusion region,

$$\frac{E}{E_o} = \frac{1}{\xi^{\frac{1}{2}}}\left[1 - \frac{9\tau}{32\xi^2} + \frac{3675\tau^2}{2048\xi^4} - O(\frac{\tau^3}{\xi^6})\right] \operatorname{erfc}\frac{1-\xi}{\sqrt{4\tau}} \tag{10}$$

where $\tau \ll 1$. One should note that fewer terms of this solution are needed as $\xi \longrightarrow 1$ and $\tau \longrightarrow 0$. Thus, at short times the electric field penetrates as the erfc of distance from the edge of the conductor divided by the square root of time. We thus define a penetration depth, which is analogous to the skin-depth of a sinusoidal signal, as

$$d_p = \sqrt{t/\mu\sigma}. \tag{11}$$

The solutions developed in this, the diffusion regime, contain all the physics of equation 1 that occur on the time frame of τ_o. We

should now like to investigate the consequences of dropping the second order time derivative that provided these results and to elucidate the physics that occur *immediately* following the application of the electric field.

Inner Solution

To obtain the short-time or inner solution, we shall first define the variable $\xi' = 1 - \xi$, a dimensionless distance from the edge of the conductor, and then define new independent variables by stretching ξ' and τ by powers of δ. That is, let

$$\bar{\xi} = \frac{1 - \xi}{\delta^n} \quad \text{and} \quad \bar{\tau} = \frac{\tau}{\delta^m}.$$

Setting m = 2 and n = 1, substituting them into equation 3, and keeping terms multiplied by the smallest powers of δ, we obtain the equation

$$\frac{\partial^2 E}{\partial \bar{\xi}^2} = \frac{\partial^2 E}{\partial \bar{\tau}^2} + \frac{\partial E}{\partial \bar{\tau}}, \tag{12}$$

with boundary conditions,

$E = E_o$, at $\bar{\xi} = 0$;

E is well behaved, as $\bar{\xi} \longrightarrow \infty$;

and initial conditions,

$E = 0$, at $\bar{\tau} = 0$;

$\frac{\partial E}{\partial \bar{\tau}} = 0$, at $\bar{\tau} = 0$.

(Note the absence of the $1/\xi$ term on the left of equation 12, implying that the curvature of the wire has little effect in this time

regime.) These equations were solved by the Laplace-transform technique to give

$$\bar{E}(s) = E_o \frac{\exp[-(s^2 + s)^{1/2} \bar{\xi}]}{s}. \tag{13}$$

Applying the complex inversion formula to this solution while integrating around the branch cut between 0 and -1, we get the solution

$$E = E_o \left[1 - \frac{1}{\pi} \int_0^1 \frac{e^{-x\bar{\tau}} \sin[\sqrt{|x||1-x|}\ \bar{\xi}]}{x} dx \right] u(\bar{\tau}-\bar{\xi}), \tag{14}$$

where $u(\bar{\tau}-\bar{\xi})$ is the Heaviside function.[21] We extract more information from this time regime by expanding equation 13 for large and small values of s to obtain the short and long time solutions, respectively. Expanding 13 for large values of s and taking the inverse Laplace transform to get the short-time solution of the inner region gives

$$E = E_o e^{-\bar{\xi}/2} \left[1 + \frac{\bar{\xi}}{8}(\bar{\tau}-\bar{\xi}) - \frac{\bar{\xi}(8-\bar{\xi})}{256} (\bar{\tau}-\bar{\xi})^2 + \frac{\bar{\xi}(120-24\bar{\xi}+\bar{\xi}^2)}{18432} (\bar{\tau}-\bar{\xi})^3 + O(\bar{\xi}\bar{\tau}^4) \right] u(\bar{\tau}-\bar{\xi}). \tag{15}$$

This solution indicates that the electric field initially penetrates the conductor essentially as a front, traveling at the speed of light, with a magnitude that is exponentially damped with distance from the surface. The characteristic length of penetration is $2r_o\delta$.

Beyond the distance of $\bar{\tau} = \bar{\xi}$ the field is zero.

Allowing s to approach 0 in equation 13 and inverting to obtain the long-time solution of the inner region gives

$$\frac{E}{E_o} = \operatorname{erfc}\left[\frac{\bar{\xi}}{(4\bar{\tau})^{\frac{1}{2}}}\right]. \tag{16}$$

Thus after an initial period of ϵ/σ the field penetrates as the erfc of the distance divided by the square root of time. This is of the same form as the solution obtained as the short-time solution in the diffusion region, equation 11.

To summarize, when an electric field with an axial component of magnitude E_o is applied to the surface of a conductor at time 0, the field penetrates the conductor at the speed of light with a magnitude that is dramatically damped within in a distance of δr_o. This occurs within the time 0+ and $\delta^2 r_o^2 \mu\sigma = \epsilon/\sigma$. This is a very short time frame. For comparison, the time it takes light to reach the center of the conductor is $\delta r_o^2 \mu\sigma$. After this initial period, the field penetrates the conductor as the erfc of the distance from the surface divided by the square root of four times the time divided by $r_o^2 \mu\sigma$. Finally, as t approaches $r_o^2 \mu\sigma$, the field approaches the uniform, steady-state field distribution.

From this analysis, we shall develop the solutions of the total current as a function of time.

Current

From the expressions given for the electric field, one can determine the instantaneous total current. This value is derived from Ohm's law and integration of i over the cross-sectional area,

$$I = 2\pi r_o^2 \sigma \int_0^1 E\ \xi d\xi . \tag{17}$$

Solving for the instantaneous current allows us to compare the results of the above cases more readily by eliminating the independent variable ξ. The instantaneous current for the full solution and diffusion solution are, accordingly,

$$\text{Full} \quad \frac{I}{\pi r_o^2 \sigma E_o} = 1 - \sum_{k=1}^{\infty} \frac{4}{\lambda_k^2} \left[\cosh(\omega_k \tau) + \frac{\sinh(\omega_k \tau)}{2\delta^2 \omega_k} \right] \exp\left[-\frac{\tau}{2\delta^2} \right], \tag{18}$$

$$\text{Diffusion} \quad \frac{I}{\pi r_o^2 \sigma E_o} = 1 - \sum_{k=1}^{\infty} \frac{4}{\lambda_k^2} \exp(-\lambda_k^2 \tau). \tag{19}$$

Another approach to the full solution is first to integrate the Laplace transform of the electric field, equation 4, with respect to ξ from 0 to 1. Using the method of residues, we obtain the above solution; but expanding this equation for large s and inverting gives a solution useful at short times,

$$\frac{I}{\pi r_o^2 \sigma E_o} = \frac{2\tau e^{-\tau/2\delta^2}}{\delta} [I_o(\tau/2\delta^2) + I_1(\tau/2\delta^2)]$$

$$- [\tau - \delta^2(1 - e^{-\tau/\delta^2})] - \frac{\tau^2 e^{-\tau/2\delta^2}}{6\delta} [I_1(\tau/2\delta^2) + I_2(\tau/2\delta^2)]$$

$$- \frac{1}{8} [\tau^2 - 2\delta^2\tau(2 + e^{-\tau/\delta^2}) + 6\delta^4(1 - e^{-\tau/\delta^2})] \tag{20}$$

$$- \frac{5\tau^3 e^{-\tau/2\delta^2}}{48\delta} [I_2(\tau/2\delta^2) + I_3(\tau/2\delta^2)] + O(\tau^3)$$

for $\tau \ll 1$. Allowing s to get *very* large provides the very-short-time solution,

$$\frac{I}{\pi r_o^2 \sigma E_o} = 2\tau/\delta. \tag{21}$$

In the diffusion region, if we start with the transformed solution of the electric field, equation 10, integrate over the cross-sectional area of the conductor, take the limit as s gets very large, and invert it, we get the short-time solution to the diffusion region,

$$\frac{I}{\pi r_o^2 \sigma E_o} = \left(\frac{2\tau}{\pi}\right)^{1/2}. \tag{22}$$

For the inner region, we shall first integrate equation 13 with respect to $\bar{\xi}$ from 0 to ∞ and then take the inverse Laplace transform. Here, the current is given as

$$\text{Inner} \qquad \frac{I}{\pi r_o^2 \sigma E_o} = 2\delta\bar{\tau} e^{-\bar{\tau}/2} [I_o(\bar{\tau}/2) + I_1(\bar{\tau}/2)]. \tag{23}$$

Since $\bar{\tau} = \tau/\delta^2$, we see that the first term of the expanded full solution, equation 20, is equivalent to the short-time solution given here. The rest of the terms of equation 20 are corrective terms for large τ which tend to bend the solution down to the long-time

solution. If we take the limit of the Laplace transformed solution of the inner region, equation 13, for very small s, and again integrate with respect to $\bar{\xi}$ from 0 to ∞, we get the long-time solution of the inner region,

$$\frac{I}{\pi r_o^2 \sigma E_o} = \delta \left[\frac{2\bar{\tau}}{\pi}\right]^{1/2}, \tag{24}$$

and for *very* large s, we get the short-time solution of the inner region,

$$\frac{I}{\pi r_o^2 \sigma E_o} = 2\delta\bar{\tau}. \tag{25}$$

From this analysis of the current distribution, we see that at short times ($t<\epsilon/\sigma$) the current is proportional to time to the first power and at long times ($t>\epsilon/\sigma$) is proportional to time to the one half power until t is of order $r_o^2\mu\sigma$ where it approaches the steady-state value (see figure 3). In the former case, the short-time solution of the inner region overlaps the very-short-time solution of the full solution. In the latter case, the long-time solution of the inner region overlaps the short-time solution of the diffusion region. We can conclude that the "displacement current," which is responsible for this difference in solutions, is important only for $\bar{\tau} = \tau/\delta^2 \leq O(1)$ where $\delta^2 \ll 1$. One further note, figure 2 shows that the current approaches the final steady-state asymptotically with an exponential time constant of $r_o^2\mu\sigma$. This is as predicted by the lumped-inductance analysis — the only thing in this work predicted

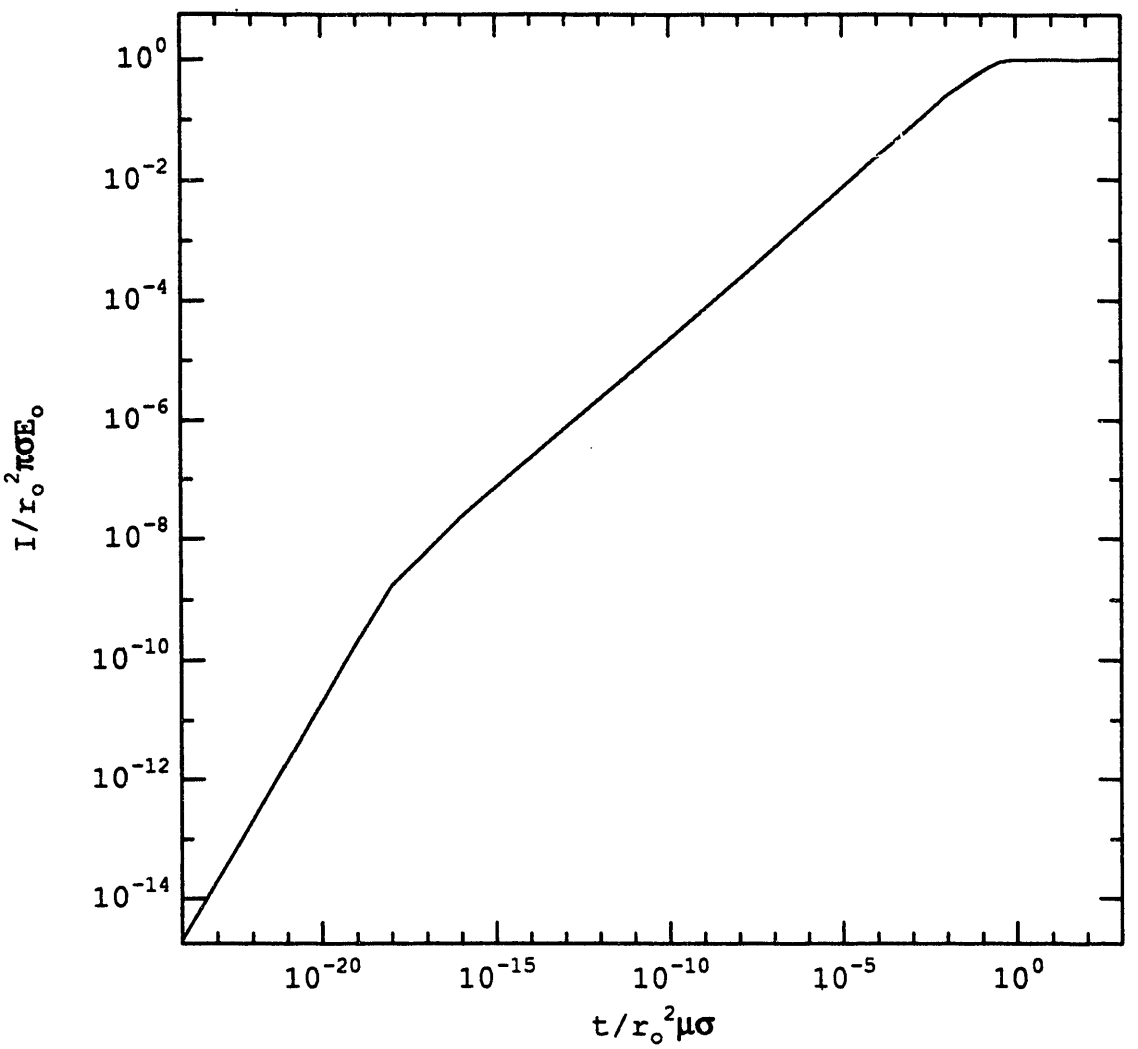

Figure 3. Dimensionless current *versus* dimensionless time for $\delta = 1\text{x}10^{-9}$.

by the lumped-inductance analysis.

Summary

This analysis describes the penetration of a steadily applied electric field into a cylindrical conductor from the initial time to steady state. This is recognized as a crude first approximation to the current distribution in a bipolar battery. The solution scheme used introduced two distinct time regimes referred to as the inner and diffusion solutions. A long-time and short-time solution of the electric field distribution were determined in each regime and then confirmed as consistent by direct comparison and comparison of the instantaneous current distributions. The current initially penetrates the wire at a rate proportional to time up to a time of the order of ϵ/σ and then at a rate proportional to the square root of time. It is this same order of time after which the omission of the displacement current is justified. The lumped inductance analysis is appropriate for times on the order of $r_o^2\mu\sigma$.

It part II we shall include the cylindrical wire in a radial circuit. That analysis will describe the interactions of the fields in the conductor with the rest of the circuit in terms of the time constant of the complete system.

(It should be noted that all calculations in this paper have been performed assuming that σ, ϵ, and μ are independent of time; *i.e.*, the conductor is nondispersive.)

List of Symbols

Roman

d_p	penetration depth, m
E	axial electric field component, V/m
E_o	magnitude of axial electric field component at the outer edge of conductor, V/m
I	total current, A
i	current density, A/m^2
L	inductance, V-s/A
r	distance from center of wire, m
r_o	radius of wire, m
R	resistance, Ω
s	Laplace transform variable, s^{-1}
t	time, s
x	variable of integration

Greek

δ	dimensionless stretching parameter
ϵ	permittivity, $C^2/N\text{-}m^2$
λ_k	k^{th} zero of Bessel function $J_o(x)$
μ	permeability, N/A^2
π	3.14159265358979
σ	electric conductivity, S/m
τ	dimensionless time
τ_o	dimensionless time constant

$\bar{\tau}$ stretched dimensionless time

ξ dimensionless distance from center

$\bar{\xi}$ stretched dimensionless distance from edge

References

1. P. L. Kapitza, "A Method of Producing Strong Magnetic Fields," *Proc. Roy. Soc. Lond.*, **105A**, 691-710 (1924).

2. E. Willihnganz, "The Voltage of the Sponge Lead Plate During Discharge of the Storage Battery," *Trans. Electrochem. Soc.*, **79**, 243-251 (1941).

3. H. F. Gibbard, "High Temperature, High Pulse Power Lithium Batteries," *Journal of Power Sources*, **26**, 81-91 (1989).

4. H. F. Gibbard, "Ultra-High-Power Batteries," *Electrochemical Society Proc.*, **86**-12, 193-205 (1986).

5. R. M. LaFollette and D. N. Bennion, "Design Fundamentals of High Power Density, Pulsed Discharge, Lead Acid Batteries: I Experimental," *J. Electrochem. Soc.*, **137**, 3693-3701 (1990).

6. R. M. LaFollette and D. N. Bennion, "Design Fundamentals of High Power Density, Pulsed Discharge, Lead Acid Batteries: II Modeling," *J. Electrochem. Soc.*, **137**, 3701-3707 (1990).

7. B. McKinney, W. Tiedemann, and J. Newman, "Short Circuit Currents in Uninterruptible Power Source Batteries," *Proceedings of the Symposium on Advances in Lead-Acid Batteries*, Pennington N. J., 3336-3347 (1984).

8. B. D. Cahan, M. L. Daroux, and E. B. Yeager, "Effect of Physical and Geometrical Factors on the Impedance of Electrochemical Power Sources," *Proc. - Electrochemical Soc.*, **87**-12, 137-151 (1987).

9. W. G. V. Rosser, "What Makes an Electric Current Flow," *Am. J. Phys.*, **31**, 884 (1963).

10. M. A. Heald, "Electric Fields and Charges in Elementary Circuits," *Am. J. Phys.*, **52**, 522-526 (1984).

11. A. Marcus, "The Electric Field Associated with a Steady Current in Long Cylindrical Conductor," *Am. J. Phys.*, **9**, 225-226 (1941).

12. A. Sommerfeld, *Electrodynamics*, Academic Press, New York, 125-133 (1952).

13. D. Marcuse, "Comment on 'The Electric Field Outside a Long Straight Wire Carrying a Steady Current,'" *Am. J. Phys.*, **38**, 935-936 (1970).

14. J. C. Maxwell, *A Treatise on Electricity and Magnetism*, 3rd Edition, Dover Publications, Inc., New York (1954).

15. J. D. Jackson, *Classical Electrodynamics*, 2nd Edition, John Wiley & Sons, New York (1975).

16. M. A. Shakur, "Solution to the Problem on Page 785," *Am. J. Phys.*, **52**, 849 (1984).

17. J. G. Chervenak, "The Back Electric Field from a Long Wire," *Am. J. Phys.*, **54**, 946-947 (1986).

18. P. Silvester, "AC Resistance and Reactance of Isolated Rectangular Conductors," IEEE Transactions on Power Apparatus and Systems, **86**, 770-774 (1967).

19. J. R. Carson, "Wave Propagation over Parallel Wires: The Proximity Effect." *Phil. Mag.*, **41**, 607-633 (1921).

20. J. R. Gosselin, P. Rochon, and N. Gauthier, "Study of Eddy Currents in a Cylindrical Wire: An Undergraduate Laboratory Experiment," Am. J. Phys., **50**, 440-443 (1982).

21. M. Abramowitz and I. A. Stegun, *Handbook of Mathematical Functions*, Dover Publications, Inc., New York (1965).

Chapter 2

Magnetic Field Effects in High-Power Batteries

Part II: Time Constant of a Radial Circuit Terminated by a Cylindrical Cell with Inductance

Foreword

The time constant to steady-state of an electric signal applied to the outer boundary of a radial circuit that propagates to a centrally located cylindrical conductor is determined rigorously by a transmission-line analysis. Two cases are reported: the perfect radial conductor and a radial conductor with a finite resistance. The time constant is featured as a function of the ratio of the radius of the radial conductive leads to the radius of the inner conductor. As the ratio is increased, the time constant departs from that of an electric field penetrating a cylindrical conductor and approaches the inductive time constant of the leads. An analytic approximation of the time constant of the system is also provided. This analysis should assist in the development of high-power circuitry design when the discharge time is on the order of the inductive time constant.

Introduction

The intent of this research is to determine the inductive time constant of a circuit that contains a battery. As discussed by

Rosser,[1] the rate at which the current rises in one portion of a circuit is a function of the configuration and properties of the rest of the circuit. Therefore, this problem cannot be solved in parts. The rigorous method for handling the inductance effects is to solve Maxwell's equations of electromagnetism throughout the entire circuit and surrounding medium, simultaneously with the equations that govern battery performance. This would require an enormous effort. As such, we direct our investigation to the simpler case of determining rigorously the rate of discharge of a radial circuit with an inductive, coaxial, cylindrical core. Applying the same arguments as found in part I, the cylindrical core is assumed to approximate the behavior of a bipolar battery. Furthermore, the electromotive force is assumed rooted at some radial distance, r_o, away.

In part I we developed the solution to the rate at which an electric field penetrates a cylindrical conductor. As discussed, a solid conductor is a poor approximation of the inner workings of a battery. However, that analysis provided an adequate first approximation of the inductive behavior of the battery. In this section, we shall use a transmission-line analysis in conjunction with the preceding work to determine the time constant of the total circuit configuration. The solution to this full problem may suggest where the limitation to instantaneous discharge resides and may then be used for design criteria for systems intended to be discharged at high rates.

Analytic Approach

An analytic approach is possible if a simplified circuit geometry is proposed. The following configuration is considered: a cylindrical conductor of finite length d, conductivity σ_i, and radius r_i sandwiched between two circular plates of radius r_o, where $r_o > r_i$ (see figure 1.) The system is initially at open-circuit, and the potential is zero everywhere. A constant voltage source is then applied at time zero at $r = r_o$. We wish to determine the time it takes the system to reach steady-state. A transmission-line analysis shall be used to characterize the propagation of the signal along the radial conductors to the inner cylindrical conductor. The solution derived in part I section for the penetration of an electric field into a conductor shall be converted into a boundary condition at $r = r_i$. The problem is solved using Laplace transforms. Two cases are considered: the first is where the outer radial conductors are assumed to have an infinite conductivity; and the second is where they have a finite conductivity. Before proceeding to the solution, we shall first develop, through the elementary laws of statics and electrodynamics, the transmission-line equations.

Transmission-Line Analysis

A measure of the ease by which charge q migrates through a medium is characterized by its resistivity, ρ. This parameter is lowest for conductors, of moderate value for semiconductors, and highest for insulators. The total resistance of a bar of a conducting material of length l and area A is

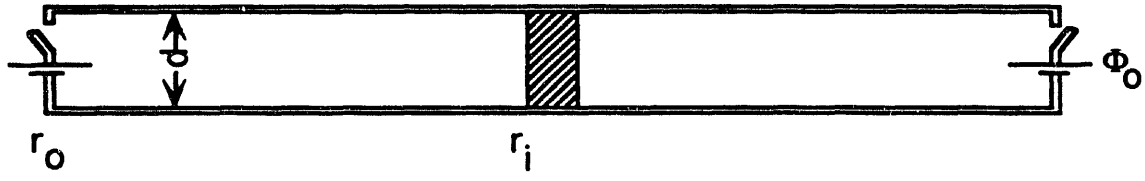

Figure 1. Radial circuit of radius r_o containing a cylindrical conductor of radius r_i.

$$R = \frac{\rho l}{A}. \tag{1}$$

Thus the resistance is defined by two parameters: the physical geometry and resistivity.

According to Gauss's law, an electric field outside of a conductor acting perpendicular to the conductor is given by

$$\mathbf{E}\cdot\mathbf{n} = \frac{q}{\epsilon A}. \tag{2}$$

The potential is defined as

$$-\nabla\Phi = \mathbf{E}. \tag{3}$$

For two parallel plates of equal and opposite charge and distance d apart we obtain

$$\Phi = \frac{qd}{\epsilon A}, \tag{4}$$

or

$$q = C\Phi, \tag{5}$$

where C is the capacitance. The capacitance, like the resistance, is a function of the physical geometry and a parameter, ϵ, that describes the medium separating the conductive material. For the parallel plates, capacitance per unit area is defined as

$$c = \frac{C}{A} = \epsilon/d. \tag{6}$$

Current is defined as the amount of charge that passes a particular point per unit of time. In differential form

$$I = \frac{\partial q}{\partial t} = C\frac{\partial \Phi}{\partial t} \tag{7}$$

for a capacitive current.

Ampere's law shows that with the passing of any current there is an associated magnetic field,

$$\nabla \times \mathbf{B} = \mu \mathbf{i}. \tag{8}$$

For a current flowing in a wire, the magnetic field is proportional to the amount of current and inversely proportional to the square of the distance from the center of the wire,

$$B \propto \mu I_L / r^2. \tag{9}$$

The magnetic flux, ϕ, is the sum of the magnetic fields of current-carrying elements from different positions in the conductor. The magnetic linkage, λ, is the sum of the total magnetic flux in the system. The magnetic linkage is proportional to the current,

$$\lambda = L I_L. \tag{10}$$

L, the self-inductance, is a proportionality constant between the flux linkage and the current and again is a function of the physical geometry and μ, a parameter describing the surrounding medium. For a parallel-plate configuration, it can be shown that the self-inductance is

$$L = \mu d. \tag{11}$$

To relate the flux linkage back to a potential, we turn to Faraday's law,

$$\nabla \times \mathbf{E} = -\frac{\partial \mathbf{B}}{\partial t}, \tag{12}$$

which mathematically states that a magnetic field that is varying in time has associated with it an electric field. These definitions

ultimately lead to the expression

$$-\nabla\Phi = L\frac{\partial i_L}{\partial t}. \tag{13}$$

We can now discuss the transmission of a signal in the radial direction between two conducting plates. If the conductors are "perfect," *i.e.* have a resistivity of zero, charge travels between the plates on the surfaces and is referred to as the skin current. If the plates have a finite resistance, the current penetrates within the plates and it can be integrated over the thickness ℓ. In either case, the current density will have units of A/cm. Charge flowing in the radial direction behaves as a purely inductive current, i_L, if the plates are perfect, and will contain an ohmic term if they are not. Some of the charge goes to charging the plates and is referred to as the capacitive current, i_c, with units of A/cm^2. A shell balance of the current traveling in the radial direction along a plate with no resistance entering the shell at r and leaving at $r+\Delta r$ appears as

$$2\pi r i_L\big|_r = 2\pi r i_L\big|_{r+\Delta r} + 2\pi r\Delta r i_c. \tag{14}$$

Dividing through by $r\Delta r$ and taking the limit as Δr approaches zero gives the differential form

$$\frac{1}{r}\frac{\partial(r i_L)}{\partial r} = -i_c. \tag{15}$$

Differentiation of equation 15 with respect to time and the subsequent substitution of the previously derived current-potential relationships,

$$\frac{\partial \Phi}{\partial r} = -L\frac{\partial i_L}{\partial t} \tag{16}$$

and

$$i_c = c\frac{\partial \Phi}{\partial t}, \tag{17}$$

gives the transmission-line equation for a radial circuit of infinite conductivity,

$$\frac{1}{r}\frac{\partial}{\partial r}\left(r\frac{\partial \Phi}{\partial r}\right) = Lc\frac{\partial^2 \Phi}{\partial t^2}. \tag{18}$$

If the conductor maintains a finite resistivity, the equation

$$-\frac{\partial \Phi}{\partial r} = L\frac{\partial i_L}{\partial t} + \frac{i_L}{\sigma l}, \tag{19}$$

(σ, the conductivity, is equal to $1/\rho$.) which contains an additional term for the ohmic drop, is substituted into equation 15 in the place of equation 16. This substitution gives the transmission-line equation for a radial circuit with finite conductivity,

$$\frac{1}{r}\frac{\partial}{\partial r}\left(r\frac{\partial \Phi}{\partial r}\right) = Lc\frac{\partial^2 \Phi}{\partial t^2} + \frac{c}{\sigma l}\frac{\partial \Phi}{\partial t}. \tag{20}$$

Case 1:

Outer Conductors of Infinite Conductivity.

As shown above, the following transmission-line equation for the potential applies to radial conductors of infinite conductivity:

$$\frac{\partial^2 \Phi}{\partial r^2} + \frac{1}{r}\frac{\partial \Phi}{\partial r} = Lc\frac{\partial^2 \Phi}{\partial t^2}. \tag{21}$$

Substitution of the dimensionless variables,

$$\xi = r/r_i, \quad \tau = t/r_i^2\mu_i\sigma_i, \quad \text{and} \quad \phi = \Phi/\Phi_o, \tag{22}$$

leads to the equation

$$\frac{\partial^2\phi}{\partial\xi^2} + \frac{1}{\xi}\frac{\partial\phi}{\partial\xi} = \delta_o^2\,\frac{\partial^2\phi}{\partial\tau^2}, \tag{23}$$

where $\delta_o = r_i\sqrt{Lc}/r_i^2\mu_i\sigma_i$.

We shall solve this equation by means of a Laplace transformation. The Laplace transform of equation 23 is

$$\frac{\partial^2\bar{\phi}}{\partial\xi^2} + \frac{1}{\xi}\frac{\partial\bar{\phi}}{\partial\xi} = \delta_o^2 s^2\bar{\phi} - s\phi(+0) - \phi'(+0). \tag{24}$$

The following is a list of the initial and boundary conditions.

Initial Conditions

$$\phi = 0 \quad \text{at} \quad \tau = 0, \tag{25}$$

$$\frac{\partial\phi}{\partial\tau} = 0 \quad \text{at} \quad \tau = 0. \tag{26}$$

The first condition mathematically states that the potential is zero everywhere at time zero. The second condition states that the change of the potential with respect to time at time zero is also zero. This implies that some type of "inertia" or inductance must be overcome before the potential will change at time zero.

Boundary Conditions

$$\phi = 1 \qquad \text{at} \quad \xi = r_o/r_i, \tag{27}$$

$$2\pi\int i_i r dr = 2\pi r_i i_o \qquad \text{at} \quad \xi = 1. \tag{28}$$

The first boundary condition states that at $r = r_o$ the potential is

instantaneously set to Φ_o. The second condition is interpreted as the integral of the current density over the area in the inner conductor is equal to the line integral of the skin-current density that enters the inner conductor at $r = r_i$.

We shall now derive the Laplace transformation of the boundary conditions. The Laplace transformation of equation 27 gives

$$\bar{\phi} = 1/s \qquad \text{at} \quad \xi = r_o/r_i. \tag{29}$$

On the right side of equation 28, i_o, the skin-current density, defined in equation 16, is

$$i_o = -\frac{1}{L}\int_0^t \frac{\partial \Phi}{\partial r} dt = -\frac{r_i \mu_i \sigma_i \Phi_o}{L}\int_0^\tau \frac{\partial \phi}{\partial \xi} d\tau. \tag{30}$$

The Laplace transformation of this equation is

$$\bar{i}_o = -\frac{r_i \mu_i \sigma_i \Phi_o}{L}\,\frac{1}{s}\frac{\partial \bar{\phi}}{\partial \xi}. \tag{31}$$

Ohm's law gives the relation for current density in the central conductor in terms of a component of electric field

$$i_i = \sigma_i E. \tag{32}$$

We have shown in part I that inside a cylindrical conductor the Laplace transform of the axial component of the electric field distribution due to a steady field of unit magnitude applied at the surface is

$$\bar{E} = -\frac{\Phi_o \bar{\phi}}{d} = \frac{I_o[(\delta_i^2 s^2 + s)^{\frac{1}{2}}\xi]}{s\, I_o[(\delta_i^2 s^2 + s)^{\frac{1}{2}}]}, \tag{33}$$

I_o is the modified Bessel function of the first kind, of order 0.[2] Duhamel's superposition formula,[2] an integration of the solution to the linear equations applicable to the system, is used to describe the current in the conductor

$$i_i = \sigma_i \int_0^{\tau} E(\xi, \tau-\tau') \frac{\partial E(\tau')}{\partial \tau} d\tau'. \tag{34}$$

The Laplace transform of this equation is equal to the product of the Laplace transform of its parts.[2] The Laplace transform of $E(\xi, \tau-\tau')$ is given in equation 33. The Laplace transform of the derivative of E with respect to τ is

$$\overline{\frac{\partial E}{\partial \tau}} = s\bar{E}. \tag{35}$$

Taking the Laplace transform of equation 34 and substituting into it equations 33 and 35 gives

$$\frac{2\pi r_i^2 \sigma_i \Phi_o \bar{\phi}}{d} \int_0^1 \frac{\xi\, I_o[(\delta_i^2 s^2 + s)^{\frac{1}{2}}\xi]}{I_o(\delta_i^2 s^2 + s)^{\frac{1}{2}}} d\xi = \frac{2\pi r_i^2 \mu_i \sigma_i \Phi_o}{L} \frac{1}{s} \frac{\partial \bar{\phi}}{\partial \xi}. \tag{36}$$

After integrating and some rearrangement, we get the boundary condition,

$$\frac{\bar{\phi}\, I_i(\delta_i^2 s^2 + s)^{\frac{1}{2}}}{(\delta_i^2 s^2 + s)^{\frac{1}{2}} I_o(\delta^2 s^2 + s)^{\frac{1}{2}}} = \frac{\mu_i}{Ld} \frac{1}{s} \frac{\partial \bar{\phi}}{\partial \xi} \qquad \text{at} \quad \xi = 1. \tag{37}$$

Solution

Solution of equation 24 with the conditions of 25, 26, 29, and 37 is

$$\bar{\phi} = AI_o(\delta_o s\xi) + BK_o(\delta_o s\xi). \tag{38}$$

$$A = \frac{\frac{1}{s} - BK_o\left(\delta s\frac{r_o}{r_i}\right)}{I_o\left(\delta_o s\frac{r_o}{r_i}\right)}, \tag{39}$$

and

$$B = \frac{I_o(a)Y(s) - cI_i(a)}{s\,[K_o(b)I_o(a) - K_o(a)I_o(b)]Y(s) - c\,[K_o(b)I_1(a) - K_1(a)I_o(b)]}, \tag{40}$$

where

$$a = \delta_o s, \quad b = \delta_o s r_o/r_i, \quad c = \delta_o \mu_i/Ld, \tag{41}$$

and

$$Y(s) = \frac{I_1(\delta_i^2 s^2 + s)^{\frac{1}{2}}}{(\delta_i^2 s^2 + s)^{\frac{1}{2}} I_o(\delta_i^2 s^2 + s)^{\frac{1}{2}}}. \tag{42}$$

Inversion of this solution to position and time coordinates is formidable. The transformation may be performed by the method of residues, application of which requires the poles of the equation. The poles are also equal to the negative of the time constants.

Time Constants

Since our primary concern in this investigation is the rate at which a conductor in a circuit can be brought to full current, we

shall focus our efforts on deriving the time constant of the above solution. The poles of the solution are the roots of the denominator of B. To emphasize the effect of circuit size on the time constant, we rearrange the denominator of B to

$$c[K_o(b)I_1(a)+K_1(a)I_o(b)]Y(s)\left\{\frac{K_o(b)I_o(a)-K_o(a)I_o(b)}{[K_o(b)I_1(a)-K_1(a)I_o(b)]\,c}-\frac{1}{Y(s)}\right\} \quad (43)$$

The term on the left within the brackets, from here on referred to as K, is a function of s, the properties of the radial part of the circuit, and r_o/r_i. The term on the right within the brackets is a function of s and the properties of the inner conductor. A plot of both terms within the brackets is provided in figure 2, where the ratio of r_o/r_i is a parameter. K appears as a straight line with a slope which becomes more negative as r_o/r_i is increased. $Y(s)$ is unaltered by changes in the radius ratio. The root of equation 43 is the value of s where the two terms in the brackets are equal (the point of intersection in figure 2). As the size ratio approaches infinity, one sees in figure 2 that the point of intersection approaches zero, and, thus, the time constant approaches infinity. Figure 2 further shows that $1/Y(s)$ intersects the abscissa at the value of $s = s_o$ where $\delta_i^2 s_o^2 - s_o = \lambda_o^2$. λ_o is the first zero of J_o, the Bessel function of the first kind, of order 0. $\lambda_o^2 = 5.783186$.[3] K intersects the abscissa at $s = 0$. The time constant, $\tau' = -1/root \equiv -1/s_r$, is therefore bound between $-1/s_o$ and infinity, and is a function of the size ratio r_o/r_i.

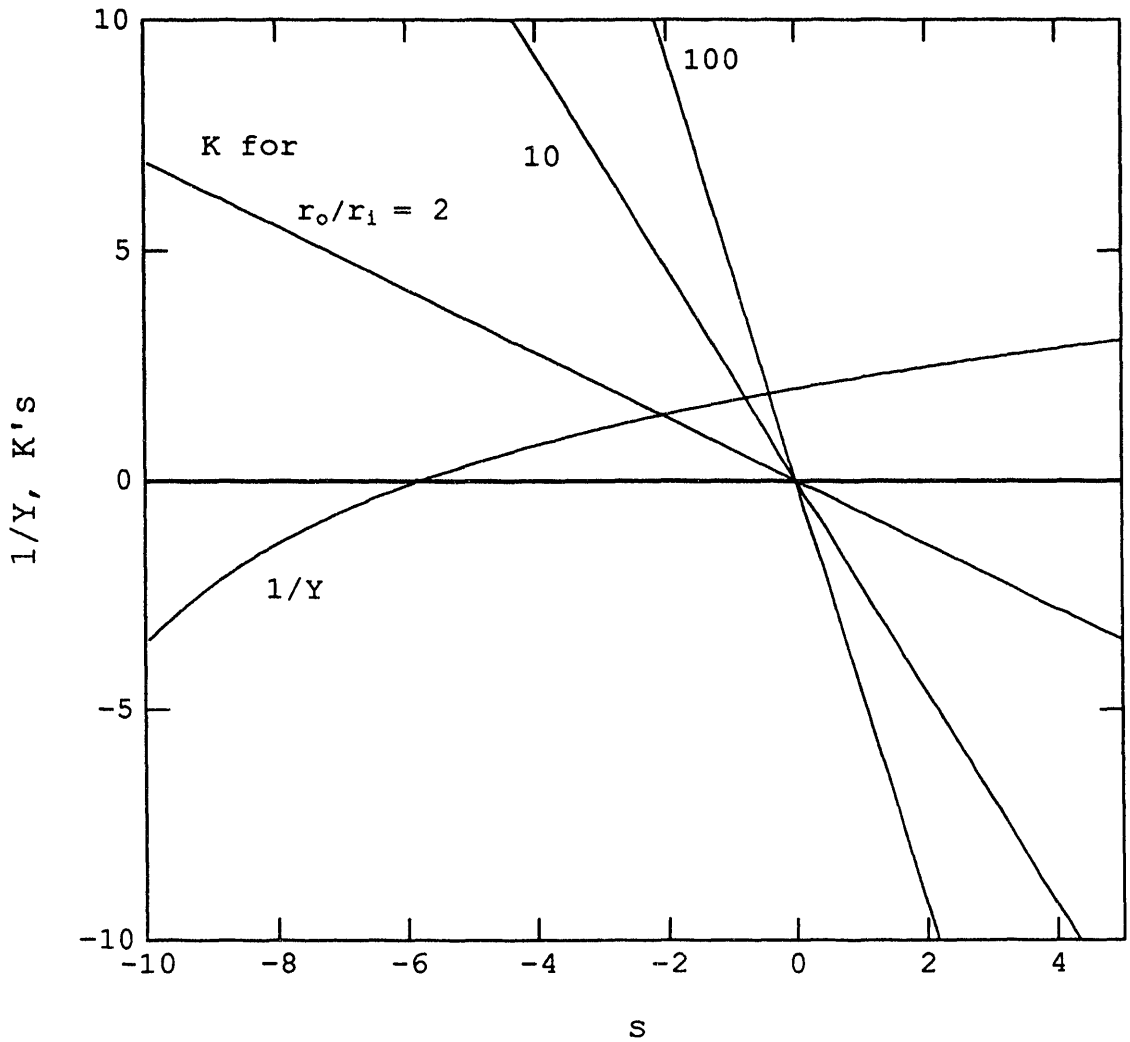

Figure 2. 1/Y and K *versus* s for three values of r_o/r_i. $\delta_i = \delta_o = 10^{-5}$.

We now wish to develop an approximate analytic expression of the time constant as a function of the size ratio. The limit of K as s approaches zero is

$$\lim_{s \to 0} K = -\frac{s\delta_o}{c} \ln \frac{r_o}{r_i}. \tag{44}$$

(c is defined in equation 41.) An approximation of $1/Y(s)$ for small s is

$$\lim_{s \to 0} \frac{1}{Y(s)} \approx 2\left(1 - \frac{s}{s_o}\right). \tag{45}$$

Combination of the above equations leads to

$$\frac{\tau'}{\tau_o} = \frac{s_o}{s_r} = 1 + \frac{|s_o|\delta_o}{2c} \ln \frac{r_o}{r_i}. \tag{46}$$

This approximation of the time constant as a function of the size ratio is plotted in figure 3 along with the roots of equation 43. This figure shows that the time constant increases without bound as the ratio of the radius of the perfectly conducting outer leads to the radius of the inner conductor is increased.

Case 2:

Outer Conductors of Finite Conductivity.

The radial circuit geometry is again used here; however, this time the circuit maintains a finite conductivity. The transmission-line equation for a radial conductor with a finite conductivity is

$$\frac{\partial^2 \Phi}{\partial r^2} + \frac{1}{r}\frac{\partial \Phi}{\partial r} = Lc\frac{\partial^2 \Phi}{\partial t^2} + \frac{c}{\sigma_o \ell}\frac{\partial \Phi}{\partial t}, \tag{47}$$

as derived earlier. Substituting into the above equation the

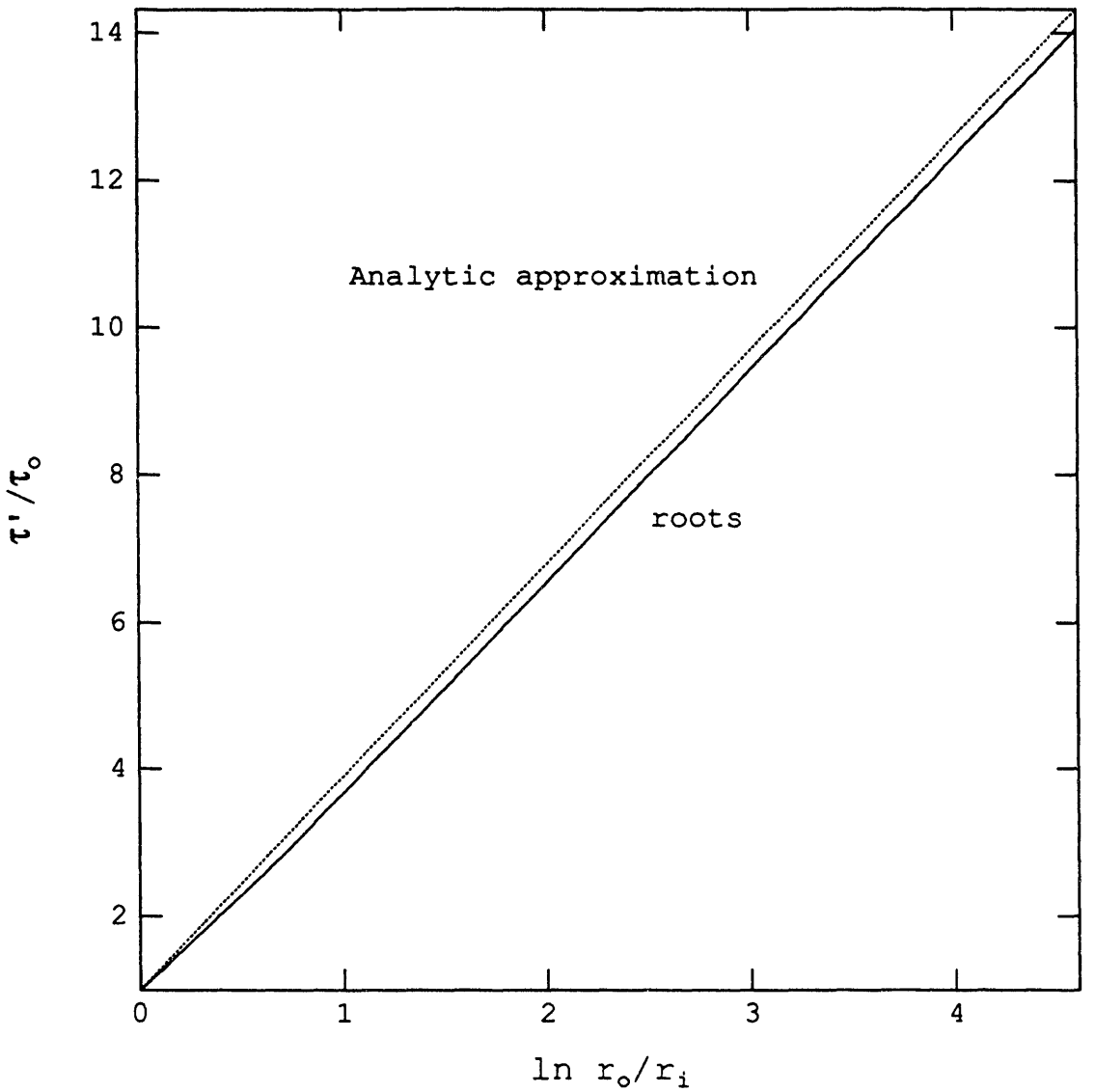

Figure 3. The time constant, and an analytic approximation, of the circuit of infinite conductivity *versus* the logarithm of the size ratio.

previously defined dimensionless parameters from equation 22 gives

$$\frac{\partial^2\phi}{\partial\xi^2} + \frac{1}{\xi}\frac{\partial\phi}{\partial\xi} = \delta_o^2\left[\frac{\partial^2\phi}{\partial\tau^2} + \beta\frac{\partial\phi}{\partial\tau}\right], \tag{48}$$

where

$$\beta = \frac{r_i^2\mu_i\sigma_i}{\sigma_o\ell L}. \tag{49}$$

The self-inductance of the inner conductor is proportional to its permeability, μ_i. The resistance of the inner conductor is inversely proportional to the radius squared and the conductivity, $1/r_o^2\sigma_i$. Likewise, the resistance of the outer conductor is inversely proportional to the conductivity and the thickness of the plates, $1/\ell\sigma_o$. Thus, β can be thought of as the ratio of the inductive time constants, L/R, of the inner conductor and outer radial leads.

The Laplace transform of equation 23 is

$$\frac{\partial^2\bar{\phi}}{\partial\xi^2} + \frac{1}{\xi}\frac{\partial\bar{\phi}}{\partial\xi} = \delta_o^2\,[s^2\bar{\phi} - s\phi(+0) - \phi'(+0) + \beta(s\bar{\phi} - \phi(+0))]. \tag{50}$$

The same initial and boundary conditions apply as in case 1; however, i_o obeys the equation from the transmission-line analysis for a conductor of finite conductivity equation 19, which is rewritten here as

$$-r\frac{\partial\Phi}{\partial r} = Lr\frac{\partial i_o}{\partial\tau} + \frac{r}{\sigma l}i_o. \tag{51}$$

The dimensionless Laplace transform form of this equation is

$$-\frac{\Phi_o}{r_i}\frac{\partial\bar{\phi}}{\partial\xi} = \left(\frac{Ls}{r_i^2\mu_i\sigma_i} + \frac{1}{\sigma_o l}\right)\bar{i}_o. \tag{52}$$

Combination of equations 28, 36, and 52 and some rearrangement provides the boundary condition

$$\frac{\mu_i}{(s+\beta)Ld}\frac{\partial\bar{\phi}}{\partial\xi} = \frac{I_1(\delta_i^2 s^2 + s)^{1/2}}{s(\delta_i^2 s^2 + s)^{1/2} I_o(\delta_i^2 s^2 + s)^{1/2}}\phi \quad \text{at} \quad \xi = 1. \tag{53}$$

Solution

Solution of equation 48 with the derived initial and boundary conditions in equations 25, 26, 29, and 53 gives the Laplace transform solution

$$\bar{\phi} = A I_o[\delta_o(s^2 + \beta s)^{1/2}\xi] + B K_o[\delta_o(s^2 + \beta s)^{1/2}\xi]. \tag{54}$$

$$A = \frac{\frac{1}{s} - B K_o(b)}{I_o(b)}. \tag{55}$$

$$B = \frac{\frac{a}{\delta_o cs} Y(s) I_o(a) - I_1(a)}{sY(s)[K_o(b)I_1(a) + K_1(a)I_o(b)]\left\{\frac{a}{\delta_o cs}\frac{K_o(b)I_o(a) - K_o(a)I_o(b)}{K_o(b)I_1(a) + K_1(a)I_o(b)} - \frac{1}{Y(s)}\right\}}. \tag{56}$$

$$a = \delta_o(s^2 + \beta s)^{1/2}, \quad b = \delta_o(s^2 + \beta s)^{1/2} r_o/r_i, \quad c = \delta_o\frac{\mu_i}{Ld}, \tag{57}$$

and Y(s) is the same as in case 1, equation 42.

As in the first case, inversion of this solution to time coordinates is difficult; we shall again focus on obtaining the time constant of the problem.

Time Constants

We show in figure 4, as we did in figure 2, a plot of the two terms within the large brackets of equation 58 for several values of

β and a r_o/r_i ratio of 10/1. When β is set to zero, we recover the analysis in Case 1. As β is increased, the K line from the original analysis is offset to the left by β. Again, the poles of the solution are those values of s where the two curves intersect. The shift of K by variations in β precludes the time constant from approaching infinity even as the size of the circuit approaches this limit. We see that as β is increased, the time constant, which is the inverse of the absolute value of the roots, decreases. The dimensionless time constant of a circuit of finite conductivity is constrained between the two limits $-1/\beta$ and $-1/s_o$.

Again we search for an analytic expression of the time constant. Taking the limit of the left term in the large brackets of equation 58 as $s \longrightarrow 0$ gives

$$\lim_{s \longrightarrow 0} K = \frac{a^2}{\delta_o c s} \ln \frac{r_o}{r_i} = \frac{(s + \beta)\delta_o}{c} \ln \frac{r_o}{r_i}. \tag{58}$$

The approximation of $1/Y(s)$ for small s was derived in case 1, equation 45. Combination of the two limiting forms provides an analytic approximation of the time constant

$$\frac{\tau'}{\tau_o} = \frac{s_o}{s_r} = \frac{1 - \dfrac{s_o \delta_o}{2c} \ln \dfrac{r_o}{r_i}}{1 + \dfrac{\beta \delta_o}{2c} \ln \dfrac{r_o}{r_i}}. \tag{59}$$

The time constants derived from the roots of equation 58 and those satisfying the above approximation are plotted *versus* the size of the system in figure 5 for two values of β: one $> s_o$ and the other $< s_o$.

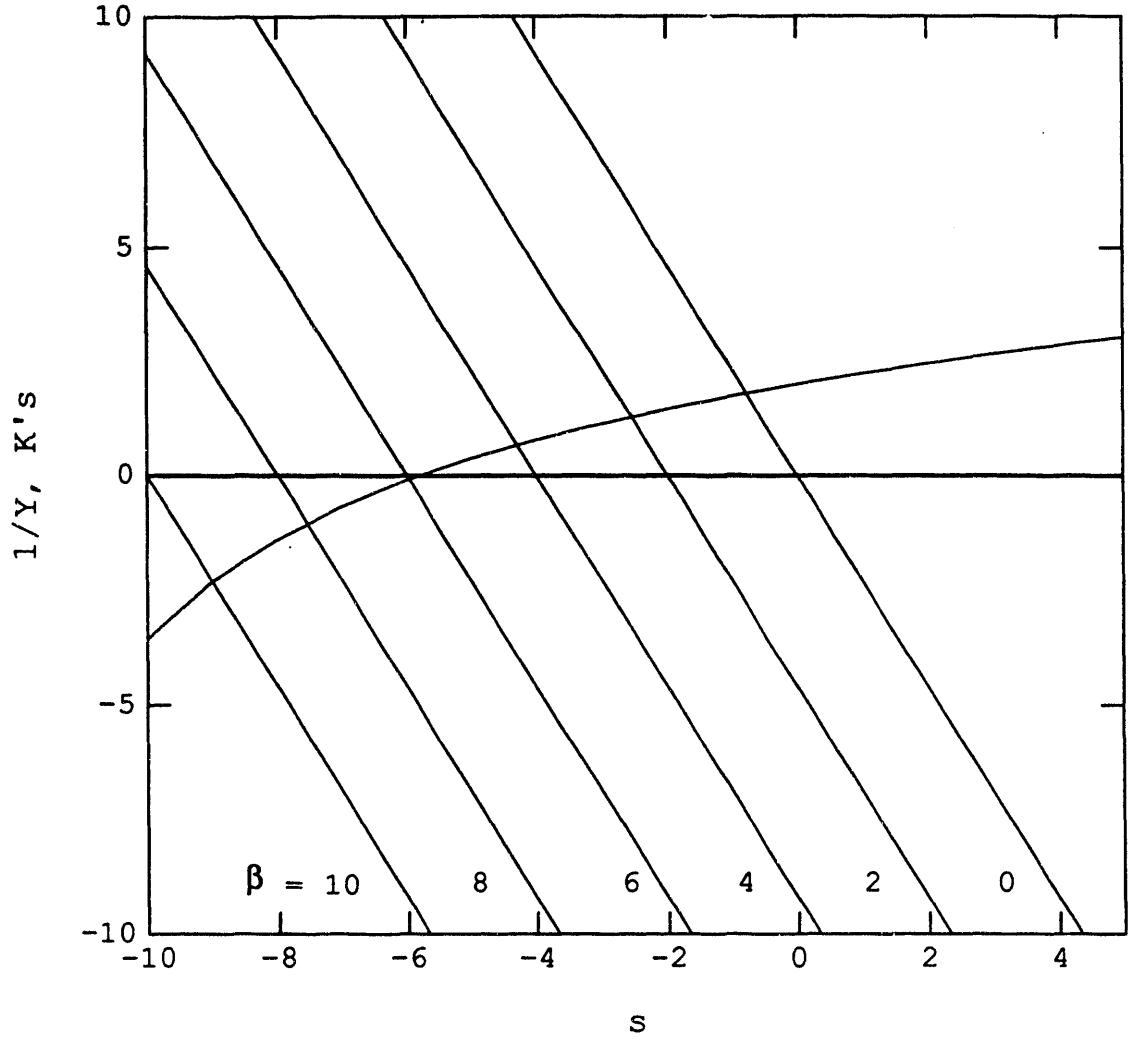

Figure 4. 1/Y and K's *versus* s for different values of β. $r_o/r_i = 10$.

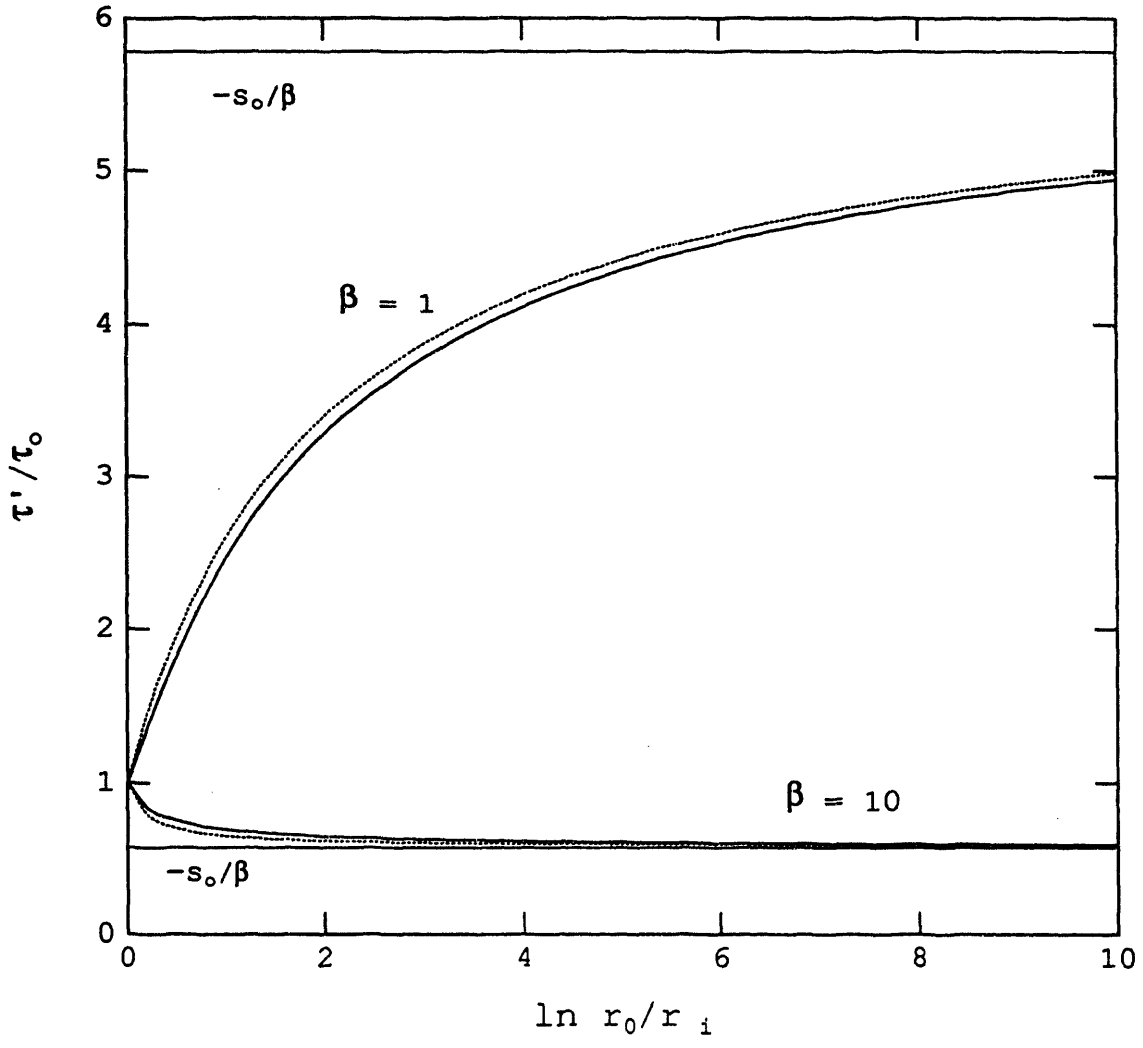

Figure 5. Time constants *verses* size for two values of β. The dashed curves are analytic approximations.

Discussion

δ_o and δ_i are both typically much less than 1 and were set equal to each other and to 1×10^{-5} in all of the figures. Only for very short times, s on the order of $1/\delta^2$, does the exact value of δ play a significant role. In the time frame of interest, which is the long time referred to in chapter 1, s is $O(1)$. The above equations can, therefore, all be simplified by setting the δ's to zero. This approximation has little effect on the present "long-time" results and explains why values of the δ's are implicitly eliminated from the analytic approximations of the time constant derived in cases 1 and 2.

As mentioned, β is the ratio of the inductive time constants of the inner conductor to the outer radial leads. In case 1, where the leads are of infinite conductivity or zero resistance, the inductive time constant of the leads is infinite, and β is zero. Setting β to zero in case 2 reduces the solutions to those of case 1.

For the system with infinitely conductive leads, the time constant is proportional to the logarithm of the ratio of the size of the leads to the size of the inner conductor. On the other hand, the system with leads of finite conductivity has a time constant that is bound between the time constant of the inner conductor and that of the leads. In general, the time constant of the system may either increase or decrease with the size ratio of the system, but it becomes independent of the size of the system as the size ratio approaches infinity.

The problem we have just addressed is analogous to the problem of determining the time constant of a circuit with two inductors in series. In that situation, the inductances are added, and the resistances are added. The time constant for the circuit is then[4]

$$\tau' = \frac{L_o + L_i}{R_o + R_i}. \tag{60}$$

Some rearrangement gives

$$\frac{\tau'}{L_i/R_i} = \frac{1 + L_o/L_i}{1 + R_o/R_i}, \tag{61}$$

which is analogous to the analytic approximation provided in equation 61. This investigation demonstrates that the present method of adding inductances to determine the overall time constant is an approximation (see figures 3 and 5) and that the approximation is less accurate for the smaller size ratios ($\ln r_o/r_i = O(1)$).

Conclusions

A rigorous investigation has been undertaken to determine the time constant of a radial circuit with and without resistance. The circuit with an infinite conductivity has a time constant that is proportional to the logarithm of the size of the system: as the size approaches infinity, so does the time constant. For a circuit with finite conductivity, the time constant is bound between two limits and is independent of size ratio for large systems. An analytic approximation to the time constant is provided for comparison with the rigorous evaluation and shows that the approximation, which is used in most texts of circuit analysis, is less accurate for smaller

systems — circuits where the leads are approximately as wide as the cell of interest. This analysis is a first approximation to the time constant of a circuit containing an electrochemical power source and is an applicable design tool for rapidly discharging systems.

List of Symbols

Roman

C	capacitance, C/V
c	capacitance per area, C/V-cm^2
d	distance between radial conductors, cm
E	electric field, V/cm
$\bar{E}$	Laplace transform of E, V/cm
i_i	current density in inner conductor, A/cm^2
i_o	current density in outer leads, A/cm
$\overline{i_o}$	Laplace transform of i_o
l	thickness of radial leads, cm
L	inductance, V-s^2/C-cm^2
r	radial coordinate, cm
r_i	radius of inner conductor, cm
r_o	radius of outer leads, cm
R	resistance, Ω
s	Laplace transform of dimensionless time, τ
t	time, s

Greek

β	ratio of the inductive time constants
δ	dimensionless parameter
μ	permeability, V-s^2/C-cm
ξ	dimensionless radial coordinate
σ	conductivity, S/cm
τ	dimensionless time
ϕ	dimensionless potential
$\bar{\phi}$	Laplace transform of ϕ
Φ	potential, V

subscripts

i	property of inner conductor
o	property of outer leads

References

1. W. G. V. Rosser, "What Makes an Electric Current Flow," *Am. J. Phys.*, 31, 884-5 (1963).

2. F. B. Hildebrand *Advanced Calculus for Applications*, 2nd Edition, Prentice-Hall, Inc., Englewood Cliffs, New Jersey (1976).

3. M. Abramowitz and I. A. Stegun, *Handbook of Mathematical Functions*, Dover Publications, Inc., New York, p.409 (1964).

4. R. E. Thomas and A. J. Rosa, *Circuits and Signals: An Introduction to Linear and Interface Circuits*, John Wiley and Sons, Inc., New York (1984).

Chapter 3

The Modeling of a Growing Oxide Film

Foreword

The full set of equations necessary for describing the growth of an oxide film is presented. The analysis includes methods of combining equations for systems with rapid kinetics and a derivation of the high-field equation. The boundary conditions on the flux equations, Poisson's equation, and the velocity of the interface are also discussed. The methodology is then applied to the iron/iron oxide system, and includes the reactions of electrons and iron interstitials at the metal/oxide and oxide/solution interfaces. Simulations, using the low-field equation, are compared to experimental results. It is found, in agreement with experiments, that passivation does not occur until 200 mV above the potential where the formation of an oxide is thermodynamically possible. This results because the oxide formation reaction is overwhelmed by the fast kinetics of the iron dissolution to ferrous ions.

Introduction

Oxide films are present on nearly all metal surfaces subjected to oxidative environments. Those films that are compact and poor current conductors are referred to as passivating films. Experimentally it has been shown that passive films on metals, subject to an anodic current or potential, grow with a thickness that is roughly

proportional to the logarithm of time. For over fifty years, many theories have been proposed that predict such a growth rate; and still, the most prominent theories today are but subtle improvements of some of the earliest work. (Reviews of the experiments and theories can be found in Young,[1,2] Vetter,[3] and Choa *et al.*[4])

In 1935 Verwey[5] proposed that the anodic growth of oxides is limited by the rate of transport of cationic interstitials. The driving force for migration is described by a high-field mechanism, which is exponentially dependent on the local electric field. Cabrera and Mott[6] agreed that ionic transport is dominated by cation migration by a high-field mechanism, but argued that the rate of film growth is limited by the reaction rate at the metal/oxide interface. Fehlner and Mott[7] stated that ionic transport is dominated by the conduction of anions and that the limitation to growth is the reaction rate at the oxide/solution interface. Maurer[8] suggested that the electric-field-dependent production of Frenkel defects — interstitials formed within the oxide by a field assisted jump of an ion from a lattice site — is the rate limiting step to forming mobile cationic species.

These theories have since been used as they stand, or combined to describe multiple phenomena, or slightly modified to fit particular system data. Vermilyea[9] modified the high-field theory to describe the transport in Ta_2O_5 films to include two consecutive energy barriers to ionic transport. Burnstein and Davenport[10] adjusted the high-field model by developing an improved integration of the high-field equation. Cahan *et al.*[11] argued that the passive

film on iron consists of Fe^{2+}, Fe^{3+}, and Fe^{4+} cations, the concentrations of which vary across the film due to the presence of a strong electric field. This description is then used to characterize properties of the film and its growth. Bean *et al.*[12] relied on a combination of cation interstitials formed through Frenkel defects and a high-field mechanism to describe the growth kinetics of tantalum oxide whereas Odynets[13] claimed that the creation of defects at the interface and subsequent transport across the film are equally responsible for the limited rate of film growth. Many researchers, such as Dewald,[14,15] Dignam,[16] and Greyling *et al.*,[17] ascribed the differences between experimental data and the high-field transport model to neglect of the space charge in the oxide, while others[18,19] have suggested that the data can be explained by a place-exchange model.

More recent work relies on a defect model, originally developed by Frenkel.[20] This model emphasizes that current is conducted by mobile charged defects. Macdonald's point-defect models[4,21,22] do not include a high-field mechanism of migration, and only the most recent paper attempts to include finite interfacial kinetics. MacDougall's point-defect models[23,24] are concerned mostly with the structure of the oxide and suggest that transient changes of currents at a given potential are due to a reduction of the number of oxide imperfections. The models of Macdonald and MacDougall were recently compared by Dagan and Tomkiewicz[25] for the growth of films on permalloy. They found that Macdonald's model did not fit the data as well

as MacDougall's (although, MacDougall's paper is based solely on qualitative arguments).

In each of the above theories, only one mechanism at a time is considered such that an analytic expression for film growth is derived. These equations usually take one of the following forms: a logarithmic growth law, an inverse logarithmic growth law, or a modified inverse logarithmic growth law. Lukac *et al.*[26] have gone on to show that these three laws can equally describe the growth kinetics and that none of the models is completely consistent with the experimentally observed temperature and potential dependences.

We believe that any or all of the above mentioned phenomena may play a significant role in oxide growth, where the predominant mechanism is a function of the system being examined and the stage to which growth has transpired. Therefore, in order to follow the progress of the growth of any oxide film through all of its stages, a model is developed that contains all of the physics. The equations of this model are then solved simultaneously with a computer. Starting with the framework of Macdonald's point defect model, we shall present a general model that includes any number of species that may react homogeneously and heterogeneously. The model will also include effects due to variations in the adjacent solution phase and track film growth or dissolution.

In the model development we shall consider only those species that are typically present. We shall then provide the equations necessary to describe the system and touch on electric-field effects

and thermodynamic consistency. The method used to increase the computational efficiency shall also be discussed. Upon completion of the general model development, we present results specific to the iron/iron oxide system. The first thing to be considered, however, is a description of the system.

General System Description

Figure 1 provides a schematic of the system. (This figure is similar to that introduced by Vetter,[3] figure 328.) A metal substrate interacts with a solution through an oxide. The interaction is described by reactions at both interfaces, the properties of the oxide, and the properties of the solution. The concern here is with variations occurring in a direction perpendicular to the metal interface while neglecting all parallel interactions. In other words, a one-dimensional model is developed. Furthermore, we assume that an oxide is present from the start, completely ignoring initial oxide formation (which, rigorously, occurs through nucleation sites and is inherently two-dimensional). A mathematically one-dimensional description of a film formed on a bare metal surface has been developed by Russell and Newman.[27]

Transport in an oxide can be interpreted in terms of mobile vacancies and defects; see Wagner.[27] A general model of an oxide must have the flexibility to accept various types of defects and associated reactions. Moreover, oxides may also be semiconductors; thus, electrons and holes as well as any dopant species must also be easily incorporated into the model. An account of the dominant modes

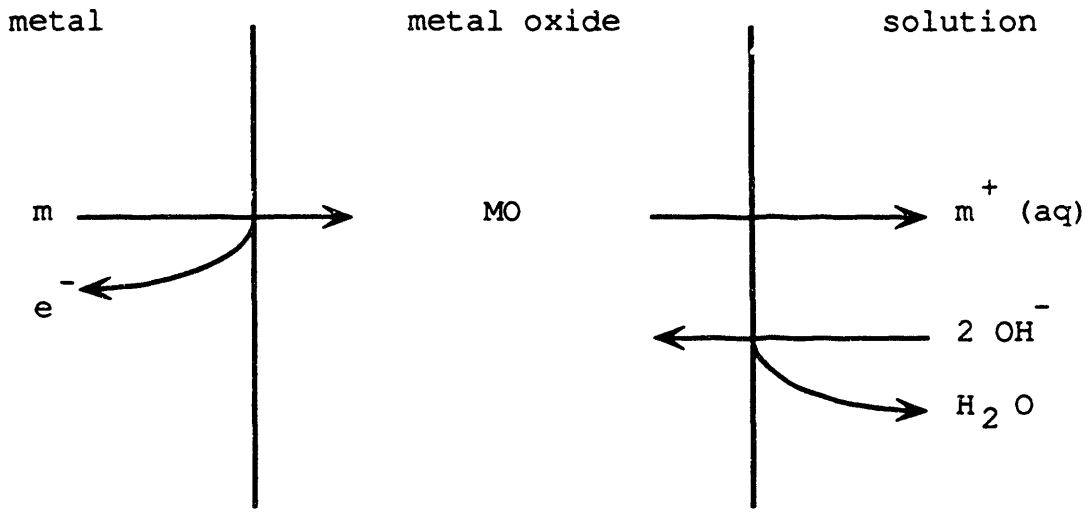

Figure 1. System.

of conduction in oxides can be found in Shewmon[28] and Sørensen.[29]

To simplify the description while still providing a general framework, we shall consider only the following charge carriers: anion and cation vacancies, anion and cation interstitials, and electrons and holes. Again, we assume that the lattice itself has no charge: only the defects possess charge. More specifically, the oxide shall be viewed as an MO background (a schematic of which appears in figure 2), where cations and anions assume their respective lattice sites, are absent from their sites, or take up interstitial locations. Kroger-Vink notation is adopted for distinguishing the species. As Choa *et al.*[4] explain, X_Y denotes an X site occupied by a Y species. Hence, $V_M^{\chi-}$ describes a metal vacancy carrying χ negative charges. Following this criterion, a cation of plus two charge in a cation site, a cation vacancy, and a cation interstitial are denoted as M_M, V_M^{2-}, and I_M^{2+}, respectively. Analogous notation is used for the anionic species. Electrons and holes appear as e^- and h^+, respectively. For our simplified description, this leads to the following types of species:

$$e^- \quad h^+ \quad V_M^{2-} \quad V_O^{2+} \quad I_M^{2+} \quad I_O^{2-} \quad M_M \quad O_O$$

We shall now consider the equations necessary to describe a system consistent with this construct.

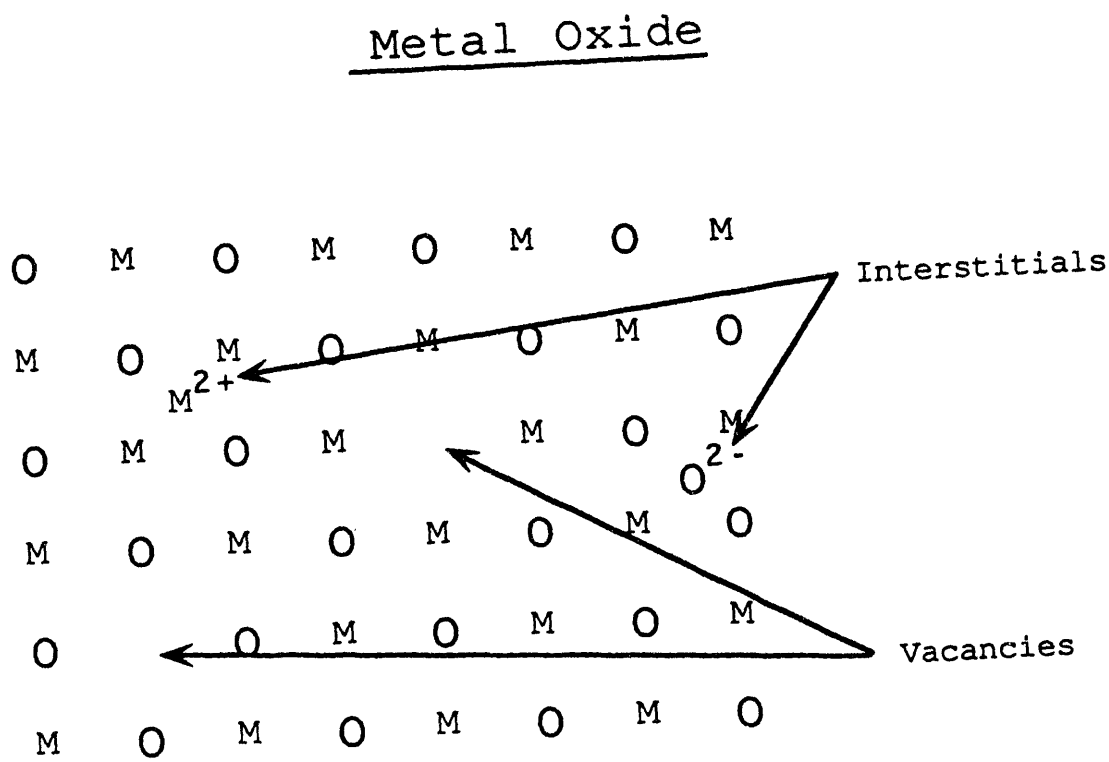

Figure 2. Schematic of an MO oxide.

Equations

Mole Flux Balance.

A mole flux balance for each of the species listed above may be written as

$$\frac{\partial c_k}{\partial t} + \nabla \cdot \mathbf{N}_k = -\sum_{\ell} s_{k,\ell} R_{\ell}$$

and read as the accumulation of a species in a differential volume plus the divergence of its flux through the faces of that volume is equal to its net generation per unit volume. The reaction rate can normally be written as the difference of forward and backward reaction terms which are a function of the activities of the species (see Newman,[30] chapter 23). For example, a reaction that can be described by the mechanism

$$V_O^{2+} + I_O^{2-} \longrightarrow O_O$$

would typically react at a rate

$$R_1 = k_1 c_{V_O^{2+}} c_{I_O^{2-}} - k_{-1},$$

where the activity coefficients of the vacancies and interstitials and the activity of the lattice species are considered constant and are contained in the rate constants, k_1 and k_{-1}. Thermodynamic consistency requires k_1/k_{-1} to be equal to the equilibrium constant, K_1, which is the ratio of the secondary-reference states of the species involved in the reaction. This particular reaction is an example of the formation of a Frenkel defect and may also be a function of the

magnitude of the electric field. (Further discussion is deferred to the **Reactions** section.)

For a dilute species (which excludes M_M and O_O), the flux can be written as the sum of fluxes created by separate driving forces, plus a convective term.

$$N_k = c_k v_k = \text{diffusion} + \text{migration} + \text{convection}$$

The convective term is defined as the concentration of the species times a reference velocity, chosen for convenience.

The diffusion and migration terms can be interpreted as a reaction. For example, the mechanism of the transport of a cation interstitial may be depicted as an interstitial at position α combining with open interstitial site at position δ to form an interstitial at position δ and an interstitial site at position α,

$$(I_M^{2+})^\alpha + I_S^\delta \rightleftarrows I_S^\alpha + (I_M^{2+})^\delta \ .$$

Such a mechanism can be described by an Arrhenius type rate expression (Newman,[31] chapter 23). Assuming constant activity of the interstitial sites, the rate of transport appears as

$$R_{trans} = kc^\alpha_{I_M^{2+}} \exp\left(\frac{z_k F(\Phi^\alpha - \Phi^\delta)}{2RT}\right) - kc^\delta_{I_M^{2+}} \exp\left(\frac{-z_k F(\Phi^\alpha - \Phi^\delta)}{2RT}\right).$$

The difference in the electrochemical potential at α and δ is defined as

$$\mu_k^\alpha - \mu_k^\delta = z_k F \eta_s = z_k F(\Phi^\alpha - \Phi^\delta - V^o),$$

where V^o is the potential difference when the net rate of transport

equals zero. In this case, V^o equals

$$V^o = \frac{RT}{z_k F} \ln\left[\frac{c_k^\delta}{c_k^\alpha}\right].$$

Substitution of these definitions into the rate expression gives the high-field rate expression

$$R_{trans} = 2k(c^\alpha_{I_M^{2+}} c^\delta_{I_M^{2+}})^{1/2} \sinh\left[\frac{\mu^\alpha_{I_M^{2+}} - \mu^\delta_{I_M^{2+}}}{2RT}\right].$$

The difference in the electrochemical potential can be approximated as

$$\frac{\mu_k^\alpha - \mu_k^\delta}{a} = -\nabla\mu_k,$$

where a is some short distance. Substitution of this equation into the rate expression and assuming a small gradient in the electrochemical potential simplifies the rate expression to the linear form used in solution electrochemistry

$$R_{trans} = -\frac{ka}{RT}(c_k^\alpha c_k^\delta)^{1/2} \nabla\mu_k.$$

where ka is thus recognized as the diffusion coefficient, D_k, in dilute solutions (Newman[31], chapter 11). Upon defining an electrochemical activity A_k according to

$$\exp\left[\frac{\mu_k - \mu_k^\theta}{RT}\right] = c_k \exp\left[\frac{z_k F\Phi}{RT}\right] = A_k$$

and substituting into the rate expression, we obtain the simplified expression

$$R_{trans} = \frac{2D_k A_k}{a \exp\left[\frac{z_k F\Phi}{RT}\right]} \sinh\left[-\frac{a\nabla \ln A_k}{2}\right].$$

Finally, combination of the flux terms provides the high-field flux expression

$$N_k = \frac{2D_k A_k}{a \exp\left[\frac{z_k F\Phi}{RT}\right]} \sinh\left[-\frac{a\nabla \ln A_k}{2}\right] + c_k v_{ref}.$$

The mole flux balance equation for the dilute species can now be expressed in terms of the dependent variables: concentration, potential, and reference velocity. Before addressing the potential, we shall first describe the method of handling homogeneous reactions that occur at such rapidity as to be considered at equilibrium.

Summing Equations

In many instances, homogeneous reactions occur at such a fast rate that it is a good approximation to assume that the reaction is at equilibrium. When this is the case, the mole flux equations are combined to eliminate the presumed equilibrium reaction from all but one of the mole balance equations. Then this one equation is replaced with the equilibrium expression,

$$K_\ell = \prod c_k^{-s_{k,\ell}},$$

where $s_{k,\ell}$ are the stoichiometric coefficients of reaction ℓ. We have designed a subroutine called "eqnprod" that sums the mole flux equations in such a way that each reaction, starting with the fastest reaction, is eliminated from every mole balance but one (if the

specified reactions are not independent, multiple reactions may appear in the final form of the combined equations). This translates our set of i mole balance equations to $i-j$ equations of the form

$$-\sum_{l} \nu_{i,l} R_l = \sum_{k} \mu_{i,k} \left(\frac{\partial c_k}{\partial t} + \nabla \cdot \mathrm{N}_k \right),$$

and j equilibrium equations. (ν and μ are combinations of the stoichiometric coefficients derived through the elimination of the equilibrium reactions.) For those mole balance equations containing reactions that are fast but not considered at equilibrium, the equation can be divided through by the backward rate of the fast reaction. The logarithm of this equation appears as

$$\ln K_{l_{max}} + \sum_{k} s_{k,l_{max}} \ln c_k = \ln \left[1 - \frac{\sum_{k} \mu_{i,k} \left(\frac{\partial c_k}{\partial t} + \nabla \cdot \mathrm{N}_k \right) - \sum_{l \neq l_{max}} \nu_{i,l} R_l}{k_{b,l_{max}} \prod c_k^{q_{k,l_{max}}}} \right].$$

The departure from equilibrium now appears as the logarithm of 1 minus a small number.

Poisson's Equation

Many oxide films, especially those that exist as compact crystal structures, possess a small number of defects, suggesting a small number of charge carriers and a large space-charge region. For a thin oxide film, the space-charge layer may extend across a significant portion of the oxide. As Dewald[14] and others have shown, space charge in the oxide can have an appreciable effect on the growth rate of films. We shall therefore incorporate Poisson's equation into our

model development

$$\nabla^2\Phi = -\frac{F}{\epsilon}\sum_k z_k c_k.$$

This electrostatically derived formula is thermodynamically consistent for infinitely dilute solutions.

Because a double layer also exists in the solution phase near the oxide/solution interface, Poisson's equation is also invoked in this phase, replacing the electroneutrality equation,

$$\sum_k z_k c_k = 0,$$

(which is often substituted, as a first approximation, for Poisson's equation in electrolytic solutions).

Velocity

We have yet to develop an expression for the mole flux of M_M or O_O in terms of concentration and potential, nor have we defined the reference velocity. We shall show how these two subjects are interrelated.

The diffusion of anion and cation vacancies occurs through the mechanisms

$$O_O + V_O^{2+} \longrightarrow V_O^{2+} + O_O,$$

and

$$M_M + V_M^{X-} \longrightarrow V_M^{X-} + M_M,$$

respectively. The mechanism for anion transport can be described mathematically as,

$$N_{O_O} - c_{O_O} v_L = -(N_{V_O^{2+}} - c_{V_O^{2+}} v_L).$$

The flux of V_O^{2+} relative to the convective flux is equal and opposite to the flux of O_O relative to its convective flux. An analogous relationship applies to the transport of the cation. Rearrangement of these equations leads to the definition of the lattice velocity

$$v_L = \frac{\sum_i^{O\ \text{sites}} N_k}{cO^o} = \frac{\sum_i^{M\ \text{sites}} N_k}{cM^o} = \frac{\sum_i^{\text{all sites}} N_k}{cMO^o},$$

where c_O^o, c_M^o, and c_{MO}^o are the concentrations of O, M, and MO sites, respectively, and are constants. Summation of the mole flux balance equations over the species occupying O, M, or both sites leads to the single equation

$$\nabla \cdot v_L = 0.$$

This is a continuity equation consistent with the notion that the site density is constant.

In the solution, the equations that describe the velocity are the momentum-balance equations. We would prefer not to solve these equations, and instead enter velocity profiles that have been determined analytically. We shall assume that the oxide is growing on a rotating disk electrode and use the high Sc number approximation to the normal component of the velocity relative to a disk surface with no axial velocity (Newman,[31] chapter 15),

$$v_x = -0.51023\zeta^2\sqrt{\Omega\nu},$$

where ζ equals $x\sqrt{\Omega/\nu}$ and x is the distance normal to the disk

surface.

Summarizing, we have a mole balance for each minor species, Poisson's equation, and a continuity equation for the velocity. This completes the mathematical description of the transport in the bulk of the film. Completion of the problem, however, consists of a description of the boundary conditions.

Boundary Conditions

We shall now discuss the boundary conditions for a multi-phase, one-dimensional problem. For any physically realizable system there exists a certain number of degrees of freedom,

$$f = c + 2 - \pi - r,$$

at equilibrium (c is the number of species, π is the number of phases, and r is the number of independent reactions). Two of these are covered by specifying the temperature and pressure of the system. Since we typically are not at equilibrium, this equation does not necessarily apply; however it does suggest that some of the boundary conditions in one phase can not be arbitrarily set with indifference to the adjoining phases.

One method for setting boundary conditions is to mimic the experimentalist. This procedure usually leads to the correct number of constraints. For example, when a metal surface is placed in a solution with intent to form an oxide, the composition of the solution and either the potential difference across the cell or the total cell current are at the experimentalist's control. The same

conditions are applied here. The number of degrees of freedom suggests that the boundary conditions for the oxide phase, the phase sandwiched between the metal and solution phases, are flux relationships that relate the concentration of the species in the oxide to the concentration of the species just outside the oxide. For those species that do not react at either interface nor homogeneously, there exists an additional degree of freedom. In this instance, only the initial condition is necessary for a transient problem, but for a steady-state problem one should set either the concentration of that species at one of the interfaces or an average concentration of that species. We shall proceed through the boundary conditions from one end of the system to the other for the mole flux balance, Poisson, and continuity equations.

Mole Balance

A mole flux balance equation is written for every solute species in the solution and every minor species in the oxide. This equation is second-order with respect to the concentration and therefore requires a boundary condition involving concentrations at each side of each phase. We shall start with the solution phase and go from right to left as in figure 1 with positive flux going from left to right.

Experimentally, the solution composition is typically set. We too choose to fix the concentrations in this phase. Far from the electrode we assume that the species are at equilibrium and that the fluxes of the species are constant. Combining the mole balance

equations, as was shown above, to eliminate each reaction from all but one equation reveals the number of independent equilibrium reactions and the form of the mole balance equations. If the solvent is a dissociative species, that is, it reduces to one or more minor species, such as

$$H_2O \longrightarrow H^+ + OH^-,$$

then there are two ways of handling the boundary conditions: the total amount of added components is specified and the pH is solved for; or the pH is specified and the amount of added acid or base is solved for. If the pH is specified, the electroneutrality equation is used to determine the amount of base or acid that is required. If the amounts of each species that is added to the solution is known, then the electroneutrality equation may have to be included to determine the amount of H^+ or OH^- present.

We provide a simple example. Ammonium hydroxide is added to 1 N aqueous solution of completely dissociated ferrous sulfate such that the final pH is 10. We assume that the solution consists of the following six solute species,

$$NH_4OH,\ NH_4^+,\ Fe^{2+},\ SO_4^{2-},\ H^+,\ \text{and}\ OH^-.$$

We require six equations. There are two equilibrium equations, one relating NH_4OH, NH_4^+, and OH^-

$$K_{NH_4OH} = \frac{c_{NH_4^+}\, c_{OH^-}}{c_{NH_4OH}},$$

and one relating H^+ and OH^-

$$K_w = c_{H^+} c_{OH^-}$$

(the water equilibrium reaction.) Combining the mole balances to eliminate these reactions from all but two equations leads to the four total mole balances,

$$c_{Fe^{2+}} = c^o_{Fe^{2+}},$$

$$c_{SO_4^{2-}} = c^o_{SO_4^{2-}},$$

$$c_{NH_4OH} + c_{NH_4^+} = c^o_{NH_4OH2} + c^o_{NH_4^+},$$

and

$$c_{NH_4OH} + c_{OH^-} + c_{H^+} = c^o_{NH_4OH} + c^o_{OH^-} + c^o_{H^+}.$$

Since the original amount of ammonium hydroxide added is not known and neither is $c^o_{OH^-}$, we replace the last two equations with

$$-\ln c_{H^+} = pH,$$

and the electroneutrality equation,

$$\sum_k z_k c_k = 0.$$

This gives us our six equations.

We now move to the oxide/solution interface, focusing on the species on the solution side. Since the concentrations of each of these species has been set "far away," and since we intend to set the total potential across the system, we use flux expressions at this interface to relate the concentrations in the adjoining phase (an

alternative would be to use flux expressions for all but one of the species and to set the concentration of that one; this would implicitly determine the total current and preclude setting the total potential). The following general mole balance equation applies for the right side of the interface:

$$\frac{\partial \Gamma_k}{\partial t} + \left(N_k - c_k v_I\right) = \sum_l s_{k,l} R_{A,l},$$

where v_I is the velocity of the interface. In words this equation reads: the accumulation of moles of k at the the solution side of the surface plus the flux of k from the surface relative to the convective flux of k at the surface is equal to the rate of generation of k at the surface. Γ_k is the surface concentration of adsorbed species at the interface and is related to the concentration just outside the interface through the rate expression

$$R = k_f c_k \exp\left[\frac{(1-\beta)nF}{RT}(\Phi^\alpha - \Phi^s)\right] - k_b \Gamma_k \exp\left[-\frac{\beta nF}{RT}(\Phi^\alpha - \Phi^s)\right].$$

If the reaction rate is fast enough to assume equilibrium, the relationship is,

$$\Gamma_k = K_s c_k \exp\left[\frac{nf}{RT}(\Phi^\alpha - \Phi^s)\right],$$

where $K_s = k_f/k_b$ has units of length. The surface reaction, $R_{A,l}$ is written in terms of the potential and concentrations through the Butler-Volmer equation (see Newman,[31] chapter 8, for details)

$$R_{A,l} = k_a \prod_k c_k^{p_{k,l}} \exp\left[\frac{(1-\beta)nF(\Phi^o - \Phi^s)}{RT}\right] - k_c \prod_k c_k^{q_{k,l}} \exp\left[-\frac{\beta nF(\Phi^o - \Phi^s)}{RT}\right].$$

Those interfacial reactions that are so fast as to be considered at equilibrium are replaced by an equilibrium expression, and the rest of the equations are combined to eliminate that reaction from all but one equation.

On the oxide side of the oxide/solution interface (the left side of the oxide/solution interface according to figure 1), the following equation holds for all those species which react,

$$\frac{\partial \Gamma_k}{\partial t} - \left(N_k - c_k v_I\right) = \sum_l s_{k,l} R_{A,l},$$

where Γ_k is the concentration per unit area of adsorbed species on the oxide side (left side) of the interface. For those species which do not react at either interface, heterogeneously or homogeneously, the boundary condition takes on one of the following forms: the concentration of that species at the interface is fixed; the average concentration of the species across the film is fixed,

$$\frac{1}{x_2 - x_1} \int_{x_1}^{x_2} c_k dx = c_{k,avg};$$

or the mole flux balance equation is used and one of the other two options is applied at the metal/oxide interface. If one of the first two options is used here, then the mole flux balance can be applied at the metal/oxide interface.

The boundary conditions of the oxide phase at the metal/oxide interface have implicitly been covered: the same equations developed for the right side of the oxide/solution interface are used here along with the conditions considered above for those species which do

not react.

In the metal phase, we assume that the activities of the metal atoms and electrons are constant.

Potential

Poisson's equation is solved from one end of the system to the other. This second-order equation requires a specification of the potential at some position, the absolute value of which is arbitrary, and is chosen for convenience. For our system, the potential at the end of the solution phase farthest from the oxide is set to zero.

Gauss's law is required at the interfaces. On the solution side of the oxide/solution interface, Gauss's law takes the form

$$\nabla\Phi^s - \frac{\Phi^s - \Phi^o}{\delta_{o/s}} = -\frac{F}{\epsilon_s}\sum_k z_k\Gamma_k.$$

In the oxide, on the left side of the oxide/solution interface, Gauss's law appears as

$$\frac{\Phi^s - \Phi^o}{\delta_{o/s}} - \nabla\Phi^o = -\frac{F}{\epsilon_o}\sum_k z_k\Gamma_k.$$

On the right side of the metal/oxide interface, we apply Gauss's law as on the right side of the oxide/solution interface, and, finally, on the metal side we specify the potential, V.

At one of the interfaces we are required either to fix the potential or set the current. During a potentiostatic experiment, the potential of the metal relative to a reference electrode in the solution is fixed. We too set the potential of the metal for simu-

lating a potentiostatic experiment. To simulate a galvanostatic experiment, either the current is set and the potential is determined from the equation

$$i = F \sum_k z_k(N_k - c_k v_I) = -F \sum_k z_k \left(\frac{\partial \Gamma_k}{\partial t} + \sum_l s_{k,l} R_{A,l} \right)$$

or the potential is set and iterated upon until the desired current density is obtained.

Velocity

The equation for the velocity of the lattice was derived by summing the mole flux equations of the species occupying lattice sites. The boundary condition is analogously developed. Depending on whether the mole flux balance equations are on the right side or the left side of the interface, summation gives

$$v_L - v_I = \pm \frac{\sum_k \sum_\ell^{\text{all sites}} s_{k,\ell} R_\ell}{c^o_{MO}}$$

(the plus sign applies to the right side of the interface). The right side of the above equation can also be written as

$$\frac{\sum_l R_l \sum_k^{\text{all sites}} s_{k,l}}{c^o_{MO}}.$$

This indicates that film growth is realized only at interfaces where the sum of the stoichiometric coefficients of species occupying lattice sites is not equal to zero.

Velocity is a relative quantity, which allows us to set its value arbitrarily at any position. In other words, we can set the velocity of any one interface or set v_L (since $\nabla \cdot \mathbf{v}_L = 0$) to a convenient constant. We set the velocity of the metal/oxide interface to zero.

At the metal/oxide interface, where the velocity of the interface is set to zero, the above equation yields the lattice velocity, v_L. At the oxide/solution interface it yields the velocity of the interface, since v_L is known by integration of the continuity equation across the oxide. This v_I can then be added directly to the velocity distribution specified in the solution phase (as shown by Acrivos[31]).

Initial Conditions

In a transient case, an initial concentration of each species is required. One way to proceed is to set the potential of the metal to the value where the film, metal, and solution exist in mutual equilibrium. (If no such potential exists, an alternative would be to solve for a quasi-steady state at a given potential.) The steady-state concentration and potential distributions are solved for at this potential. The potential is stepped to a new value, and growth of the film is followed from this initial condition. To march through time, one can either use a Crank-Nicholson time stepping algorithm or assume quasi-steady state. The first method is a better approximation, especially for rapid film growth.

Reactions

Electric Fields on Homogeneous Reactions

As we have mentioned, the gradient of the potential may enhance the forward or backward rate of certain homogeneous reactions. Why does this appear in oxides, and not in aqueous solutions? Because in oxides we are speaking of the formation or depletion of vacancies and interstitials in a lattice structure: a structure where the molecules maintain some fixed position, Thus the occupied sites and interstitials are distinguishable. A similar means of transport in a solution is described by the high-field equation.

A typical homogeneous reaction which is susceptible to influence by the electric field is the formation of Frenkel defects. This, again, is defined as interstitial species created by ions leaving the ionic sites. Oxides consist of some equilibrium concentration of interstitials and vacancies related through the relations,

$$K_O = \frac{a_{O_O}}{a_{I_O^{2-}} a_{V_O^{2+}}}$$

and

$$K_M = \frac{a_{M_M}}{a_{I_M^{2+}} a_{V_M^{2-}}}.$$

In a nonequilibrium situation, there is reason to believe that these relationships should be independent of the potential distribution. However, if there is an alignment of the product species with the

gradient of the potential there does exist a potential dependence. Following the procedures of chapter 23 of Newman[31], we write the reaction

$$I_O^{2-} + V_O^{2+} \longrightarrow O_O$$

in two ways:

$$1. \quad (I_O^{2-})^{\delta} + (V_O^{2+})^{\alpha} \longrightarrow O_O^{\alpha},$$

and

$$2. \quad (I_O^{2-})^{\alpha} + (V_O^{2+})^{\delta} \longrightarrow O_O^{\delta},$$

where α is at one position and δ is at another position to the right. The rate of the first reaction is

$$R_1 = k_{f,1}\, c^{\delta}_{I_O^{2-}} c^{\alpha}_{V_O^{2+}} \exp\left[\frac{(1-\beta)nF}{RT}(\Phi^{\alpha}-\Phi^{\delta})\right] - k_{b,1}\, c^{\alpha}_{O_O} \exp\left[-\frac{\beta nF}{RT}(\Phi^{\alpha}-\Phi^{\delta})\right]$$

and the rate of the second reaction is

$$R_2 = k_{f,2}\, c^{\alpha}_{I_O^{2-}} c^{\delta}_{V_O^{2+}} \exp\left[\frac{-(1-\beta)nF}{RT}(\Phi^{\alpha}-\Phi^{\delta})\right] - k_{b,1}\, c^{\delta}_{O_O} \exp\left[\frac{\beta nF}{RT}(\Phi^{\alpha}-\Phi^{\delta})\right]$$

The activity coefficients of the minor species and the activity of O_O are considered constant. The summation of the two rates gives the overall rate of reaction. Substituting in the relationships

$$c_k^{\alpha} = c_k^{\delta} = c_k\ , \quad k_{f,1} = k_{f,2} = k_{f,s}\ , \quad k_{b,1} = k_{b,2} = k_{b,s}\ , \quad R_s = \tfrac{1}{2}(R_1 + R_2)\ ,$$

$$\text{and} \quad -a\nabla\Phi = \Phi^{\alpha} - \Phi^{\delta}$$

gives the overall rate of reaction

$$R_s = k_{f,s}\, c_{I_O^{2-}} c_{V_O^{2+}} \cosh\left[\frac{(1-\beta)naF}{RT}\nabla\Phi\right] - k_{b,s}\, c_{O_O} \cosh\left[\frac{\beta naF}{RT}\nabla\Phi\right].$$

At steady-state, $R_s = 0$ and the rate equation gives

$$\frac{\cosh\left[\frac{(1-\beta)naF}{RT}\nabla\Phi\right]}{\cosh\left[\frac{\beta naF}{RT}\nabla\Phi\right]} = \frac{1}{K_s c_{I_{O_{2-}}} c_{V_O^{2+}}}.$$

This equation shows that the product of the concentration of species in a system at steady-state in the presence of an applied field is greater than or equal to the equilibrium constant. Further ramifications of this result are left to the reader.

Thermodynamic Consistency of Heterogeneous Reactions

Values from thermodynamic tables indicate the potential and pH at which a metal, in contact with an aqueous solution, will coexist simultaneously as a metal, metal oxide, and aqueous metal ions. For the system we are considering, a compact oxide covers the entire metal surface, and although the oxide is in contact with the other two phases, the other two phases are not in contact with each other. Nevertheless, if the system is at equilibrium, the same potential should be read as when there is mutual contact. This potential is, however, distributed over two interfaces, and we shall now give an example of how thermodynamic consistency is assured.

The standard-state potential *versus* the standard hydrogen reference electrode, SHE, of the reaction

$$Hg + 2\,OH^- \rightleftarrows HgO + H_2O + 2\,e^-,$$

is

$$U = 0.926 - 0.0591\,pH$$

for red oxide. We shall exclude the possibility of a predominance of interstitials, vacancies, electrons, and holes in the oxide, and submit that the aqueous solution is at a certain pH and contains a non-obtrusive supporting electrolyte. The following reactions are considered:

at the metal/oxide interface,

$$1.)\quad Hg \rightleftarrows Hg_{Hg} + V_O^{\cdot\cdot} + 2e^-$$

and

$$2.)\quad Hg + V_{Hg}'' \rightleftarrows Hg_{Hg} + 2e^-;$$

at the oxide/solution interface,

$$3.)\quad 2OH^- + V_O^{\cdot\cdot} \rightleftarrows O_O + H_2O,$$

and

$$4.)\quad 2OH^- \rightleftarrows O_O + V_{Hg}'' + H_2O.$$

The individual reaction rates take the form

$$R_1 = k_1 \prod c_k^{p_{k,1}} \exp\left[\frac{(1-\beta)nF(\Phi^\alpha - \Phi^\delta)}{RT}\right] - k_{-1} \prod c_k^{q_{k,1}} \exp\left[-\frac{\beta nF(\Phi^\alpha - \Phi^\delta)}{RT}\right]$$

At equilibrium, the forward rate is equal to the backward rate; rearrangement gives

$$\frac{nF}{RT}(\Phi^\alpha - \Phi^\delta) = \ln\frac{k_{-1}}{k_1} + \sum_k s_{k,1} \ln c_k.$$

Summing reactions 1 and 3 and 2 and 4 to eliminate the vacancies leads to the overall reaction listed at the start. For a film at equilibrium, thermodynamic consistency requires

$$\Phi^m - \Phi^o + \Phi^o - \Phi^s = U = U^\theta - 0.0591\,pH$$

$$= \frac{RT}{2F}\ln\frac{k_{-1}k_{-3}}{k_1k_3} - \frac{RT}{F}\ln c_{OH^-} = \frac{RT}{2F}\ln\frac{k_{-2}k_{-4}}{k_2k_4K_w^2} - \frac{RT}{F}pH.$$

where U^θ is equal to 0.926 for Hg/HgO and 2.303 RT/F equals 0.0591 at 25 ° C. More simply,

$$K_1K_3K_w^n = K_2K_4K_w^n = \exp\left(\frac{nF}{RT}U^\theta\right).$$

Knowledge of the equilibrium concentrations of the defects in the oxide and of the cavity potentials across the interfaces provides a quantitative assessment of the individual K's. The corresponding K at the other interface is set such that the total potential drop is consistent with the overall standard-state potential drop and the local interfacial concentrations at that interface.

Solving Computationally

The equations above are linearized and differentiated with Newman's Autoband subroutine (Newman[31], Appendix C). They are then solved simultaneously with Newman's Band subroutine. However, before the equations are entered, a coordinate transformation is performed.

Coordinate Transformation

To avoid extrapolation or interpolation of the concentration and potential profiles as the oxide grows or shrinks, we shall invoke a coordinate transformation. This transformation, used in each phase, is applied before assuming a quasi-steady-state condition.

$$x,\ t \longrightarrow y,\ t,$$

where

$$y = \frac{x - x'}{x'' - x'} + m' - m_o.$$

x' is the position of the interface to the left of x. x'' is the position of the interface to the right of x. m' is the mth interface from the left end of the system and is the interface to the left of x. m_o is the mth interface from the left where y is set to zero.

Equations in Finite Difference

The equations are solved using finite differences. A giant 3-width banded matrix is created of nxn matrices, where n is equal to the total number of species in each phase, plus the number of phases where the potential is solved for, plus the number of phases where the velocity is solved for. These equations a. linearized and then solved simultaneously using Newman's[31] Autoband, Band, and Matinv subroutines. Iteration is required because the equations are non-linear. The giant matrix maintains a width of three through the bulk and interfaces by following the work of Russell.[32] Here, as there, the equations are applied over a mesh spacing that is half a space wide on either side of each node. After the coordinate transformation, the mole flux balance takes the form,

$$\frac{\partial c_k}{\partial t} - \frac{(y - m' + m_o)(v_I'' - v_I') + v_I'}{L'}\frac{\partial c_k}{\partial y}$$

$$+ \frac{1}{L'}\frac{\partial N_k}{\partial y} = \sum_l s_{k,l} R_l$$

which in finite difference form appears as

$$\frac{\partial c_k(J)}{\partial t} - \frac{(J/NJ(m))(v_I'' - v_I') + v_I'}{L'} \frac{c_k(J+1) - c_k(J-1)}{2h}$$

$$+ \frac{1}{L'} \frac{N_k(J+\frac{1}{2}) - N_k(J-\frac{1}{2})}{h} = \sum_l s_{k,l} R_l .$$

The flux expression is written in terms of concentrations, potentials, and velocities (as described earlier), and put into finite difference form. To handle the time derivative, the equation can then be put into a Crank-Nicholson form, or the time derivative can be dropped (the quasi steady-state approximation alluded to earlier).

This analysis applies through the interfaces with the half mesh points that surround each interface. Poisson's equation and the continuity equation are handled likewise.

This concludes the general formalism for describing oxide film growth. We shall now apply this methodology to the specific system of iron/iron oxide in a basic solution.

The Iron/Iron Oxide System

The iron/iron oxide system has received a considerable amount of attention, dating back over 100 years. Vetter, Bonhoeffer, Weil, Franck, and Sato are just a few of the researchers who have performed numerous studies to try to elucidate the mechanism of its passivation. However, the system remains poorly understood. More recent research is centered on determining the structure of the oxide with spectroscopic techniques.[33,34,35,36]

Vetter[3] provides an excellent review of much of the early work. In the rest of this chapter we shall outline the information provided

in his investigation. We shall then provide a physical model that is consistent with those findings and with the defect model proposed by Wagner.[37] Finally, we shall compare results from our computer simulations with the experimental data provided by Jovancicevic *et al.*[38] and Lukac *et al.*[25]

Summary of Earlier Work as Provided by Vetter

The Flade potential (an experimentally measured, typically nonequilibrium, potential that marks the onset of passivation) of iron is approximately 200 mV more positive than the potential at which the oxide Fe_3O_4 is stable in a basic solution at pH = 8.4.[39] Vetter argues that the passive film is made up of a conductive layer of Fe_3O_4 that faces the metal and a nonconducting layer of Fe_2O_3 that faces the electrolyte. As the potential of the metal in contact with the solution (no oxide present) is increased, the metal preferentially dissolves as a ferrous species. The electronically conducting Fe_3O_4 oxide, the first thermodynamically stable oxide (-600 mV *versus* the NHE), does not appear due to its rapid rate of dissolution. As the potential is further increased, the Fe_3O_4 is oxidized to Fe_2O_3. This oxide is a poor conductor and features slow dissolution kinetics. Its presence leads to passivation. The Flade potential thus falls between the potentials defined by the overall reactions[37]

$$3\,Fe + 8\,OH^- \rightleftarrows Fe_3O_4 + 4\,H_2O + 8\,e^-,$$

and

$$2\,Fe_3O_4 + 2\,OH^- \rightleftarrows 3\,Fe_2O_3 + H_2O + 2\,e^-.$$

The second reaction is approximately 200 mV more positive than the first.

Another thought provided on the 200 mV discrepancy is that Fe_3O_4 and Fe_2O_3 form mixed phases with each other. ("γ-Fe_2O_3 lacks each ninth Fe ion compared to Fe_3O_4. The O^{2-} ions have the same crystal lattice."[3]) If Fe_3O_4 is preferentially formed near the metal and Fe_2O_3 near the electrolyte, a concentration gradient of iron ions and electrons must exist. A concentration gradient of iron ions is attended by a diffusion potential variation across the oxide. It is this potential variation that constitutes the difference between the predicted thermodynamic formation of oxide and the experimentally measured onset of passivation.

Vetter further notes that thin steady-state films (< 100 nm) form on metals when dissolution occurs simultaneously with film formation. His investigation revealed that the films on iron are between 2 and 10 nm and that 100 ±2 % of the dissolution results as $Fe^{3+}(aq)$.

Model

Starting with the assumption that Fe_3O_4 and Fe_2O_3 maintain the same lattice structure but differ by the presence of either cation or anion interstitials or cation or anion vacancies leads to the four possible descriptions of the oxide presented in figure 3. a. and b. are schematics of Fe ions in a fixed lattice of 12 O ions. c. and d.

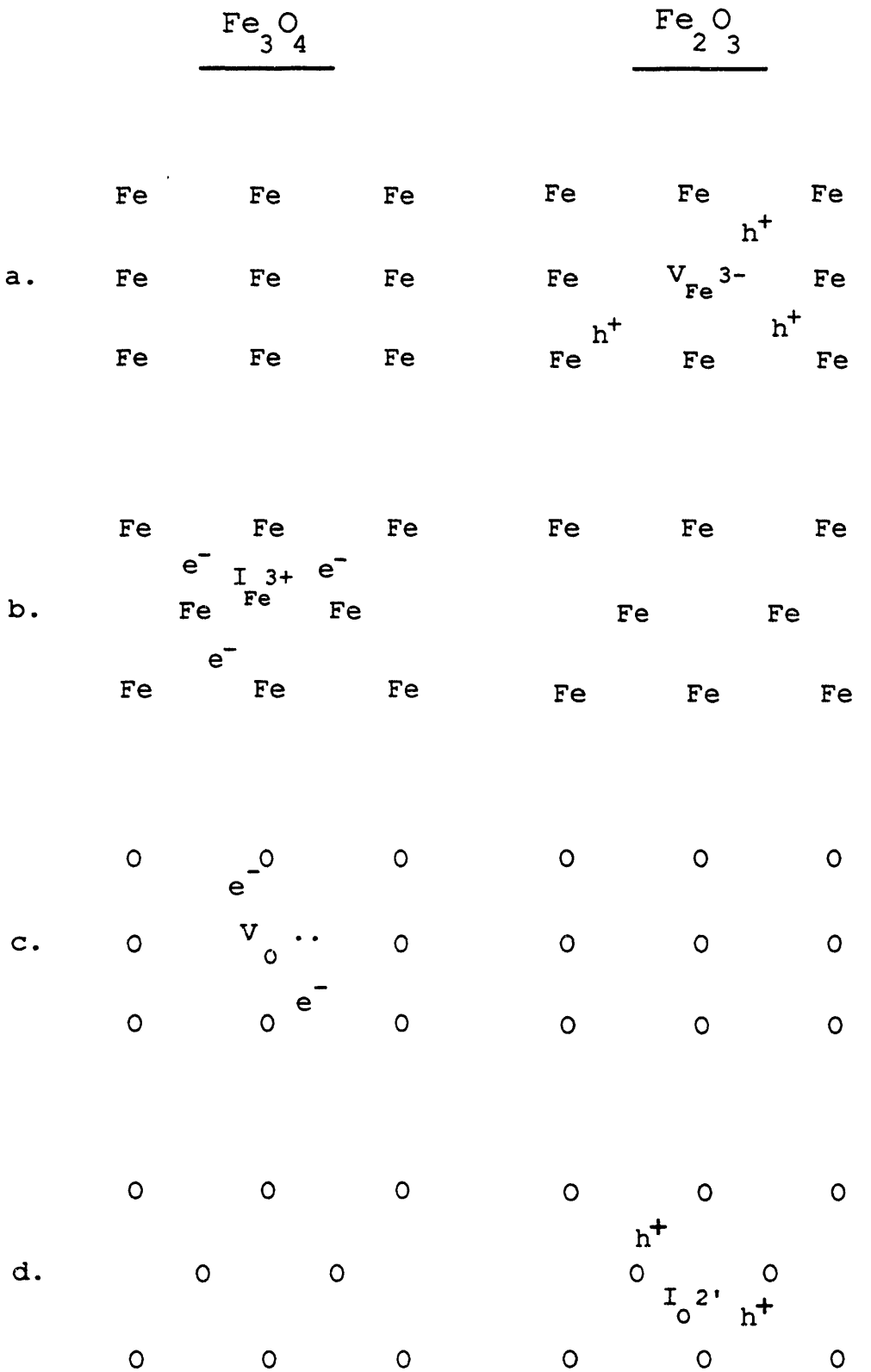

Figure 3. Schematic configurations of iron oxide.

$$2\,Fe_3O_4 + 2\,OH^- \rightleftarrows 3\,Fe_2O_3 + H_2O + 2\,e^-.$$

The second reaction is approximately 200 mV more positive than the first.

Another thought provided on the 200 mV discrepancy is that Fe_3O_4 and Fe_2O_3 form mixed phases with each other. ("γ-Fe_2O_3 lacks each ninth Fe ion compared to Fe_3O_4. The O^{2-} ions have the same crystal lattice."[3]) If Fe_3O_4 is preferentially formed near the metal and Fe_2O_3 near the electrolyte, a concentration gradient of iron ions and electrons must exist. A concentration gradient of iron ions is attended by a diffusion potential variation across the oxide. It is this potential variation that constitutes the difference between the predicted thermodynamic formation of oxide and the experimentally measured onset of passivation.

Vetter further notes that thin steady-state films (< 100 nm) form on metals when diss. .ution occurs simultaneously with film formation. His investigation revealed that the films on iron are between 2 and 10 nm and that 100 ±2 % of the dissolution results as $Fe^{3+}(aq)$.

Model

Starting with the assumption that Fe_3O_4 and Fe_2O_3 maintain the same lattice structure but differ by the presence of either cation or anion interstitials or cation or anion vacancies leads to the four possible descriptions of the oxide presented in figure 3. a. and b. are schematics of Fe ions in a fixed lattice of 12 O ions. c. and d.

are schematics of O ions in a fixed lattice of 6 Fe ions. Because the Fe_3O_4 is considered the more conductive phase, a. and d. are eliminated as possible choices: these models lack mobile species in the Fe_3O_4 phase. X-ray diffraction experiments indicate that the oxygen lattice is fixed and that the Fe_2O_3 structure appears to be missing every ninth iron ion compared with the Fe_3O_4 structure, and work by Franck *et al.*[40] indicates that cation migration is the predominate mode of ionic transfer in the oxide. Thus, b. is chosen as the best description of the oxide. In words, we are assuming that the oxide takes on the structural form of Fe_2O_3 and contains mobile Fe^{3+} interstitials and electrons.

The following reactions are used to describe the interactions of the oxide with the adjoining metal and electrolyte phases. This is in agreement with the above model description and the information provided by Vetter.

At the metal/oxide interface:

$$1.) \qquad Fe(m) \rightleftarrows I_{Fe}^{3+} + 3\,e^-(m).$$

$$2.) \qquad e^-(ox) \rightleftarrows e^-(m);$$

At the oxide/solution interface:

$$3.) \qquad 2\,I_{Fe}^{3+} + 6\,OH^-(aq) \rightleftarrows 2\,Fe_{Fe} + 3\,O_O + 3\,H_2O;$$

$$4.) \qquad I_{Fe}^{3+} + 2\,OH^- \rightleftarrows Fe(OH)_2^+(aq.);$$

$$5.) \qquad I_{Fe}^{3+} + e^-(ox) \rightleftarrows Fe^{2+}(aq.);$$

The reactions are considered to be the elementary reactions with rates of the form:

$$R_1 = k_1 \exp\left[\frac{(1-\beta)3F}{RT}(\Phi^m - \Phi^o)\right] - k_{-1} c_{I^{3+}_{Fe}} \exp\left[-\frac{\beta 3F}{RT}(\Phi^m - \Phi^o)\right]$$

$$R_2 = k_2 c_{e^-} \exp\left[\frac{(1-\beta)F}{RT}(\Phi^m - \Phi^o)\right] - k_{-2} \exp\left[-\frac{\beta F}{RT}(\Phi^m - \Phi^o)\right]$$

$$R_3 = k_3 c^{1/3}_{I^{3+}_{Fe}} c_{OH^-} \exp\left[\frac{(1-\beta)F}{RT}(\Phi^o - \Phi^s)\right] - k_{-3} \exp\left[-\frac{\beta F}{RT}(\Phi^o - \Phi^s)\right]$$

$$R_4 = k_4 c_{I^{3+}_{Fe}} c^2_{OH^-} \exp\left[\frac{(1-\beta)3F}{RT}(\Phi^o - \Phi^s)\right] - k_{-4} c_{Fe(OH)^+_2} \exp\left[-\frac{\beta 3F}{RT}(\Phi^o - \Phi^s)\right]$$

$$R_5 = k_5 c_{I^{3+}_{Fe}} c_{e^-} \exp\left[\frac{(1-\beta)2F}{RT}(\Phi^o - \Phi^s)\right] - k_{-5} c_{Fe^{2+}} \exp\left[-\frac{\beta 2F}{RT}(\Phi^o - \Phi^s)\right]$$

Equilibrium requires:

1.) $$\frac{c_{I^{3+}_{Fe}}}{K_1} = \exp\left[\frac{3F}{RT}(\Phi^m - \Phi^o)\right]$$

2.) $$\frac{1}{K_2 c_{e^-}} = \exp\left[\frac{F}{RT}(\Phi^m - \Phi^o)\right]$$

3.) $$\frac{1}{K_3 c^{1/3}_{I^{3+}_{Fe}} c_{OH^-}} = \exp\left[\frac{F}{RT}(\Phi^o - \Phi^s)\right]$$

4.) $$\frac{c_{Fe(OH)^+_2}}{K_4 c_{I^{3+}_{Fe}} c^2_{OH^-}} = \exp\left[\frac{3F}{RT}(\Phi^o - \Phi^s)\right]$$

and

$$5.)\qquad \frac{c_{Fe^{2+}}}{K_5 c_{I_{Fe}^{3+}} c_{e^-}} = \exp\left[\frac{2F}{RT}(\Phi^o - \Phi^s)\right]$$

Combinations of these reactions lead to the overall reactions:

$$\frac{3}{4}Fe(m) + 2\,OH^- \longrightarrow \frac{2}{3}Fe_{Fe} + O_O + \frac{1}{12}I_{Fe}^{3+} + \frac{1}{4}e^-(ox) + H_2O + 2\,e^-(m);$$

$$Fe(m) + 2\,OH^- \longrightarrow Fe(OH)_2^+(aq) + 3\,e^-(m);$$

and

$$Fe(m) \longrightarrow Fe^{2+}(aq) + 2\,e^-(m).$$

It is these overall reactions for which thermodynamic constants can be found in the literature.

We shall now present the system parameters: how they were chosen or determined.

System Parameters

Table 1 provides a list of the mobile species and properties of the phases.[29,41] The electronic conductivity of Fe_3O_4 is high; therefore, an arbitrarily high diffusion coefficient for the electrons is chosen (100 cm^2/s, the same order of magnitude as found in some semiconductors). In the aqueous phase, we could not find the diffusion coefficient for the two boric species or the ferric species; however, since the current density through passive films is low ($\approx$ 5 $\mu A/cm^2$) and limited by transport of ions in the film, an estimate in the solution phase should be sufficient. The diffusion coefficient of interstitials for an oxide is typically small and in

Table 1		
Phase 1: γ-Fe_2O_3		
density (g/cm^3)	mol. wt. (g/mol)	dielectric coeff.
5.24	55.847	9.
Mobile Species	Conc. (M)	Diff. coeff. (cm^2/s)
IFe^{3+}	8.2	$2.\times10^{-16}$
e^-	24.6	$1.\times10^{2}$
Phase 2: H_2O		
density (g/cm^3)	mol. wt. (g/mol)	dielectric coeff.
1.	18.0	78.
Mobile Species	Conc. (M)	Diff. coeff. (cm^2/s)
Na^+	0.20	1.334×10^{-5}
Fe^{2+}	3.9×10^{-6}	0.72×10^{-5}
$Fe(OH)_2^+$	1.3×10^{-18}	$1.\times10^{-5}$
$B_4O_7^{2-}$	0.0500039	$1.\times10^{-5}$
$HB_4O_7^-$	0.1	$1.\times10^{-5}$

this model is the mass-transfer limitation to oxide growth. Thus, the current density is limited by the rate of transport of interstitials and is directly related to the diffusion coefficient of the iron interstitials. As we shall demonstrate, this value is on the order of 10^{-16} cm^2/s.

Although the equilibrium constants of the overall reactions can be found in the literature,[37] the values of equilibrium constants for each reaction at each interface remain to be determined.

As demonstrated earlier, the equilibrium constants of the individual reactions must be consistent with the equilibrium constants of the overall reactions. The three overall reactions can be in equilibrium simultaneously if we set the Fe^{2+} concentration at 3.9×10^{-6} M, the $Fe(OH)_2^+$ concentration to 1.3×10^{-18} M, the pH to 8.4 and the potential *versus* a hydrogen reference electrode in the same solution to −103 mV (-600 mV *versus* the NHE). How does the potential vary from the metal to the reference electrode to account for this 103 mV? This is an important question because we are solving Poisson's equation throughout the system and Gauss's law at the interfaces simultaneously with equilibrium relationships. Thus, knowledge of the exact potential distribution across all phases is critical. This variation in potential is an equilibrium situation and is not the result of a passage of current as is the potential gradient associated with ohmic effects.

We shall now demonstrate how the potential varies from the metal to the reference electrode using our best judgement and the little data we have. We expect a potential drop between the reference electrode and the solution phase. Since we are not interested in the physics in this region, we simply require an estimate of its value to subtract from the total of −103 mV. From potential-of-zero-charge data of the hydrogen/mercury reference electrode, it is estimated that the potential difference between the electrode and the solution is -248.2 mV. Adding this potential to the potential difference from the metal to the reference electrode gives a potential difference

from the metal to solution of −351.2 mV. This potential difference can occur as a drop across the metal/oxide interface, a drop across the double layers of the oxide at both interfaces, a further drop across the oxide/solution interface, and one last drop through the solution double layer to the bulk of the solution.

The iron phase adjacent to the oxide can be thought to consist of iron ions and electrons. Since these two species are the only mobile species in both the oxide and metal phases, we shall assume that the equilibrium potential drop across this interface is zero.[42] We are left with distributing the −351.2 mV between the oxide and the solution. We do not have information on the absorption equilibrium constants of the electrons, interstitials, sodium ions, ferrous ions, *etc.* at the oxide/solution interface; therefore, we shall assume that there is no specific absorption of any of the species on either side of this interface. We shall also assume that the interfacial region has a finite thickness of 0.35 nm and a dielectric constant that is equal to the average of the dielectric constant of the two adjacent bulk phases. With the absence of absorbed species, Gauss's law is reduced to a form that states that the gradient of the potential times the dielectric constant in the oxide just outside of the interfacial region is equal to the gradient of the potential times the dielectric constant through the interfacial region, which is also equal to the gradient of the potential times the dielectric constant in the solution double layer. Even though we do not account for specific adsorption, an equal and opposite amount of diffuse charge

accumulates on each side of the interface to account for the potential variation and satisfy Poisson's equation.

To arrive at a first approximation of the potential and concentration distributions, which will lead to a reasonable guess of the equilibrium constants at the interface, the following iterative procedure is followed. The net accumulation of charge near an interface is related to the potential distribution near the interface by the equation[29]

$$q = \pm 2RT\epsilon \sum_k c_{k,\infty}\left[\exp\frac{z_k F(\Phi_2 - \Phi_1)}{RT} - 1\right]^{1/2},$$

where Φ_2 is the potential at the interface and Φ_1 is the potential far away in the bulk. The potential difference across the 0.35 nm interfacial region is related to the charge by the equation

$$\frac{\Phi_3 - \Phi_2}{0.35\ \text{nm}} = \frac{q}{\epsilon_{avg}}.$$

Thus, we pick a value for the charge, q, determine the potential drops across the oxide, interface, and solution regions, sum them to see if the total is equal to the total potential drop that is required (−351.2 V), and then pick another q until the difference is satisfactory. Once the proper q is found, we determine the concentrations at the interfaces through the equation[29]

$$c_k = c_{k,\infty}\exp\left[\frac{F}{RT}(\Phi_2 - \Phi_1)\right].$$

This calculation gives us an initial guess at the potentials and concentrations at near the interfaces, and thus an initial guess in a computer program.

The equilibrium constants of the five reactions must be consistant with the equilibrium constants of the three overall reactions. This leaves us with two degrees of freedom. The assumption that the equilibrium potential potential drop across the metal/oxide interface is zero eliminates one degree of freedom, and the assumption that the concentration of iron interstitials is equal to the bulk concentration of iron intrestitials required to make the Fe_2O_3 lattice structure into Fe_3O_4 (which is 8.2 M) eliminates the second degree of freedom. These values are substituted into the first equilibrium relation to obtain K_1. The concentration of electrons is related to the concentration of interstitials through electroneutrality, thus, K_2 is determinable. Substituting into the lastthree equilibrium relations the bulk concentrations and potentials provides the remaining three equilibrium constants. The equilibrium constants of reactions 1, 2, 3, 4, and 5 are accordingly

$$K_1 = 0.04065 \text{ l/mol}, \quad K_2 = 8.2 \text{ mol/l}, \quad K_3 = 8.57272 \times 10^5 \text{ (l/mol)}^{1/3},$$

$$K_4 = 4.07739\times10^{-1} \text{ l/mol}, \quad \text{and } K_5 = 1.44466\times10^4 \text{ l/mol}.$$

We shall now present the results of our simulations and discuss the attributes and inadequacies of the model as compared to experimental findings.

Results and Discussion

The growth of an oxide on iron in a basic medium of boric acid and sodium borate, pH of 8.4 is predicted by computer simulation.

Generated curves are compared to experimental data. It is not our intention to present a parametric study of the diffusion coefficients and the rates of the interfacial reactions. For this reason we shall present only our best fits to the experimental data and simply describe the results of varying certain parameters. For easy comparison to experimental data, our simulations are corrected by 248.8 mV such that the potential of the metal is consistent with the potential one would read *versus* the NHE.

Equilibrium

The first result is the potential distribution for the equilibrium conditions. The system consists of a 0.1 nm thick oxide sandwiched between an iron surface on the left and a borate buffer solution to the right. The metal phase is set to the equilibrium potential of −600 mV (with the correction as discussed above) *versus* the potential of the solution of −248.8 mV at a point just outside the mass-transfer boundary layer, 12.6 μm thick. The potential distribution across the oxide and solution phases is plotted against the position from the metal surface divided by the width of the particular phase, figure 4. The potential varies by approximately 47 mV in the double layer of the oxide at the oxide solution/interface and varies by approximately 104 mV through the double layer of the solution phase near this same interface. The rest of the 351 mV is across the oxide/solution interface.

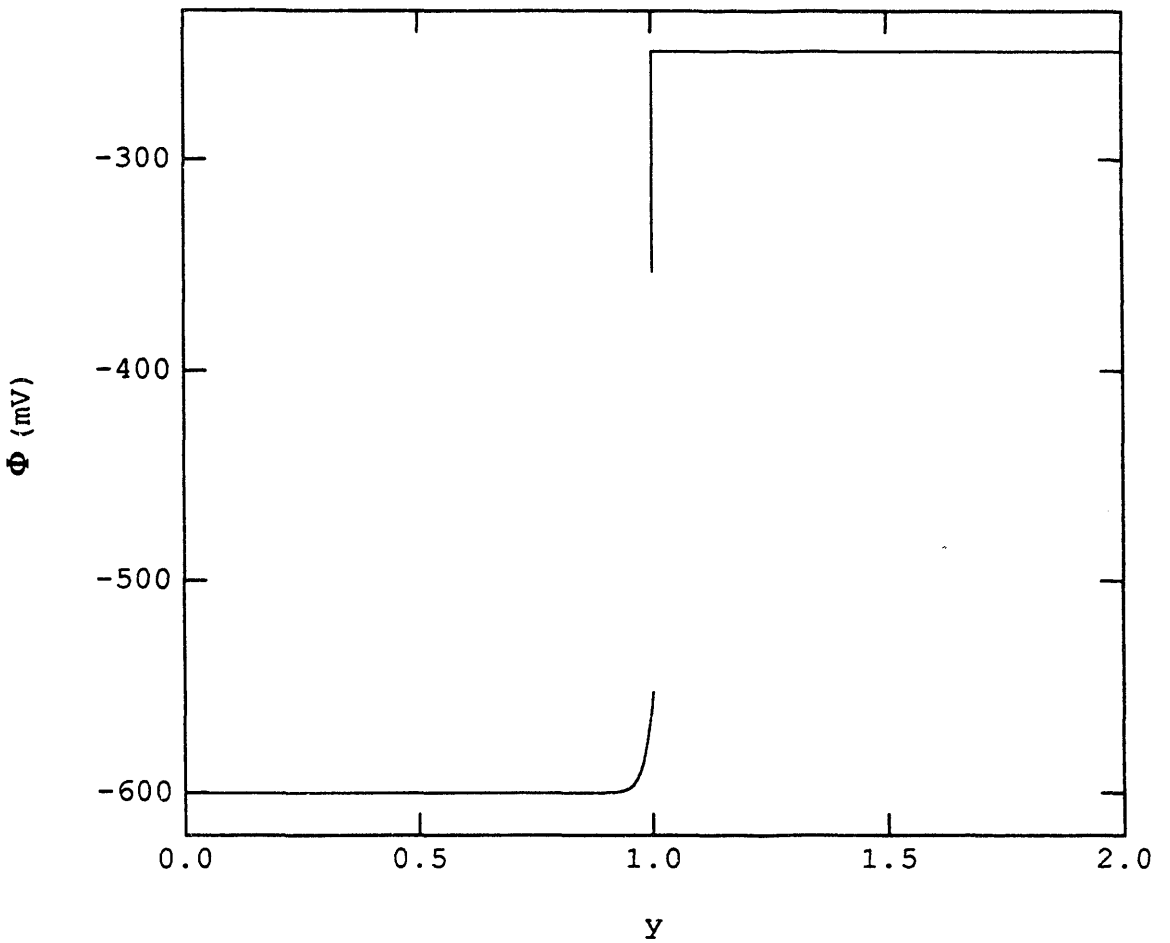

Figure 4. Potential distribution across the oxide and solution phases at the equilibrium potential, V = -600 mV *vs*. the NHE.

The potential distribution in the solution appears to drop straight down at the interface. This is an illusion created by the thinness of the solution double layer (0.61 nm) compared to the width of the mass-transfer layer (12.6 μm). The potential distribution in the oxide also reveals the thinness of the oxide double layer: about 0.015 nm. This is considered small for most oxide semiconductors but agrees with the notion of Wagner[35] for this oxide. The corresponding concentration profiles of the electrons and interstitials in the oxide are provided in figure 5. The concentration of the electrons increases by a factor of 10 near the interface, and the concentration of the interstitials drops by nearly two orders of magnitude. This is a function of the potential dependence of the concentrations as given above. Figure 6 provides the concentration and potential profiles in the solution phase *versus* the dimensionless coordinate y. This blown up view shows the curvature of the potential through the double layer near the interface and the corresponding concentration profiles. The concentrations in this region similarly obey the potential dependence given above.

the next results describe the growth of the oxide during a positive sweep of the potential.

Comparison with Experimental Data

In this part of our investigation, we introduce curves of current and length *versus* potential. The curves presented are those that best fit the experimental data in the literature with emphasis

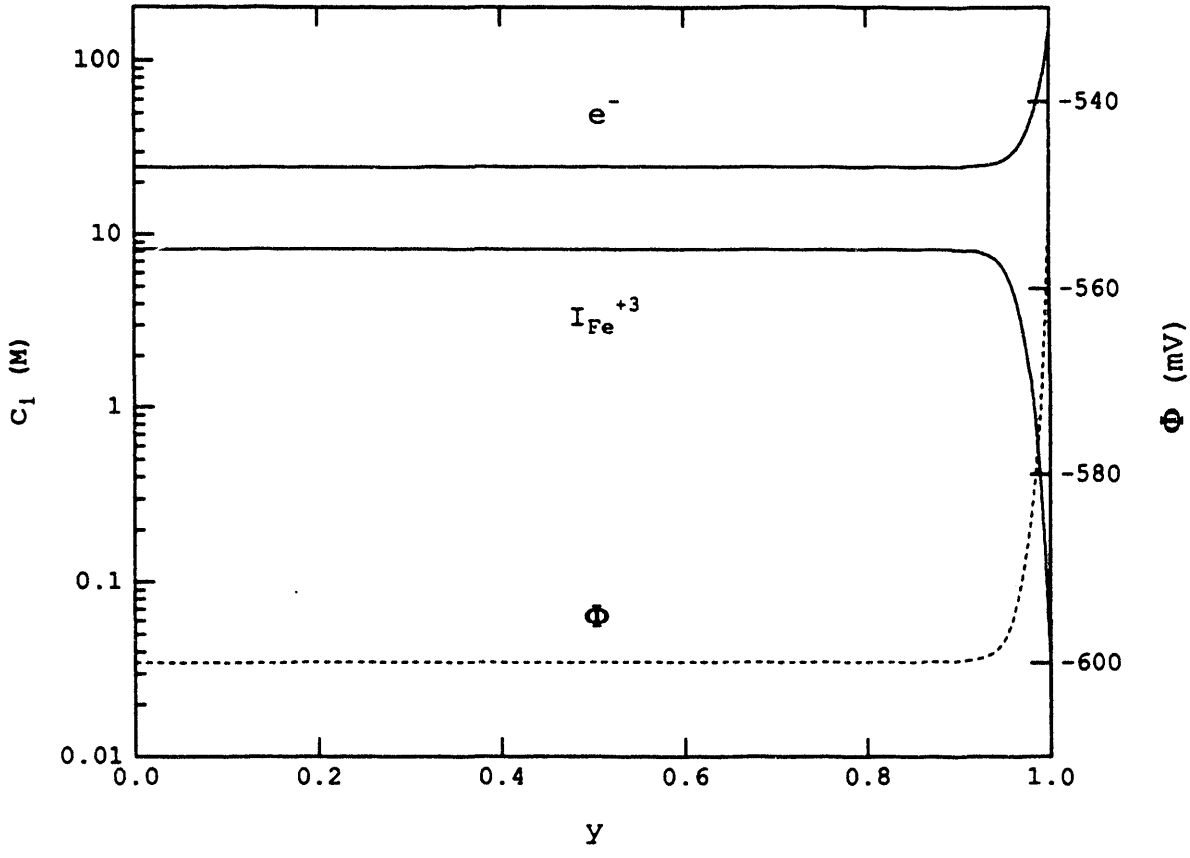

Figure 5. Potential and concentration distributions of interstitials and electrons *versus* the dimensionless coordinate, *y*, at the equilibrium potential, V = -600 mV *vs.* the NHE.

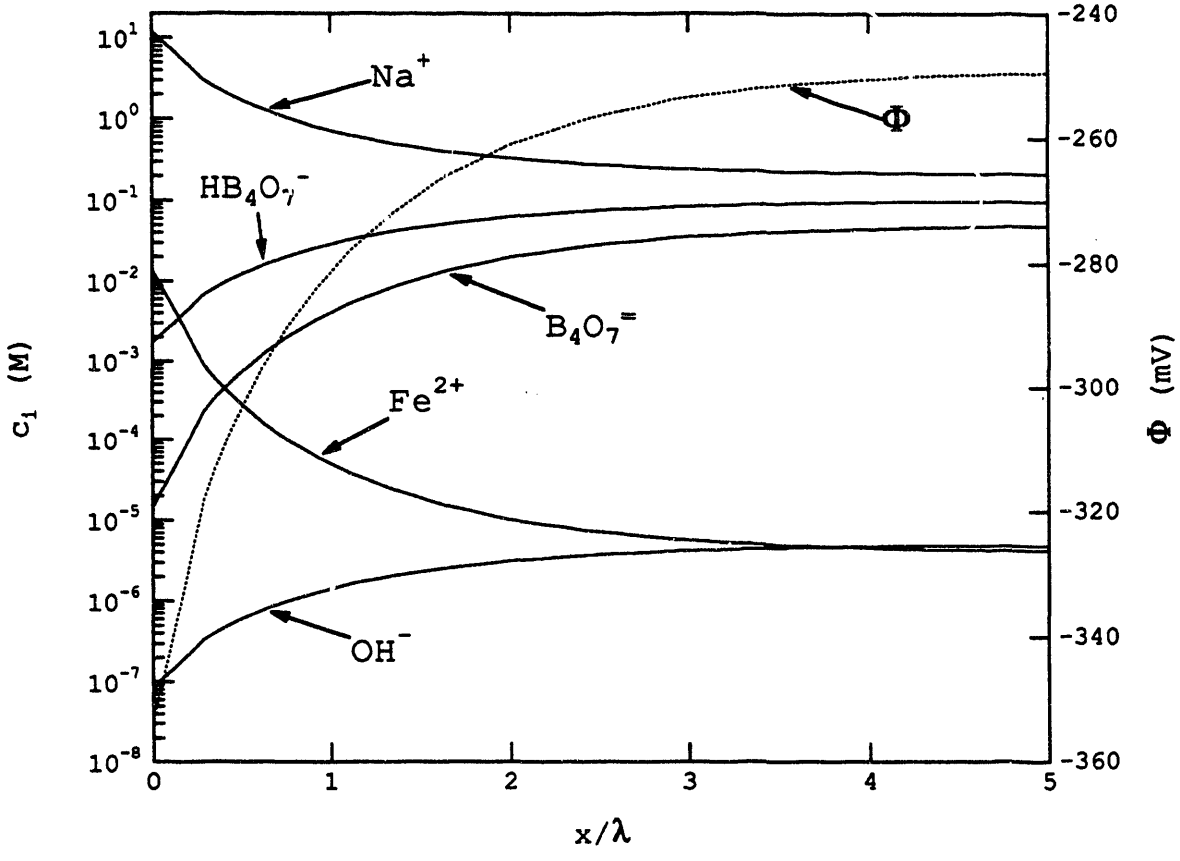

Figure 6. Concentration and potential distributions in the solution phase at the equilibrium potential *versus* the number of debye lengths from the oxide surface. V = -600 mV *vs.* NHE.

on emphasize important aspects of the effects of varying certain parameters. Also shown are results of simulations that include additional physics, performed to augment the comparison with the data.

Before proceeding we must state that we were unable to implement the high-field rate equation. The severe nonlinearity of this equation, combined with the high degree of coupling of Poisson's equation and the flux equations provided too difficult a challenge for Autoband[29] (the numerical differentiation subroutine we chose for solving our equations). Despite the months of effort to get around this problem, no satisfactory solution was obtained. This is clearly a disappointment, for preliminary results indicate that the field is initially growing in the high-field regime. It is felt that a proper linearization of the equations and perhaps techniques used for decoupling such problems would be effective. However, considering the amount of time that has already been spent, we decided to provide the low-field results. Moreover, it is felt that many of the trends seen in the low-field regime should hold for the high-field regime. Again, the results presented are the best fit achievable with the low-field equation.

Figure 7 contains experimental data reproduced from Jovancicevic *et al.*[36] The current *versus* potential is featured for a sweep rate of 0.3 mV/s. Also shown in the figure is a computer generated simulation for the same sweep rate assuming a quasi-steady state. According to Jovancicevic *et al.*,[36] an oxide of 0.03 nm is not seen until the potential equals -500 mV (this is 100 mV above the equili-

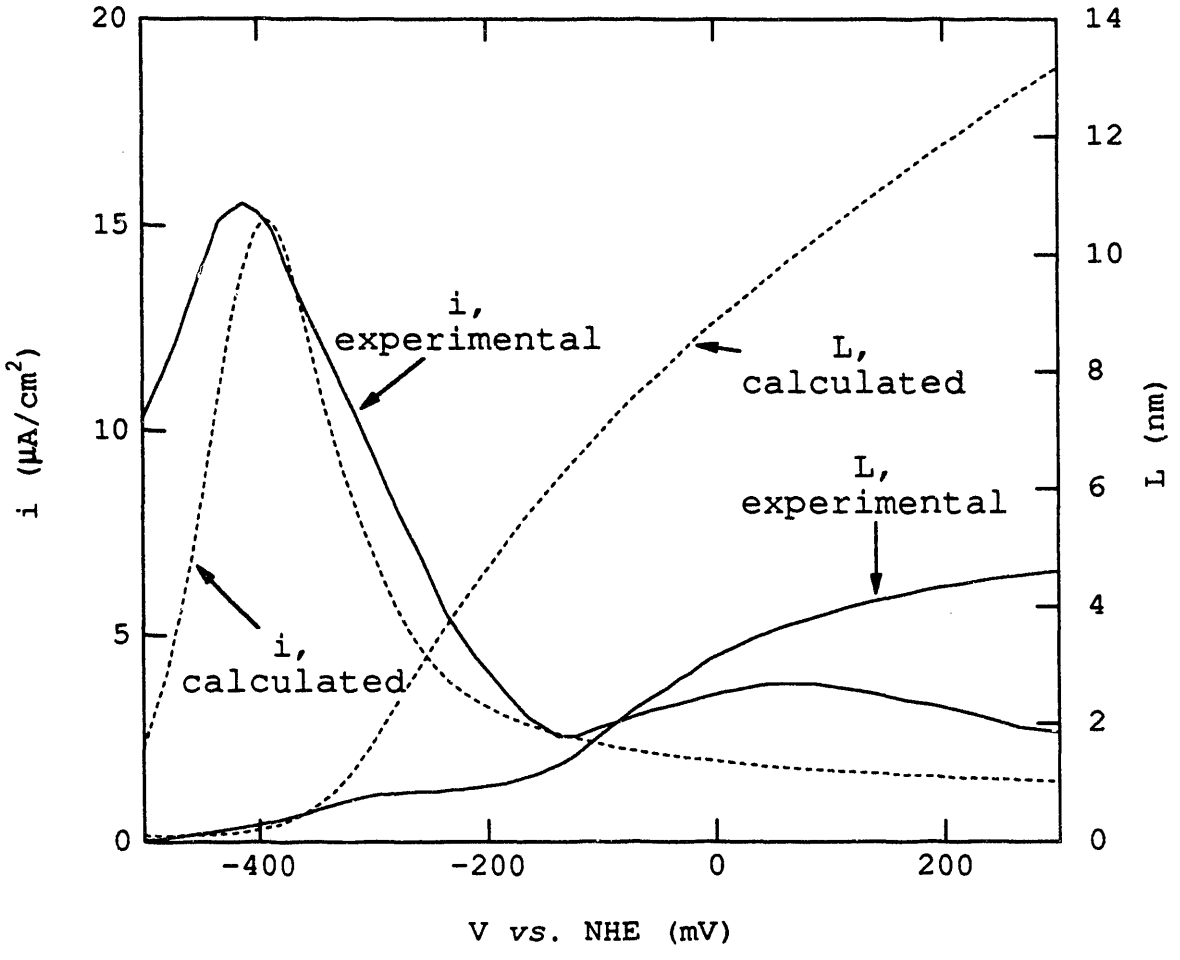

Figure 7. The solid curves are current and length *versus* potential data at 0.3 and 5.0 mV/s, respectively, from Jovancicevic *et al.*[36] The dashed curves are current and length *versus* voltage at 0.3 mV/s from simulations.

brium potential). Since we have not included nucleation in our model, we can not simulate the results of a zero thick oxide. The simulations therefore start at −500 mV. The 0.03 nm measured at this potential is thinner than an atom, and probably means that roughly 30% of the film is covered by a 1 nm thick film. Our model does not include nucleation or a means of handling the kinetics of partial coverage. The simulation will therefore provide a poor fit at the lower potentials.

To fit a curve to the data, we have at our disposal five rate constants and the diffusion coefficients of the species in the oxide. The diffusion coefficient of the interstitials is much smaller than that of any other species, and the interstitials are involved in all of the proposed reactions. It is therefore the only diffusion coefficient that we shall adjust.

The electrons move relatively easily through the oxide and, we assume, pass easily into the metal phase. Reaction 2 is therefore assumed to progress at a high enough rate to be considered at equilibrium. A variation of the rate of interstitials from the metal into the oxide should equally affect the flux of interstitials to the opposite interface. Thus, to avoid needless complications, we assume that the rate of reaction 1 progresses fast enough to be considered at equilibrium. Simulations show that the equilibrium constant for the ferric reaction, reaction 4, is too low to have an effect, independent of its rate. For this reason the reaction is assumed to be at equilibrium (hence, maximum rate). This reduces our flexibil-

ity to varying two rate constants, of reactions which occur at the oxide/solution interface, and the diffusion coefficient of the interstitials.

Simulations showed that as the rate constant of the ferrous reaction, reaction 5, is increased, the initial peak in the current in figure 7 moves up and to the right with respect to potential. An increase in the oxide-forming reaction, reaction 3, has the opposite effect. The diffusion coefficient of the interstitials moves the entire curve vertically up or down in a manner that is proportional to the change in the diffusion coefficient. What is going on?

Initially, as the current increases with potential, the current is limited by the rate of the ferrous reaction. The oxide-forming reaction also increases with potential, although it is not the dominant reaction, and the oxide thickens. When the current reaches a peak, the system is switching from a reaction-limited regime to a diffusion-limited regime, which defines the onset of passivation. In this regime, the current density decreases as the oxide thickens. In the diffusion-limited regime, the interstitials reach the surface at some finite rate. The interstitials are then consumed by one of the three reactions at the oxide/solution interface. As the potential is increased, the reaction that consumes the majority of interstitials will shift from a reaction of lower charge transfer to one of higher charge transfer. The charge transfer number in reaction 5 is equal to two, and the charge transfer number of reactions 3 and 4 is equal to three. Between reactions of the same order, the reaction with the

combination of equilibrium constant and rate of reaction that allows it to appear first as the dominant means of interstitial consumption shall continue to prevail at higher potentials. For these reasons we see in figure 8 that the dominant rate of interstitial consumption switches from reaction 5 to reaction 3. The equilibrium constant of reaction 4 is too small to allow it to compete with reaction 3, although at the higher potentials reaction 4 carries more current than reaction 5.

If the oxide were electrically neutral and the flux of electrons were equal to zero, the limiting current would obey the equation

$$i_{lim} = 3FN_{I_{Fe}^{3+}} = 3F\left(\frac{4D_{I_{Fe}^{3+}}c_{I_{Fe}^{3+}}}{L}\right),$$

where the concentration of interstitials is that at the metal/oxide interface. The diffusion-limited current of interstitials that are initially consumed primarily by the ferrous reaction is accompanied by a flux of electrons of the same direction and magnitude. The current carried by the electrons, however, is of the opposite sign and one third of the interstitial current. Thus, the limiting current appears as two thirds of that expected from the diffusive flux of interstitials alone. Figure 9 presents the current from the simulation and the theoretical limiting current and two-thirds of the theoretical limiting current when electroneutrality holds. This transition from a limiting current of interstitials accompanied by electron transport to the limiting current with no electron transport

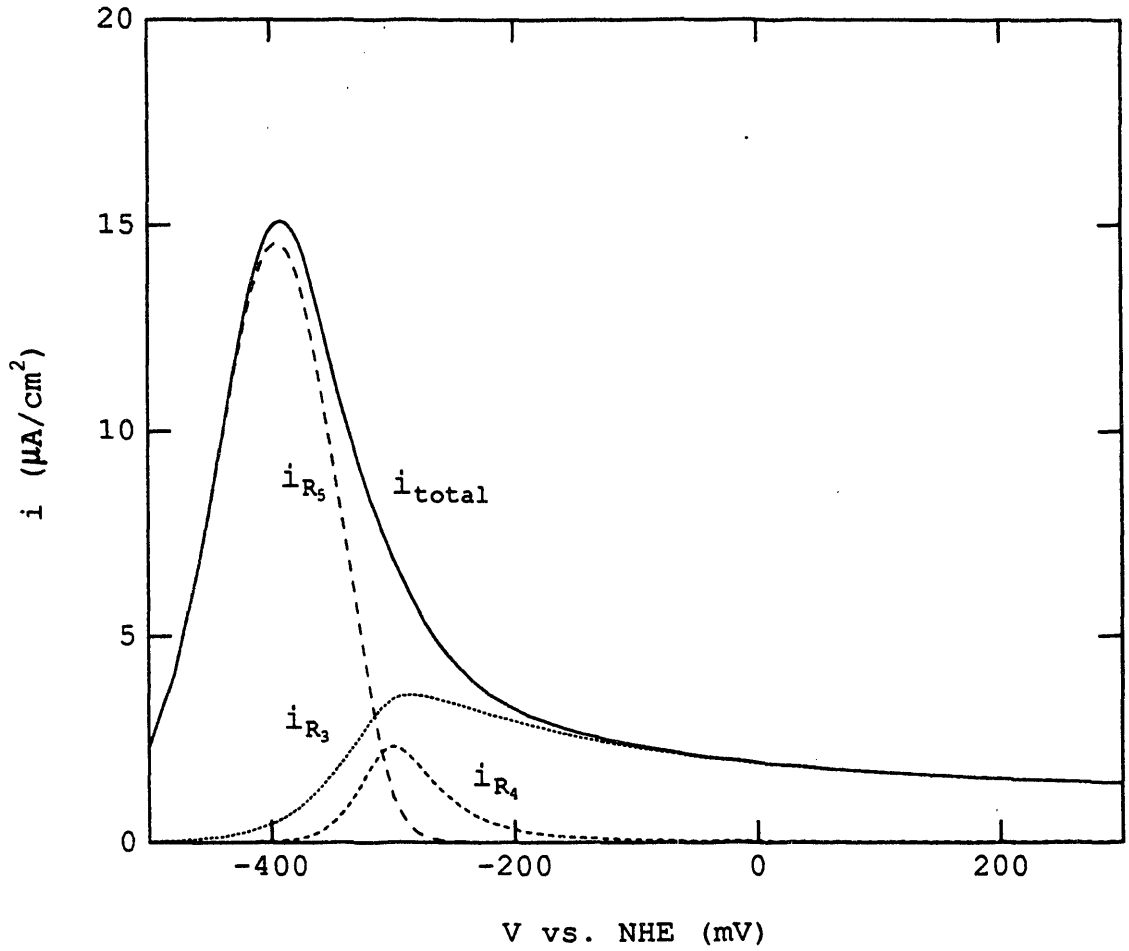

Figure 8. The currents through each reaction at the oxide/solution interface *versus* the potential. Sweep rate = 0.3 mV/s.

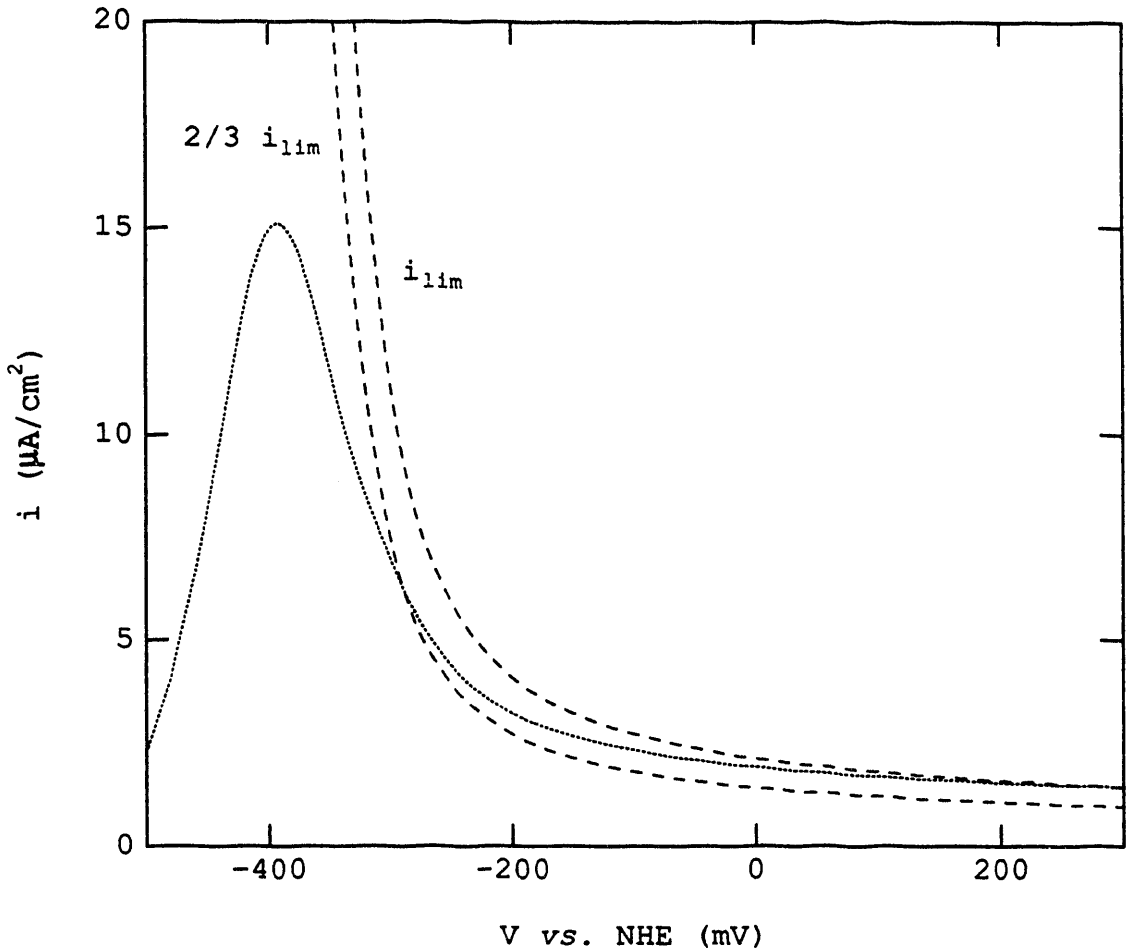

Figure 9. Current *versus* potential from simulation and an estimate of the limiting current and two-thirds of the limiting current. Sweep rate = 0.3 mV/s.

should follow the transition of the current from the ferrous reaction to the oxide-forming reaction. We therefore expect the two-thirds limiting current to lie on top of the simulation current at the potential where the peak starts to turn down and the full limiting current line to coincide with the simulation current at higher potentials. The lack of agreement at the low-potential end is a result of the nonelectroneutrality. This provides further justification for not making this assumption and using Poisson's equation instead.

In the end, the values that provide the best fit to the data are $k_{-3} = 1\times10^{-13}$ mol/cm^2-s, $k_5 = 1\times10^{-11}$ cm/s, and $D_{I^{3+}_{Fe}} = 2\times10^{-16}$ cm^2/s.

Further inspection of the data provided by Jovancicevic *et al.* reveals a second peak in the current at a potential of around 100 mV. Our first inclination was that this is the result of another reaction, perhaps the ferric reaction, reaction 4, becoming the dominant means of interstitial utilization. The simulations above were obtained assuming that reaction 4 is at equilibrium. It is therefore impossible to increase the rate of this reaction. But perhaps the equilibrium constant reported for this reaction was incorrect, and maybe there is room for adjusting its value. However, this reaction has the same reaction order as that of the oxide-film reaction. Therefore, the equilibrium constant must be increased to the point where the rate of reaction 4 overcomes the rate of reaction 3, the oxide-forming reaction. If this is done, the oxide-film reaction is diminished, and the current continues to increase with potential,

switching from the ferrous reaction to the ferric reaction. Eventually, enough oxide would be formed at the slow reaction rate to limit the rate of transport of interstitials, and the current would slowly decrease. The final result would still be one large peak in the current.

Underpotential Deposition

The thickness of the oxide measured *versus* the potential during a sweep rate of 5 mV/s is provided in figure 7. A plateau in the oxide thickness at around 7.5 nm appears between -375 and -175 mV. This leads us to believe that there may be underpotential deposition. Underpotential deposition (UPD) is the deposition of any solid on a substrate made of a different material than the deposit where the substrate is thermodynamically more stable for deposition than the deposit. Deposition of this type is analogous to the BET isotherm where the surface coverage of gas molecules is a function of the pressure of the surrounding gas. We would like to take advantage of this similarity and use the equations previously derived in the literature for the BET isotherm. A driving force for deposition that is a function of the thickness of the oxide is subsequently developed.

The BET isotherm[43] is characterized by the equation

$$v = \frac{v_m c P}{(P_o - P)\left[1 + \frac{(c-1)P}{P_o}\right]},$$

where v is the volume of the adsorbed layer, v_m is the volume of a monolayer of the absorbed layer, c is a constant related to the heat of adsorption, and P_o is the saturation pressure. In relation to our analysis, the volume of the absorbed layer is analogous to the thickness of the oxide, L, and the pressure is analogous to the applied potential, U:

$$v \longleftrightarrow L \text{ and } \ln\frac{P}{P_o} \longleftrightarrow \frac{nFU}{RT}.$$

We require an equation that gives the potential as a function of the length. Rearrangement of the above equation and substitution of L and U give

$$\frac{nFU}{RT} = \ln\frac{2P_o}{\left\{\left[c\left(\frac{L_m}{L} - 1\right) + 2\right]^2 + 4(c - 1)\right\}^{1/2} + c\left(\frac{L_m}{L} - 1\right) + 2}.$$

c is related to the width of the potential plateau, U_o, through the equation

$$c = \exp\left(\frac{FU_o}{RT}\right).$$

From the data of Jovancicevic *et al.*,[36] we estimate that U_o is approximately 200 mV.

The BET isotherm relates the volume of coverage to the gas pressure. The surface coverage is not strictly associated with either interface. In this analysis, a relationship between the potential of oxide deposition and the amount of coverage is also not strictly associated with either interface. However, we felt that the best way

to incorporate the UPD was to attribute it to the oxide-forming reaction, reaction 3, at the oxide/solution interface. Thus, the U defined above was subtracted from the potential difference of the oxide/solution interface in both the forward and reverse reaction rates of reaction 3,

$$R_3 = k_3 c_{I_{Fe}}^{1/3} c_{OH^-}^{3+} \exp\left[\frac{(1-\beta)F}{RT}(\Phi^o - \Phi^s - U)\right] - k_{-3}\exp\left[-\frac{\beta F}{RT}(\Phi^o - \Phi^s - U)\right].$$

The result of the above adjustment to reaction rate 3 on the current and the length of the oxide when the potential is swept at a rate of 0.3 mV/s is provided in figure 10. One sees a peak in the current at the same potential where the length of the film briefly levels off. The peak in the current appears because the oxide stops growing, and thus, the diffusion-limited current stops decreasing. The current tends to level off. A few millivolts further to the right in figure 11 the oxide film reaction begin to increase again, while the current drops off again.

The reason we included UPD in our analysis was not only to make our length *versus* potential curve agree with the experimental data but also to get the second peak in the current to agree as well. The peak we get is nowhere near the potential of the second peak in the experimental data. In our simulations, the leveling off of the oxide is going to appear at the same potential where the peak in the current appears. In the experiments, these two phenomena are separated by 200 mV. Figure 10 demonstrates that if we try to match the experimentally measured leveling off of the film thickness with

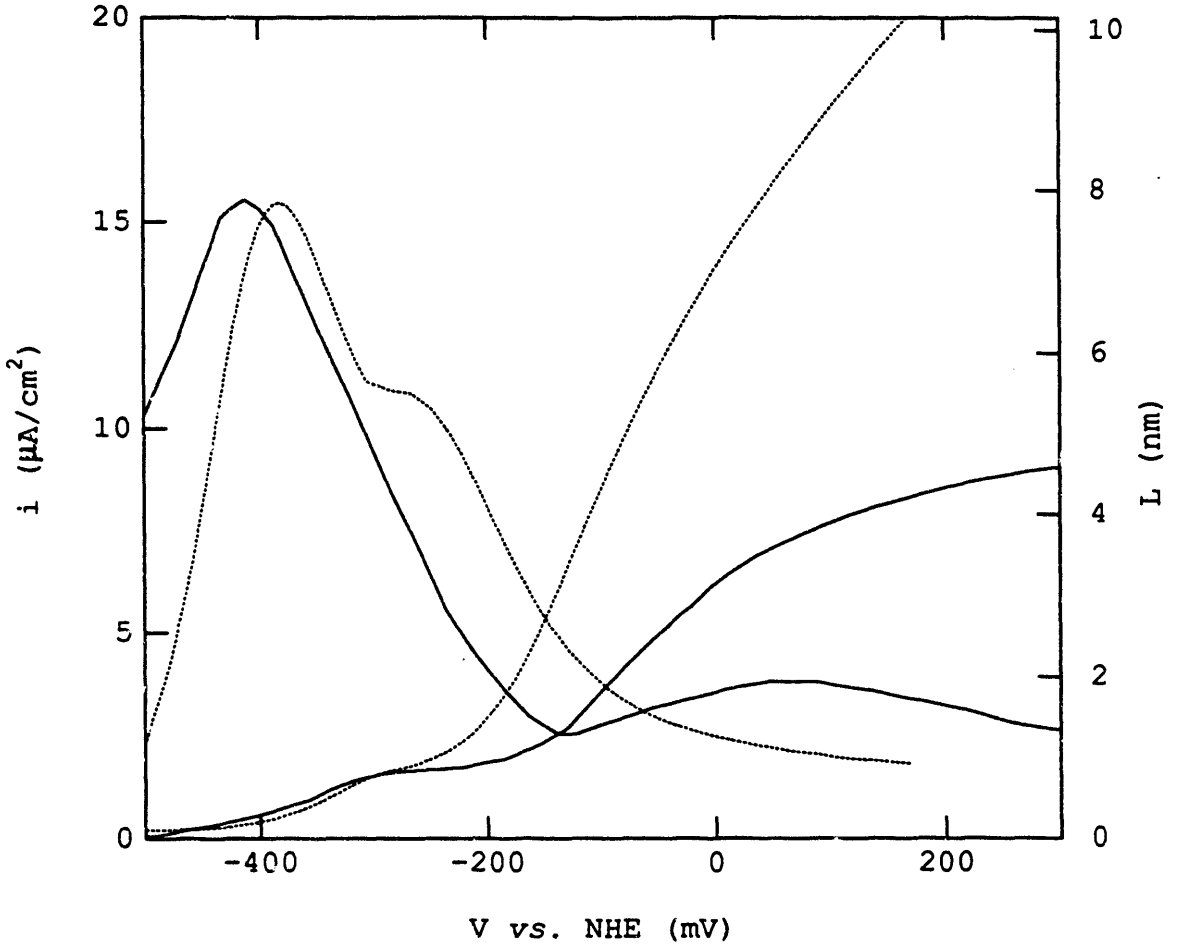

Figure 10. Solid curves are current and length *versus* potential data at 0.3 and 5 mV/s, respectively, from Jovancicevic *et al.*[36] The dashed curves are current and length *versus* voltage at 0.3 mV/s from simulations that include UPD.

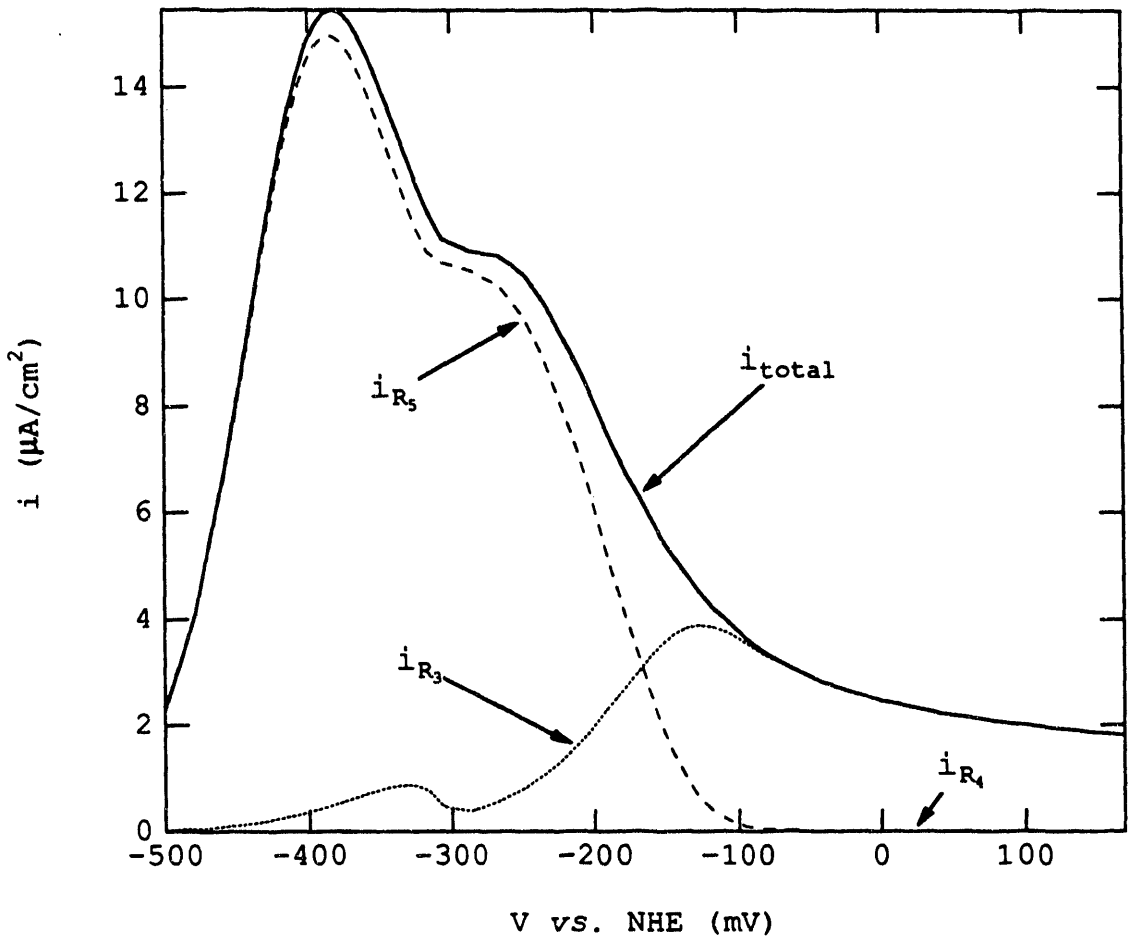

Figure 11. The currents through each reaction at the oxide/solution interface *versus* the potential with UPD. Sweep rate = 0.3 mV/s.

our simulations, the peak in the simulated current appears at too low a potential as compared to the peak in the current in the experimental data. If we attempted to match the peak in the current with our simulations at the correct potentials, we would have to delay the UPD 200 mV and allow the length to reach 6 nm before leveling off. This would allow sufficient film growth to occur to bring the mass-transfer-limited current down to the proper magnitude at the first minimum. A growing oxide that briefly levels off at 6 nm before continuing to grow again can not be explained by UPD. We conclude that the two events in the data are mutually exclusive. With the present amount of physics included in our analysis, it is impossible for us to match all of the data provided by Jovancicevic *et al.*

A final comparison to experimental data is provided. Included in figure 12 are the data from Jovancicevic *et al.*, our original simulation (without UPD), and the current *versus* potential curve reproduced from Lukac *et al.*[25] Our work appears to be in far better agreement with the work of Lukac *et al.* than that performed by Jovancicevic *et al.* After exhausting all physically reasonable avenues for creating simulations that could duplicate the results of Jovancicevic *et al.*, we come to the conclusion that perhaps the work done by Lukac *et al.* was done under better controlled conditions.

Summary

In this chapter we have presented the equations that describe the growth of a film. Methods of combining the equations to elim-

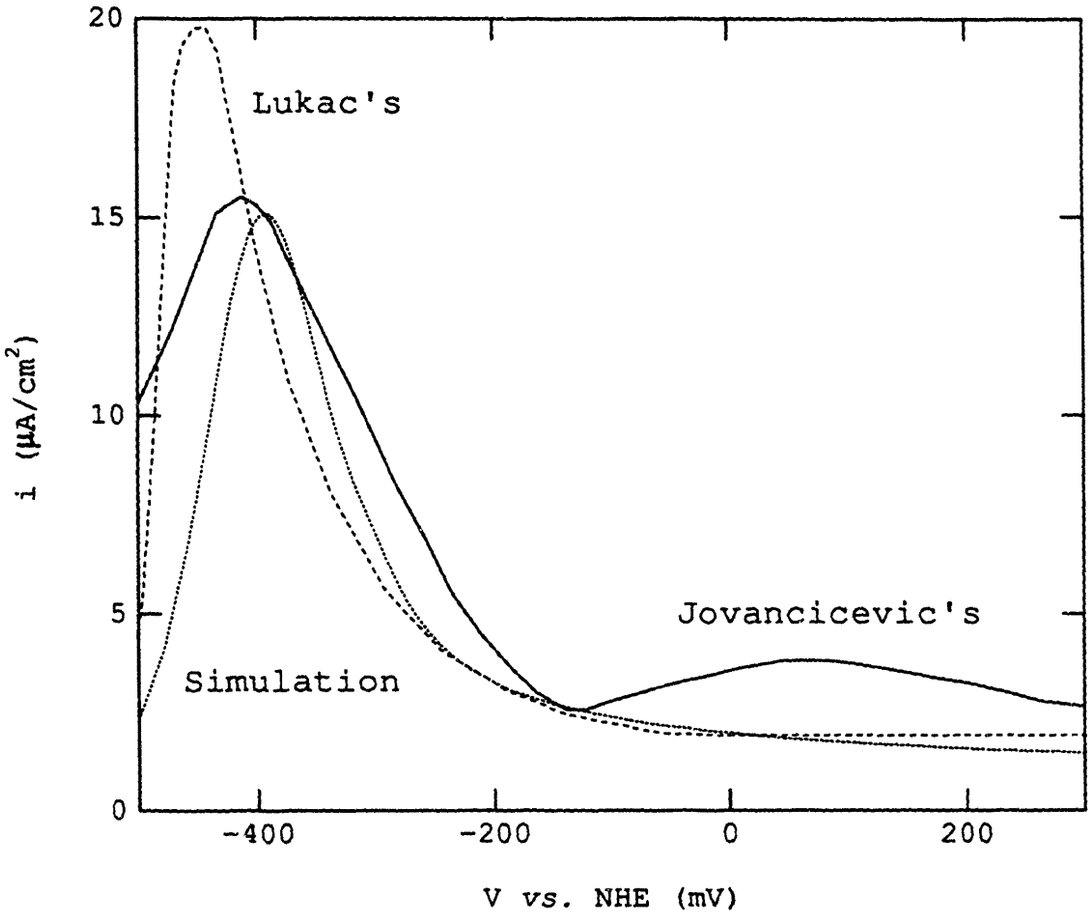

Figure 12. Current *versus* potential from Jovancicevic *et al.*[36] and the simulation at a sweep rate of 0.3 mV/s and Lukac *et al.*[25] at a sweep rate of 1/3 mV/s.

inate rapid reactions are provided, as well as the boundary conditions and a means for solving the equations. Equations that find specific application to oxide films were developed as were variables that make the computation simpler. A model was developed specifically for the iron/iron oxide system. The method by which certain parameters are determined was given. A program was then written and results of a low-field mole-flux equation were displayed. A comparison to existing experimental data and the effects of certain parameters on the final simulations were also discussed. A final comparison to experimental data showed good agreement with the work of Lukac *et al*. From this analysis we conclude that as the potential of iron in a borate buffer solution is swept in an increasing manner, iron initially reacts to form dissolved ferrous species. Eventually, at approximately 200 mV above equilibrium, an oxide is formed that is thick enough to cause a switch to the mass-transfer-limited regime and the onset of passivation. At higher potentials, the oxide-film-forming reaction becomes the dominant reaction.

List of Symbols

Roman

a	jump distance, cm
a_k	activity of species k
c_k	concentration of species k, mol/cm^3
D_k	diffusion coefficient of species k, cm^2/s

e^-	symbol for the electron
F	Faraday's constant, 96485 C/equiv
h^+	symbol for the hole
i	current density, A/cm^2
$k_{1\ell}, k_{-\ell}$	forward and backward rate constants of rxn. ℓ
K_ℓ	equilibrium constant of reaction ℓ
L	length of phase, cm
m	the mth interface from the left
m_o	the chosen stationary interface
n	number of charges transferred in a reaction
N_k	mole flux of k, mol/cm^2-s
p_k	reaction order for forward reactants
q_k	reaction order for backward reactants
R	universal gas constant, 8.3143 J/mol-K
R_ℓ	reaction rate of ℓ, mol/cm^3-s
R_{A_ℓ}	reaction rate at surface of ℓ, mol/cm^2-s
s_k	stoichiometric coefficient of species k
t	time, s
T	temperature, K
U^θ	standard electrode potential, V
v	velocity, cm/s
V	electrode potential, V
x	coordinate, cm
X_Y	X site occupied by Y
y	dimensionless coordinate

z_k charge number of species k

Greek

β symmetry factor

δ distance between charges in different phases, cm

Γ_k surface concentration of species k, mol/cm^2

ϵ permeability, F/m

ζ dimensionless distance

μ_k electrochemical potential of k, J/mol

ν viscosity, g/cm-s

Φ electric potential, V

Ω angular velocity, s^{-1}

subscripts

i,k species i and k

I interface

l reaction l

L lattice

migr migration

ref reference

trans transport

superscripts

m metal

superscripts

m metal

o	oxide
s	solution
'	position to the left of x
''	position to the right of x

References

1. L. Young, "The Theory of Formation of High Resistance Anodic Oxide Film," *Can. J. Chem.*, **371**, 276-285 (1959).

2. L. Young, *Anodic Oxide Films*, Academic Press, London (1961).

3. K. J. Vetter, *Electrochemical Kinetics. Theoretical and Experimental Aspects*, Academic Press, New York, 748-789 (1967).

4. C. Y. Choa, L. F. Lin, and D. D. Macdonald, "A Point Defect Model for Anodic Passive Films," *J. Electrochem. Soc.*, **128**, 1186-1194 (1981).

5. E. J. W. Verwey, "Electrolytic Conduction of a Solid Insulator at High Fields," *Physica*, **2**, 1059-1063 (1935).

6. N. Cabrera and N. F. Mott, "Theory of the Oxidation of Metals," *Repts. Progr. Phys.*, **12**, 163-184 (1948-49).

7. F. P. Fehlner and N. F. Mott, "Low-Temperature Oxidation," *Oxidation of Metals*, **2**, 59-99 (1970).

8. R. J. Maurer, "Deviations from Ohm's Law in Soda Lime Glass", *J. Chem. Phys.*, **9**, 579-584 (1941).

9. D. A. Vermilyea, "The Kinetics of Formation of Anodic Tantalum Oxide — Further Studies," *J. Electrochem. Soc.*, **102**, 655-659 (1955).

10. G. T. Burnstein and A. J. Davenport, "The Current-Time Relationship during Anodic Oxide Film Growth under High Electric Field," *J. Electrochem. Soc.*, **136**, 936-941 (1989).

11. B. D. Cahan and C.-T. Chen, "The Nature of the Passive Film on Iron. III. The Chemi-Conductor Model and Further Supporting Evidence," *J. Electrochem. Soc.*, **129**, 921-925 (1982).

12. C. P. Bean, J. C. Fisher, and D. A. Vermilyea, "Ionic Conductivity of Tantalum Oxide at Very High Fields," *Physical Review*, **101**, 2, 551-554 (1956).

13. L. L. Odynets, "Ionic Transport in Anodic Oxide Films in Strong Fields," *Elektrokhimiya*, **26**, 1040-1043 (1990).

14. J. F. Dewald, "The Effects of Space Charge on the Rate of Formation of Anode Films," *Acta Met.*, **2**, 340-341 (1954).

15. J. F. Dewald, "A Theory of the Kinetics of Formation of Anode Films at High Fields," *J. Electrochem. Soc.*, **102**, 1-6 (1955).

16. M. J. Dignam, "Transition Layer Model of the Oxide-Electrolyte Interface," *Can. J. Chem.*, **56**, 595-605 (1978).

17. C. J. Greyling, I. A. Kotze, and P. E. Viljoen, "The Kinetics of Oxide Film Growth on Maraging Steel as Described by Space-charge Effects," *Surf. Interface Anal.*, **16**, 293-298 (1990).

18. N. Sato and M. Cohen, "The Kinetics of Anodic Oxidation of Iron in Neutral Solution," *J. Electrochem. Soc.*, **111**, 512-522 (1964).

19. B. E. Conway, B. Barnett, H. Angerstein-Kozlowska, and B. V. Tilak, "A Surface-Electrochemical Basis for the Direct Logarithmic Growth Law for the Initial Stages of Extension of Anodic Oxide Films Formed at Noble Metals," *J. Chem. Phys.*, **93**, 8361-8373 (1990).

20. J. Frenkel, "Über die Warmebewegung in festen end flüssigen Körpern," *Z. f. Physik*, **35**, 652-669 (1926).

21. D. D. Macdonald and M. Urquidi-Macdonald, "Theory of Steady-State Passive Films," *J. Electrochem. Soc.*, **137**, 2395-2402 (1990).

22. D. D. Macdonald, S. R. Biaggio, and H. Song, "Steady-State Passive Films. Interfacial Kinetic Effects and Diagnostic Criteria," *J. Electrochem. Soc.*, **139**, 170-177 (1992).

23. B. MacDougall, "Role of Oxide Defects in the Anodic Oxidation of Nickel," *J. Electrochem. Soc.*, **127**, 789-795 (1980).

24. B. MacDougall, "Interpretation of Log*i* - Log*t* Relationships for Nickel Passivation," *J. Electrochem. Soc.*, **130**, 114-117 (1983).

25. G. Dagan and M. Tomkiewicz, "Passivation of Permalloy Thin Films. I. Kinetics of Anodic Oxidation in Neutral Solutions," *J. Electrochem. Soc.*, **139**, 461-466 (1992).

26. C. Lukac, J. B. Lumsden, S. Smialowska, and R. W. Staehle, "Effects of Temperature on the Kinetics of Passive Film Growth on Iron," *J. Electrochem. Soc.*, **122**, 1571-1579 (1975).

27. P. Russell and J. Newman, "Anodic Dissolution of Iron in Acidic Sulfate Electrolytes. I. Formation and Growth of a Porous Salt Film," *J. Electrochem. Soc.*, **133**, 59-69 (1986).

27. C. Wagner, "The Electrochemistry of Ionic Crystals," *J. Electrochem. Soc.*, **99**, 346C-354C (1952).

28. P. G. Shewmon, *Diffusion in Solids*, McGraw-Hill, New York (1963).

29. O. T. Sørensen, *Nonstoiciometric Oxides*, Academic Press, Inc., New York, New York (1981).

30. J. Newman, *Electrochemical Systems*, 2nd Edition, Prentice-Hall Inc., Englewoods Cliffs, NJ (1991).

31. A. Acrivos, "The Asymptotic Form of the Laminar Boundary-Layer Mass-Transfer Rate for Large Interfacial Velocities," *J. of Fluid Mechanics*, **12**, 337-357 (1962).

32. P. P. Russell, "Corrosion of Iron: The Active - Passive Transition and Sustained Electrochemical Oscillations," *Ph.D. Thesis*,

University of California, Berkeley (1984).

33. Y.- T. Chin and B. D. Cahan, "An Ellipsometric Spectroscopic Study of the Passive Film on Iron-Potential and Chloride Ion Dependence," *J. Electrochem. Soc.*, **139**, 2432-2442 (1992).

34. M. Hänisch and A. Otto, "Differential Reflection Spectroscopy of Passive Films on Iron," *J. of Electroanalytical Chem. and Inter. Electrochem.*," **308**, 113-126 (1991).

35. J. Gui and T. M. Devine "Obtaining Surface-Enhanced Raman Spectra from the Passive Film on Iron," *J. Electrochem. Soc.*, **138**, 1376-1384 (1991).

36. M. Kerkar, J. Robinson, and A. J. Forty, "In-Situ Structural Studies of the Passive Film on Iron and Iron/Chromium Alloys using X-Ray Absorption Spectroscopy," *Faraday. Dis. of the Chem. Soc.*, **89**, 31-40 (1990).

37. C. Wagner, "Models for Lattice Defects in Oxide Layers on Passivated Iron and Nickel," *Ber. Bunsenges. Phys. Chem.*, **77**, 1090-1097 (1973).

38. V. Jovancicevic, R. C. Kainthla, Z. Tang, B. Yang, and J. O'M. Bockris, "The Passive Film on Iron: An Ellipsometric-Spectroscopic Study," *Langmuir*, **3**, 388-395 (1987).

39. M. Pourbaix, *Atlas of Electrochemical Equilibria in Aqueous Solutions*," National Association of Corrosion Engineers, Houston,

Texas, 313-317 (1974).

40. U. F. Franck and K. G. Weil, "Zur Korrosion despassiven Eisens in Schwefelsäure," *Z. f. Elecktrochemie*, **56**, 814-822 (1952).

41. R. C. Weast, *CRC Handbook of Chemistry and Physics*, Edition 59, CRC Press, Inc., Boca Raton, Florida (1978-1979).

42. W. Schmickler and J. W. Schultze, "Electron Transfer Reactions on Oxide-Covered Metal Electrodes," *Modern Aspects pf Electrochemistry*, Edited by J. O'M. Bockris, B. E. Conway, and R. E. White, Plenum Press, New York, **17**, 357-410 (1986).

43. C. G. Hill Jr., *An Introduction to Chemical Engineering Kinetics & Reactor Design*, John Wiley & Sons, Inc., New York (1977).

Appendix

Program

This section contains the computer program that was used to create the graphs and analysis of the iron/iron oxide system of the main text. We shall briefly describe the tasks performed by the main program, its subroutines, and functions; further information is provided within the program.

Main program *iren*: initializes the variables and parameters.

Subroutine *autoband*: puts the equations in computational differentiation form.

Subroutine *eqn*: decides which equations shall be used to describe the phenomena that occur at the particular mesh point.

Subroutine *eqn1nj*: contains the equations that describe the conditions at the first and last mesh points.

Subroutine *eqni*: contains the equations that describe the conditions at the interfaces.

Subroutine *eqnj*: contains the equations that describe the conditions within a given phase.

Subroutine *eqnprod*: combines mass balance equations such that each of the reactions is present in only one equation.

Subroutine *band*: puts the parameters of equations into a banded matrix and also solves the inverted matrix returning the solution in matrix "c."

Subroutine *matinv*: inverts matrices.

Subroutine *matmul*: matrix multiplier.

Subroutine *eqlbr*: adds the logarithm of the equilibrium constant to the sum of the logarithm of the concentrations of an equilibrium reaction.

Subroutine *sms1nc*: sums the stoichiometric coefficient times the logarithm of the concentrations of a reaction.

Subroutine *rfb*: calculates the forward and backward parts of the rate constants that include the *k's* and the product of the concentrations raised to their stoichiometric coefficients.

Function *fnrt*: calculates the charge transfer number of a reaction and multiplies it by *F/RT*.

Function *flxhfpt*: calculates the diffusive and migrative flux of a species at a half mesh point.

Function *accum*: calculates the stretching term added to fluxes.

Following this program is a data file, "iren.dat," which was read by the main program and used to generate some of the data produced for the iron/iron oxide system.

Main Program

iren

```
      program iren
      implicit real*8(a-h,o-z)
      dimension ref(5,15),cre(5,15),ampd(5),mode(5),vlr(5),vi(6),db(5)
      common /ablk/a(25,25),b(25,25),c(25,401),d(25,51),g(25),
     & x(25,25),y(25,25),neqt,njt
      common /bblk/ nj(5),nmb(5),ipu(5),ivu(5),cc(25,401)
     & ,pot(5,401),z(5,25)
      common /cblk/ nph,nsp(5),mb(5,15),ivar(5,25)
      common /dblk/ kontrol,cr0,mcro,lrcro,idlr(5),den(5),zmw(5),
     & blen(6),ltcs(5,15)
      common /eblk/ nhtr(5,2),pt(5,2,15,15),qt(5,2,15,15),
     & st(5,2,15,15),inft(6,15),rkba(6,15),equilt(6,15),
     & be(6,15),zks(5,2,25),curl(6),curr(6)
      common /fblk/ vtot,mvset,moset,lrvset,lroset,pm(5,15,15),
     & qm(5,15,15),sm(5,15,15),infm(5,15)
      common /gblk/ zlen(5),ninfm(5),rkbv(5,15),h(5,401),perm(5),f
     & ,ccsav(25,401),csav(25,401),yy(5,401)
      common/rate/velsav,vel,vel1,rrxn(25),cur(401),cursav(401),jtime
     & ,flxs(401,15),flxsav(401,15),chd(401),chdsav(401),currsav(6)
      common /hblk/ mvi,nhmr(5),cin(5,15),equilm(5,15),
     & v(5,401),vl(5,401)
      common /iblk/ aj,u(5,15),dif(5,15),frt,co
      common /nblk/ rate1,rate2,rate3,time,ji(6)
      common /test/ err(5,2),jcount,jco,jcosav
      open (2,file='iren.dat',status='old')
      open (4,file='iren.len',status='unknown')
      open (3,file='iren.con',status='unknown')
      open (5,file='restart.dat',status='old')
      rewind 4
      rewind 3
      do 999 i=1,25
           do 999 j=1,401
  999           c(i,j)=0.
c
c     Program for effect of migration on current with homogeneous
c     and heterogeneous reactions and multiple phases.
c
  802 format (i1,1x,i1,1x,e11.4,1x,e11.4,1x,f5.1,1x,a6)
  803 format (32h Nernst stagnant diffusion layer)
  804 format (32h Growing drop or plane electrode)
  805 format (28h Rotating disk,  Sc**(-1/3)=,e12.5,
     &18h;  (Omega/Nu)**.5=,e12.5)
  806 format (19h Species for Sc is ,a6)
c    67 10        20        30        40        50        60        7072
  807 format (/4h nj=,I4,//' species      U       dif'
     &'     z    lat. site  mat. bal.'/(1x,a6,2x,e9.2,1x,e9.2,1x,f5.1,
```

```
     & 6x,i1,9x,i1))
  808 format (/8x,31h s(i,1) Heterogeneous Reactions)
  809 format (1x,a6,5(f5.1))
  810 format (/8x,29h s(i,1) Homogeneous Reactions)
  812 format (/38h The next run did not converge, jkon3=,i4)
  813 format (/31h species     left         right)
  814 format (1x,a6,2x,2e12.5)
  820 format (/3x,a6,12h cur. den. =,e12.5,17h (mA/cm**2) amp =,e12.5)
  821 format (/16h cur. den. set =,e12.5,6h it is,e12.5,8hin phase
     &,i1,7h to the,i1,16h(1=left,2=right))
  822 format (/22h The total potential =,e12.5,3h mv)
  823 format (/19h Potential is set =,e12.5,15h mv  cur.den. =,
     &e12.5,11h (mA/cm**2))
  824 format (/13h The conc. of,a6,28h is set.  Potential is set =
     &,e12.5,24h mv, and the cur. den. =,e12.5,9h mA/cm**2)
  830 format (/43h     Time            Velocity of Interfaces)
  831 format (1x,e11.4,2x,6(e11.4,2x))
  832 format (/35h     Time      Length of Each Phase)
c
c     f : Faraday's constant.
c     frt : Faraday's constant divided by the gas constant and the
c       absolute temperature with units of 1/mV.
c     aa, bb : constants describing flow to a rotating disk.
c
      pi=3.14159265358979
      f=96487.
      frt=f/8.3143/298.15/1000.
      aa=0.51023262
      bb=-0.61592201
c
c     Read in or define the following values.
c
c     area : area of disk.
c     cr0 : concentration of the limiting reactant.
c     ctot: total current through cell.
c     kontrol : indicates whether the program is to solve for
c       the current for a species at a set concentration at
c       the electrode surface, 1; the current for a set potential
c       at the electrode surface, 2; for the potential for a set
c       total current, 3.
c     mcro, lrcro : phase and side of phase of limiting reactant.
c     mvi : interface where velocity is set to zero.
c     moset, lroset : phase and side where potential is set to 0.
c     mvset, lrvset : phase and side where potential is set to vtot.
c     neqt : will count the total number of equations to be solved.
c     njt : will count the total number of mesh points.
c     nph : number of phases.
c     ro : radius of disk.
c     vtot : total potential across cell.
c
      read (2,*) nph,kontrol,cr0,ro
```

```
      area=pi*ro**2
      read (2,*) vtot,ctot
      if(kontrol.eq.1) read (2,*) mcro,lrcro
      read (2,*) mvi
      do 100 m=1,nph+1
  100       vi(m)=0.
      read (2,*) mvset,lrvset
      read (2,*) moset,lroset
c
c     Read in or define for each phase the following values.
c
c     aj : jump distance in each phase.
c     be : transfer coefficient.
c     blen : length of interface (1.e-8 cm = 1 angstrom.)
c     cin : initial concentrations.
c     cre : concentrations c in reference electrode.
c     den : density of phase.
c     dif : diffusion coefficient times 1.e5.
c     equilm : equilibrium constant of homogeneous reaction.
c     equilt : equilibrium constant of heterogeneous reaction.
c     idlr : identity of the limiting reactant.
c     inft : indicates if the reaction is at equilibrium.
c     infm : indicates if it is an equilibrium reaction.
c     ipu : indicates if the potential is to be solved for.
c     ltcs : indicates if it is a lattice conservative species.
c     ivu : indicates if the velocity is to be solved for.
c     mb : indicates if a matterial balance is to be done.
c     mode : indicates type of velocity profile.
c     nhmr : number of homogeneous reactions.
c     nhtr : number of heterogeneous reactions on both sides.
c     ninfm : number of equilibrium homogeneous reactions.
c     nj : number of mesh points.
c     nsp : number of species.
c     perm : permitivity of phase (C/V-cm).
c     pm : forward homogeneous stoichiometric coefficient.
c     pt : forward heterogeneous stoichiometric coefficient.
c     qm : backward homogeneous rate stoichiometric coefficient.
c     qt : backward heterogeneous stoichiometric coefficient.
c     sm : difference of coefficients.
c     ref : name of species.
c     rkba : backward rate of heterogeneous reaction.
c     rkbv : backward rate of homogeneous reaction.
c     vlr : indicates if the given velocity goes right or left.
c     u/f/1000 : z(i)u(i)F in units of inverse millivolts.
c     z : charge of species.
c     zks : equilibrium constants of surface adsorption.
c     zlen : length of phase.
c     zmw : molecular weight of phase.
c
      aj=3.5d-10
      neqt=nph
```

```
      njt=1
      ji(1)=njt
      do 19 m=1,nph
           read (2,*) nsp(m),nhmr(m),idlr(m),nj(m)
           read (2,*) zlen(m),den(m),zmw(m),perm(m)
           perm(m)=perm(m)*8.854d-14
           blen(m+1)=3.5d-8
           read (2,802) (ltcs(m,i),mb(m,i),u(m,i),
     &     dif(m,i),z(m,i),ref(m,i),i=1,nsp(m))
           nmb(m)=0
           do 1 i=1,nsp(m)
                read (2,*) cin(m,i),cre(m,i)
                nmb(m)=nmb(m)+mb(m,i)
                u(m,i)=u(m,i)/f/1000.
 1              dif(m,i)=dif(m,i)/1.d5
           ninfm(m)=0
           if(nhmr(m).eq.0) goto 45
           do 2 i=1,nsp(m)
                read (2,*) (pm(m,i,l),qm(m,i,l), l=1,nhmr(m))
                do 2 l=1,nhmr(m)
 2                   sm(m,i,l)=pm(m,i,l)-qm(m,i,l)
           do 3 l=1,nhmr(m)
                read (2,*) infm(m,l),rkbv(m,l),equilm(m,l)
                ninfm(m)=ninfm(m)+infm(m,l)
 3              continue
45         continue
           do 44 lr=1,2
                read (2,*) nhtr(m,lr)
                if(nhtr(m,lr).eq.0) goto 44
                do 4 i=1,nsp(m)
                read (2,*) (pt(m,lr,i,l),qt(m,lr,i,l), l=1,nhtr(m,lr))
                     do 4 l=1,nhtr(m,lr)
                          st(m,lr,i,l)=pt(m,lr,i,l)-qt(m,lr,i,l)
 4                        continue
44              continue
           do 5 l=1,nhtr(m,2)
              read (2,*) inft(m+1,l),rkba(m+1,l),equilt(m+1,l),be(m+1,l)
 5              continue
           do 6 i=1,nsp(m)
                read (2,*) (zks(m,lr,i), lr=1,2)
 6              continue
           read (2,*)ipu(m),ivu(m)
           ir=idlr(m)
           if(ivu(m).eq.1) goto 13
           read (2,*) mode(m),vlr(m)
           print *, m, mode(m),vlr(m)
c
c     All data for phase m has been read in at this time.
c     We shall now set up the constants for initial guess
c       of the velocity.
c
```

```
c     Define the following values.
c     ampd : limiting current with excess supporting electrolyte.
c     anu : kinematic viscosity.
c     delta : order of boundary layer thickness.
c     difmax : maximum diffusion coefficient.
c     difz : diffusion coefficient of limiting reactant.
c     h : mesh spacing.
c     ir : limiting reactant.
c     om : rotation speed.
c     omnu : om/anu
c     scm3 : Sc number for limiting reactant to the -1/3.
c     time : time.
c     ximax : dimensionless thickness of boundary layer.
c
c     Find maximum diffusion coefficient and use for Sc number.
c
          difmax=0.0
          do 7 i=1,nsp(m)
               if(mb(m,i).eq.0) goto 7
               if(dif(m,i).gt.difmax) then
                  difmax=dif(m,i)
                  idz=i
               endif
    7          continue
          difz=dif(m,ir)
          if(mode(m).ne.1) goto 9
             const=0.0
             print 803
             ampd(m)=1.0
             ximax=1.0
             delta=zlen(m)
    9     if(mode(m).ne.2) goto 10
             const=2.0
             print 804
             ampd(m)=1.128379167
             ximax=3.3*(difmax/difz)**0.5
             read (2,*)time
             delta=(12.*difz*time/7.)**0.5
   10     if(mode(m).ne.3) goto 11
             const=2.0
             print 804
             ampd(m)=1.128379167
             ximax=3.3*(difmax/difz)**0.5
             read (2,*)time
             delta=(4.*difz*time)**0.5
   11     if(mode(m).ne.4) goto 12
             const=3.0
             read (2,*) anu,om
             omnu=om/anu
             scm3=(anu/difz)**(-1./3.)
             print 805, scm3,omnu**.5
```

```
            ampd(m)=1.119846522
            ximax=2.0*(difmax/difz)**(1.0/3.0)
            delta=(3./aa)**(1./3.)*scm3*omnu**(-.5)
            print 806,ref(m,ir)
   12       zlen(m)=ximax*delta
   13       print 807, nj(m),
     &      (ref(m,i),u(m,i)*f*1000.,dif(m,i),z(m,i),ltcs(m,i),
     &      mb(m,i), i=1,nsp(m))
            print 810
            do 14 i=1,nsp(m)
   14       print 809, ref(m,i),(sm(m,i,l), l=1,nhmr(m))
c
c     We now make initial guesses of concentrations by assuming
c       the species involved in homogeneous reactions divide into
c       proportions according to their stoichiometry, of
c       velocities  of zero except for the mode of transport we,
c       selected, and of potential by setting it equal to zero
c       except for that phase which is set to vtot.
c
c     Define the following parameters.
c     c : the variables to be solved for are stored here.
c     ct : total of the concentration.
c     i : counts the number of equations.
c     ivar : identifies the equation  to which species in each phase
c       corresponds.
c     pot : the given potential.
c     v : the given velocity.
c     vl : is the given velocity plus the velocity of the interface.
c     stt : total of the soichiometric coefficients.
c     y : the dimensionless distance xi.
c     ze : the zeta in the von Karman transformation for the
c       rotating disk.
c
            i=neqt
            db(m)=0.
            do 15 ii=1,nsp(m)
                 if(mb(m,ii).ne.1) goto 15
                 i=i+1
                 ivar(m,ii)=i
                 c(i,njt)=cin(m,ii)
                 db(m)=db(m)+cin(m,ii)*z(m,ii)**2
   15            continue
            if(db(m).ne.0.) db(m)=perm(m)**.5/(f*frt*db(m))**.5
            if(ipu(m).eq.1) ivar(m,nmb(m)+1)=i+1
            if(ivu(m).eq.1) ivar(m,nmb(m)+ipu(m)+1)=i+ipu(m)+1
            if(ipu(m).eq.1) then
               i=ivar(m,nmb(m)+ipu(m))
               if(m.eq.mvset) then
                  if(lrvset.eq.-1) then
                     c(i,njt)=vtot
                     c(i,njt+nj(m)-1)=0.
```

```
                 endif
                 if(lrvset.eq.1) then
                    c(i,njt)=0.
                    c(i,njt+nj(m)-1)=vtot
                 endif
              else
                 c(i,njt)=0.
                 c(i,njt+nj(m)-1)=0.
                 if(m.eq.2) c(i,njt+nj(m)-1)=pot(m-1,njt)+47.
                 if(m.gt.1) then
                    if(ipu(m-1).eq.0) then
                       c(i,njt)=pot(m-1,njt)
                    else
                       im=ivar(m-1,nmb(m-1)+ipu(m-1)+ivu(m-1))
                       c(i,njt)=c(im,njt)
                       if(m.eq.3) c(i,njt)=0.-104.
                    endif
                 endif
                 if(m.lt.nph) then
                    if(m+1.eq.mvset) then
                       if(ipu(m+1).eq.0) then
                          c(i,njt+nj(m)-1)=vtot
                       else
                          if(lrvset.eq.-1) c(i,njt+nj(m)-1)=vtot
                       endif
                    endif
                 endif
              endif
           else
              if(m.eq.mvset) then
                 pot(m,njt)=vtot
              else
                 pot(m,njt)=0.
              endif
           endif
           if(ivu(m).eq.1) c(ivar(m,nmb(m)+ipu(m)+ivu(m)),njt)=0.
           if(kontrol.eq.1) then
              if(m.eq.mcro) then
                 if(lrcro.eq.-1) c(ivar(m,ir),njt+nj(m)-1)=
     &                           c(ivar(m,ir),njt)
              endif
           endif
c       Make an initial guess for each j.
           do 18 j=njt,njt+nj(m)-1
                 if(j.eq.njt) yy(m,j)=0.
                 if(j.gt.njt) h(m,j)=1./dfloat(nj(m)-1)
                 if(j.gt.njt) yy(m,j)=yy(m,j-1)+h(m,j)
                 if(m.eq.2) then
                    ff=0.0605
                    zjmid=dfloat(nj(m)-1)/2.+njt
                    if(j.gt.njt) yy(m,j)=1./(1.+exp(-(dfloat(j)-zjmid)
```

```
&              *ff))
               if(j.gt.njt) h(m,j)=yy(m,j)-yy(m,j-1)
            endif
            if(m.eq.3) then
               ff=0.125
               if(j.gt.njt) yy(m,j)=dexp(dfloat(j-njt-1)*ff)
&                                  /dexp(dfloat(nj(m)-2)*ff)
               if(j.gt.njt) h(m,j)=yy(m,j)-yy(m,j-1)
            endif
            if(j.eq.njt+nj(m)-1) yy(m,j)=1.
            if(j.eq.njt+nj(m)-1) h(m,j)=yy(m,j)-yy(m,j-1)
            if(ivu(m).eq.0) then
               if(vlr(m).gt.0) yd=(1.-yy(m,j))*zlen(m)/delta
               if(vlr(m).lt.0) yd=yy(m,j)*zlen(m)/delta
               v(m,j)=vlr(m)*const*yd*difz/delta
               if(mode(m).eq.4) then
                 ze=yd*(3./aa)**(1./3.)*scm3
                  v(m,j)=v(m,j)*yd
&                 *(1.0-ze/aa*(1./3.+bb/6.*ze+(bb*ze)**2/30.
&                 +aa*ze**3/180.-(1.-4.*aa*bb)*ze**4/1260.))
               endif
               vl(m,j)=v(m,j)
            else
               i=ivar(m,nmb(m)+ipu(m)+ivu(m))
               c(i,j)=c(i,njt)
            endif
            if(ipu(m).eq.1) then
               i=ivar(m,nmb(m)+ipu(m))
               if(m.eq.2) then
                  fctr=(1.-yy(m,j))*zlen(m)/db(m)
                  if(fctr.gt.9.2) then
                     c(i,j)=c(i,njt)
                  else
                     c(i,j)=c(i,njt)+(c(i,njt+nj(m)-1)-
&                        c(i,njt))*dexp(-fctr)
                  endif
               endif
               if(m.eq.3) then
                  c(i,njt+nj(m)-1)=0.
                  fctr=yy(m,j)*zlen(m)/db(m)
                  if(fctr.gt.9.2) then
                     c(i,j)=c(i,njt+nj(m)-1)
                  else
                     c(i,j)=c(i,njt)*dexp(-fctr)
                  endif
               endif
            else
               pot(m,j)=pot(m,njt)
            endif
            if(ivar(m,ir).ne.0) c(ivar(m,ir),j)=c(ivar(m,ir),njt)
            if(kontrol.eq.1) then
```

```
                  if(m.eq.mcro) then
                     if(lrcro.eq.-1) then
                        c(ivar(m,ir),j)= cr0+(c(ivar(m,ir),njt+nj(m)-1)
     &                  -cr0)*dfloat(j-njt)/dfloat(nj(m)-1)
                     else
                        c(ivar(m,ir),j)= cr0+(c(ivar(m,ir),njt)-cr0)
     &                  *dfloat(njt+nj(m)-1-j)/dfloat(nj(m)-1)
                     endif
                  endif
               endif
               do 18 ii=1,nsp(m)
                    if(i.eq.ir) goto 18
                    if(mb(m,ii).eq.0) goto 18
                    i=ivar(m,ii)
                    c(i,j)=c(i,njt)
   18               continue
            njt=njt+nj(m)-1
            ji(m+1)=njt
            neqt=neqt+nmb(m)+ipu(m)+ivu(m)
   19       continue
         njsum=3
      do 51 m=2,nph
            do 50 j=njsum,njsum+nj(m)-1
                  if(m.eq.2) then
                     read (5,*) (yyy,c(1,j)
     &               ,c(2,j),c(3,j),(c(ivar(m,i),j),
     &                              i=1,nmb(m)),c(6,j))
                  else
                     read (5,*) (yyy,c(1,j)
     &               ,c(2,j),c(3,j),(c(ivar(m,i),j),
     &                              i=1,nmb(m)),c(13,j))
                  endif
   50             continue
            njsum=njsum+nj(m)-1
   51       continue
      velsav=-c(2,4)
c
c     jtime : the time stepping loop.
c     jkon3 : the loop when converging on a particular total
c       total current (kontrol=3.)
c
      time=0.
      timetot=1.0d05
      itcount=0
      potset=+600.0
      potprint=0.0
      swr=+1.0
      dt=0.
      nflag=0
      iflg=0
      jtime=0
```

```
   20 jtime=jtime+1
      if(jtime.gt.400) goto 36
      if(time.ge.timetot) then
         print *,'time is greater than 1.3e07.'
         goto 36
      endif
      itcount=itcount+1
      if(time.eq.0.) itcount=0
      if(itcount.ge.10) then
         itcount=0
         goto 36
      endif
      if(pot(1,3).ge.potset) goto 36
      if(pot(1,3).ge.potprint) then
         potprint=potprint+500.
         goto 36
      endif
      if(pot(1,3).lt.potset) then
         if(dif(2,1).gt.2.0e-16) then
            dif(2,1)=dif(2,1)/(10.)**(1./3.)
            if(dif(2,1).lt.2.0e-16) dif(2,1)=2.0e-16
            dt=0.
         else
            if(c(9,ji(4)).gt.1.e-11) then
               c(9,ji(4))=1.e-11
               c(11,ji(4))=0.05+1.e-11
               cin(3,2)=1.e-11
               cin(3,4)=0.05+1.e-11
               dt=0.
            else
               if(inft(3,1).eq.1) then
                  inft(3,1)=0
                  dt=0.
               else
                  if(inft(3,3).eq.1) then
                     inft(3,3)=0
                     dt=0.
                  else
c                 if(inft(3,2).eq.1) then
c                    inft(3,2)=0
c                    dt=0.
c                 else
c                       if(iflg.eq.0) then
c                          iflg=1
c                          goto 36
c                       endif
c                    if(aj.lt.3.5d-8) then
c                       aj=aj*(10.)**(1./3.)
c                       if(aj.gt.3.5d-8) aj=3.5d-8
c                       dt=0.
c                    else
```

```
                    if(pot(1,3).lt.-251.2) then
                       swr=1.
                       dt=1.
                    endif
                    if(dt.gt.70) dt=70.
c                 endif
                  endif
c              endif
               endif
            endif
         endif
         if(pot(1,3).ge.-251.2) swr=0.3
         pot(1,3)=pot(1,3)+swr*dt
         vtot=vtot+swr*dt
         if(pot(1,3).le.-251.2) dt=0.
      endif
      print *,vtot,dif(2,1),jtime,'aj=',aj
c     if(dt.gt.0. .and. time.eq.0.) then
c        if(nflag.eq.0) then
c           nflag=1
c           goto 36
c        endif
c     endif
      print *,'dt = ',dt
      zleno=zlen(2)
      do 21 m=1,nph
           zlen(m)=zlen(m)+(vi(m+1)-vi(m))*dt
           if(zlen(m).le.0.) then
              zlen(m)=0.
              print *, time,'length of phase',m,'=0'
              goto 36
           endif
   21      continue
c
c     Add a mesh point at jmid of phase two.
c
      if(zlen(2).le.zleno) goto 43
      nj(2)=nj(2)+1
      njt=njt+1
      if(njt.gt.401) then
          print *,'Too many time steps = too many js'
          stop
      endif
      jmid=(nj(2)-1)/2+ji(2)
      do 46 m=nph,2,-1
            ji(m+1)=ji(m+1)+1
            jf=ji(m)
            if(m.eq.2) jf=jmid+1
            do 46 j=ji(m+1)-1,jf,-1
                     yy(m,j+1)=yy(m,j)
                     h(m,j+1)=h(m,j)
```

```
                    v(m,j+1)=v(m,j)
                    vl(m,j+1)=vl(m,j)
                    if(ipu(m).eq.0) pot(m,j+1)=pot(m,j)
                    do 48 i=1,neqt
                          c(i,j+1)=c(i,j)
                          cc(i,j+1)=cc(i,j)
 48                       continue
                 if(j.eq.jmid+1) then
                    v(m,j)=(v(m,j+1)+v(m,j-1))/2.
            vl(m,j)=(vl(m,j+1)+vl(m,j-1))/2.
                    do 49 i=1,neqt
                          c(i,j)=(c(i,j+1)+c(i,j-1))/2.
                          cc(i,j+1)=(cc(i,j+1)+cc(i,j-1))/2.
 49                       continue
                 endif
 46              continue
    zloln=zleno/zlen(2)
    yy(2,ji(2))=0.
    do 47 j=ji(2),ji(3)
          if(j.le.jmid) yy(2,j)=yy(2,j)*zloln
          if(j.eq.jmid+1) yy(2,j)=yy(2,j-1)+(1.-zloln)
          if(j.gt.jmid+1) yy(2,j)=1.-(1.-yy(2,j))*zloln
          if(j.eq.ji(3)) yy(2,j)=1.
          if(j.gt.ji(2)) h(2,j)=yy(2,j)-yy(2,j-1)
 47       continue
 43 time=time+dt
    mf=0
    nf=0
    jkon3=0
 22 jkon3=jkon3+1
    if(jkon3.gt.100) go to 36
c
c     autoband sets up the the program to fill the variables
c       necessary for band.
c
      call autoband
c
c     Now check to see if the current has converged and change
c       potential if it has not.
c     When the program comes back from autoband so does the converged
c       solution.
c
      njsum=1
      do 40 m=1,nph
           if(m.ge.mvi) then
              vi(m+1)=c(m,njsum+nj(m)-1)
           else
              vi(m)=c(m,njsum)
           endif
 40        njsum=njsum+nj(m)-1
      curmax=0
```

```
      mmax=0
      lmax=0
      do 23 m=1,nph
            if(dabs(curmax).lt.dabs(currsav(m+1))) then
               curmax=currsav(m+1)
               mmax=m+1
               endif
23             continue
      if(kontrol.eq.3) then
         dfrn=curmax-ctot
         if(ctot.eq.0.) then
            if(dabs(dfrn).le.1.d-12) goto 34
         else
            if(dabs(dfrn).le.1.d-6*ctot) goto 34
         endif
         if(nf.ne.0) goto 31
         if(mf) 27,24,28
24          if(dfrn) 25,34,26
25             potdfo=vtot
               vtot=vtot+20.
               mf=-1
            go to 22
26             potdfo=vtot
               vtot=vtot-20.
               mf=1
            go to 22
27          if(dfrn) 25,34,29
28          if(dfrn) 29,34,26
29             potdfo2=potdfo
               potdfo=vtot
30             vtot=(potdfo+potdfo2)/2.
               nf=1
            go to 22
31       if(dfrn) 32,34,33
32          potdfo2=max(potdfo,potdfo2)
            potdfo=vtot
         go to 30
33          potdfo2=min(potdfo,potdfo2)
            potdfo=vtot
         go to 30
      endif
34 continue
      print 832
      print 831, time,(zlen(m), m=1,nph)
      print 830
      print 831, time,(vi(m),m=1,nph+1)
      cife=c(4,ji(3))
      ce=c(5,ji(3))
      cfe2=c(9,ji(3))
      cfeoh=c(10,ji(3))
      coh=c(11,ji(3))/c(12,ji(3))*1.d-5
```

```
      cdp=c(6,ji(3))-c(13,ji(3))
      cpa=c(6,ji(3))
      cpb=c(13,ji(3))
      write (4,890), time,vtot,zlen(2),currsav(3),cursav(ji(4)-5)
     &,rate1,rate2,rate3,vi(3),cife,ce,cfe2,cfeoh,coh,cpa,cpb
 890  format (16(e15.8,', '))
      dt=3600.*240.
      do 35 m=1,nph
           if(dabs(vi(m+1)-vi(m)).eq.0.) goto 35
           dxv=zlen(m)/dabs(vi(m+1)-vi(m))/10.
           if(dt.gt.dxv) dt=dxv
   35      continue
      goto 20
   36 continue
c
c     Print the concentrations at the two ends of each phase.
c
      j=1
      do 38 m=1,nph
           if(nmb(m).eq.0) goto 38
           print 813
           do 37 ii=1,nsp(m)
                if(mb(m,ii).eq.0) then
                   print 814, ref(m,ii),cin(m,ii),cin(m,ii)
                else
                   i=ivar(m,ii)
                   print 814, ref(m,ii),c(i,j),c(i,j+nj(m)-1)
                endif
   37           continue
           print 814, 'phi',c(ivar(m,nmb(m)+ipu(m)),j),c(ivar
     &         (m,nmb(m)+ipu(m)),j+nj(m)-1)
           print 840, m,currsav(m)
   38      j=j+nj(m)-1
  840 format (30h The current density in phase ,i2,4h is ,e12.5,
     &9h mA/cm**2)
      write (3,*) 'time=',time,'    V=',vtot,'    L=',zlen(2),
     & '   jcount=',jcosav
      njsum=1
      do 41 m=1,nph
           do 42 j=njsum,njsum+nj(m)-1
                if(m.eq.2) then
                   write (3,893) (yy(m,j)+m-mvi,c(1,j)
     &             ,c(2,j),c(3,j),(c(ivar(m,i),j),
     &                           i=1,nmb(m)),c(6,j))
                else
                   write (3,891) (yy(m,j)+m-mvi,c(1,j)
     &             ,c(2,j),c(3,j),(c(ivar(m,i),j),
     &                           i=1,nmb(m)),c(13,j))
                endif
   42           continue
           njsum=njsum+nj(m)-1
```

```
  41      continue
 893 format (7(e15.8,1x))
 891 format (10(e15.8,1x))
c
c     Continue to next time step or not?
c
      if(jtime.lt.400) then
         if(vtot.lt.potset) goto 20
c        if(time.lt.timetot) goto 20
      endif
   39 if(jkon3.gt.100) print 812, jkon3
      if(jkon3.le.100) print *,'jkon3 =',jkon3
      if(kontrol.eq.3) print 821, ctot,curmax,mmax,lmax
      if(kontrol.eq.3) print 822, vtot
      if(kontrol.eq.2) print 823, vtot,curmax
      if(kontrol.eq.1) print 824, ref(mcro,idlr(mcro)),vtot,curmax
 102  format (i2,5(2x,e15.7))
      stop
      end
c -------------------------------------------------------
      Subroutine autoband
      implicit real*8 (a-h,o-z)
      dimension dc(25),eq(25),vi(6),small(25)
      common /ablk/a(25,25),b(25,25),c(25,401),d(25,51),g(25),
     & x(25,25),y(25,25),n,nj
      common /bblk/ njm(5),nmb(5),ipu(5),ivu(5),cc(25,401)
     & ,pot(5,401),z(5,25)
      common /cblk/ nph,nsp(5),mb(5,15),ivar(5,25)
      common /eblk/ nhtr(5,2),pt(5,2,15,15),qt(5,2,15,15),
     & st(5,2,15,15),inft(6,15),rkba(6,15),equilt(6,15),
     & be(6,15),zks(5,2,25),curl(6),curr(6)
      common /gblk/ zlen(5),ninfm(5),rkbv(5,15),h(5,401),perm(5),f
     & ,ccsav(25,401),csav(25,401),yy(5,401)
      common /iblk/ aj,u(5,15),dif(5,15),frt,co
      common /hblk/ mvi,nhmr(5),cin(5,15),equilm(5,15),
     & v(5,401),vl(5,401)
      common /mblk/ zmn(25,25),zmv(25,25),ie(25),p(25,25),
     &q(25,25),s(25,25),dum(5,2,25)
      common /test/ err(5,2),jcount,jco,jcosav
      common/rate/velsav,vel,vell,rrxn(25),cur(401),cursav(401),jtime
     & ,flxs(401,15),flxsav(401,15),chd(401),chdsav(401),currsav(6)
      common /nblk/ rate1,rate2,rate3,time,ji(6)
c
c     Define the following parameters.
c     a,b,d,g,x, and y are the matrices to be filled for
c       Newman's band subroutine.
c     cc : stores the last values of c.
c     dc : a chosen difference from the last solution to be
c       used to determine the slope to the next guess.
c     ifrt : first equation number in the phase.
c     ilst : last equation number in the phase.
```

```
c     jcount : loops through the equations due to their
c       non-linearity.
c     njmsum : sums the number of mesh points in each phase.
c     noconvg : indicates if the solution has converged (=0.)
c
c     co=c(5,3)*dexp(z(2,2)*frt*pot(1,3))+212.65078d0
      co=c(5,3)*dexp(z(2,2)*frt*pot(1,3))
c     co=c(5,3)*dexp(z(2,2)*frt*c(6,3))
c     velsav=0.d0
      jcount=0
      jco=0
      vellow=0.d0
      velhi=0.d0
    1 jcount=jcount+1
      jco=jco+1
      noconvg=0
      do 26 m=1,nph+1
            if(m.lt.mvi) vi(m)=c(m,1)
            if(m.eq.mvi) vi(m)=0.
            if(m.gt.mvi) vi(m)=c(m-1,1)
   26       continue
      nj1=1
      nj2=1
      do 2 m=1,nph
           nj2=nj2+njm(m)-1
           do 24 j=nj1,nj2
                if(ivu(m).eq.0) then
                   if(m.lt.mvi) vl(m,j)=v(m,j)+vi(m+1)
                   if(m.ge.mvi) vl(m,j)=v(m,j)+vi(m)
                endif
                do 21 i=1,n
                if(ipu(m).eq.0) po=pot(m,j)
                if(ipu(m).eq.1) po=c(ivar(m,nmb(m)+1),j)
                do 22 ii=1,nsp(m)
                      if(mb(m,ii).eq.0) goto 22
                      if(i.eq.ivar(m,ii)) then
                         if(jcount.eq.1) then
                            cc(i,j)=c(i,j)*dexp(z(m,ii)*frt*po)
                            if(m.eq.2 .and. i.eq.5) cc(i,j)=cc(i,j)-co
                         endif
                         if(jco.eq.1) ccsav(i,j)=cc(i,j)
                         if(jco.eq.1) csav(i,j)=c(i,j)
                         goto 21
                      endif
   22                 continue
                if(j.eq.nj) goto 25
                if(j.ne.nj2) goto 25
                if(ipu(m+1).eq.0) po=pot(m+1,j)
                if(ipu(m+1).eq.1) po=c(ivar(m+1,nmb(m+1)+1),j)
                if(ivu(m+1).eq.0) then
                   if(m+1.lt.mvi) vl(m+1,j)=v(m+1,j)+vi(m+2)
```

```
                if(m+1.ge.mvi) vl(m+1,j)=v(m+1,j)+vi(m+1)
            endif
            do 23 ii=1,nsp(m+1)
                 if(mb(m+1,ii).eq.0) goto 23
                 if(i.eq.ivar(m+1,ii)) then
                    if(jcount.eq.1) then
                       cc(i,j)=c(i,j)*dexp(z(m+1,ii)*frt*po)
                       if(m+1.eq.2 .and. i.eq.5) cc(i,j)=cc(i,j)-co
                    endif
                    if(jco.eq.1) ccsav(i,j)=cc(i,j)
                    if(jco.eq.1) csav(i,j)=c(i,j)
                    goto 21
                 endif
23               continue
25               continue
            cc(i,j)=c(i,j)
            if(jco.eq.1) csav(i,j)=c(i,j)
21          continue
24          continue
        nj1=nj2+1
 2      continue
   do 3 i=1,n
        do 3 k=1,n
            y(i,k)=0.d0
 3          x(i,k)=0.d0
   m=1
   ifrt=nph+1
   ilst=nph+nmb(m)+ipu(m)+ivu(m)
   njmsum=njm(m)
   j=0
   print *, 'jcount=',jcount,' vell',vell
 4 j=j+1
   if(j.eq.nj) goto 5
   if(j.eq.njmsum) then
      ilst=ilst+nmb(m+1)+ipu(m+1)+ivu(m+1)
   endif
   if(j.gt.njmsum) then
      ifrt=ifrt+nmb(m)+ipu(m)+ivu(m)
      m=m+1
      njmsum=njmsum+njm(m)-1
   endif
 5 do 6 i=1,n
        g(i)=0.0d0
        if(i.lt.ifrt) g(i)=c(i,j)
        if(i.gt.ilst) g(i)=c(i,j)
        if(i.le.nph) g(i)=0.d0
        do 6 k=1,n
            a(i,k)=0.0d0
            d(i,k)=0.0d0
            b(i,k)=0.0d0
            if(i.lt.ifrt) b(i,i)=-1.
```

```
            if(i.gt.ilst) b(i,i)=-1.
            if(i.le.nph) b(i,i)=0.
 6          continue
   call eqn(j,eq,1,1,0.0d0,m,njmsum)
    if(j.eq.ji(3)) rate1=96487.0*rrxn(1)
    if(j.eq.ji(3)) rate2=3.0*96487.0*rrxn(2)
    if(j.eq.ji(3)) rate3=2.0*96487.0*rrxn(3)
    if(j.eq.ji(3)) vell=vel
    cursav(j)=cur(j)
    chdsav(j)=chd(j)
    if(j.eq.ji(2)) currsav(2)=curr(2)
    if(j.eq.ji(3)) currsav(3)=curr(3)
    do 44 ii=1,nsp(m)
44        flxsav(j,ii)=flxs(j,ii)
   n1=1
   n2=nph
50 do 7 i=n1,n2
        dc(i)=1.d-3*cc(i,j)
        if(i.eq.6 .and. dc(i).eq.0) dc(i)=1.d-1
        if(i.eq.13 .and. dc(i).eq.0) dc(i)=1.d-1
        if(i.eq.4 .and. dc(i).eq.0) dc(i)=1.d-6
        if(i.eq.5 .and. dc(i).eq.0) dc(i)=1.d2
        if(dabs(dc(i)).eq.0.) dc(i)=1.d-3
 7      g(i)=eq(i)
   if(n1.eq.1) then
      n1=ifrt
      n2=ilst
      goto 50
   endif
   n1=1
   n2=nph
51 do 12 k=n1,n2
        call eqn(j,eq,j,k,dc(k),m,njmsum)
        m1=1
        m2=nph
52      do 8 i=m1,m2
 8           b(i,k)=-(eq(i)-g(i))/dc(k)
        if(m1.eq.1) then
           m1=ifrt
           m2=ilst
           goto 52
        endif
        if(j.eq.1) goto 10
        call eqn(j,eq,j-1,k,dc(k),m,njmsum)
        m1=1
        m2=nph
53      do 9 i=m1,m2
 9           a(i,k)=-(eq(i)-g(i))/dc(k)
        if(m1.eq.1) then
           m1=ifrt
           m2=ilst
```

```
          goto 53
        endif
10      m1=1
        m2=nph
        if(j.eq.nj) goto 12
        call eqn(j,eq,j+1,k,dc(k),m,njmsum)
54      do 11 i=m1,m2
11           d(i,k)=-(eq(i)-g(i))/dc(k)
        if(m1.eq.1) then
           m1=ifrt
           m2=ilst
           goto 54
        endif
12 continue
   if(n1.eq.1) then
      n1=ifrt
      n2=ilst
      goto 51
   endif
   call band(j)
   if(j.lt.nj) goto 4
   m=1
   njsum=njm(m)
   small(5)=1.d3
   small(4)=1.d-16
   small(8)=cin(3,1)
   small(9)=cin(3,2)
   small(10)=cin(3,3)
   small(11)=cin(3,4)
   small(12)=cin(3,5)
   do 18 j=1,nj
17         if(ipu(m).eq.1) then
              i=ivar(m,nmb(m)+ipu(m))
              if(dabs(c(i,j)).gt.1.d-8) then
   noconvg=noconvg+1
   endif
              if(cc(i,j).ne.0.) then
                 if(dabs(c(i,j)).gt.dabs(1.d-10*cc(i,j))) then
                    noconvg=noconvg+1
                 endif
              endif
              if(jcount.lt.10 .or. jtime.le.1) then
              if(c(i,j).gt.20.) c(i,j)=20.
              if(c(i,j).lt.-20.) c(i,j)=-20.
              endif
              c(i,j)=cc(i,j)+c(i,j)
           endif
           if(ipu(m).eq.0) po=pot(m,j)
           if(ipu(m).eq.1) po=c(ivar(m,nmb(m)+1),j)
           do 14 ii=1,nsp(m)
                if(mb(m,ii).eq.0) goto 14
```

```
                i=ivar(m,ii)
                if(cc(i,j).eq.0.) then
                   if(i.eq.5) then
                      if(c(i,j).lt.-co) c(i,j)=-1.e-3*co
                   else
                      if(c(i,j).lt.0.) c(i,j)=dabs(0.001*c(i,j))
                   endif
                   if(dabs(c(i,j)).gt.1.e-8) noconvg=noconvg+1
                else
                   if(jcount.lt.10 .or. jtime.le.1) then
                   if(i.eq.5) then
                      if(c(i,j).lt.-0.9*(co+cc(i,j))) c(i,j)=-.9
 &                          *(co+cc(i,j))
                      if(c(i,j).gt.9.*(co+cc(i,j))) c(i,j)=9.
 &                          *(co+cc(i,j))
                   else
                      if(c(i,j).lt.-0.9*cc(i,j)) c(i,j)=-.9*cc(i,j)
                      if(c(i,j).gt.9.*cc(i,j)) c(i,j)=9.*cc(i,j)
                   endif
                   endif
  if(i.ne.5) then
  if(dabs(c(i,j)).gt.dabs(1.e-10*cc(i,j))) then
  noconvg=noconvg+1
  endif
  else
                   if(dabs(c(i,j)).gt.dabs(1.e-10*cc(i,j))
 &                 .and. dabs(c(i,j)).gt.1.e-8) then
                   noconvg=noconvg+1
  endif
  endif
                endif
                ccc=cc(i,j)
                cc(i,j)=cc(i,j)+c(i,j)
                c(i,j)=cc(i,j)*dexp(-z(m,ii)*frt*po)
                if(m.eq.2 .and. i.eq.5) c(i,j)=(cc(i,j)+co)
 &              *dexp(-z(m,ii)*frt*po)
14              continue
            if(ivu(m).eq.1) then
               i=ivar(m,nmb(m)+ipu(m)+ivu(m))
               if(cc(i,j).eq.0.) then
                  if(dabs(c(i,j)).gt.1.e-5) then
                     if(c(i,j).lt.0.) c(i,j)=-1.e-5
                     if(c(i,j).gt.0.) c(i,j)=1.e-5
                  endif
                  if(dabs(c(i,j)).gt.1.d-10) then
                  noconvg=noconvg+1
  endif
               else
                  if(jcount.lt.10 .or. jtime.le.1) then
                  if(c(i,j).lt.-1.e-5) c(i,j)=-1.e-5
                  if(c(i,j).gt.1.e-5) c(i,j)=1.e-5
```

```
                 endif
                 if(dabs(c(i,j)).gt.dabs(1.d-10*cc(i,j))) then
                    noconvg=noconvg+1
                 endif
              endif
              c(i,j)=cc(i,j)+c(i,j)
           endif
           if(j.eq.nj) goto 16
           if(j.ne.njsum) goto 16
              m=m+1
              njsum=njsum+njm(m)-1
              goto 17
 16        do 18 mm=1,nph
              if(cc(mm,j).eq.0.) then
                 if(dabs(c(mm,j)).gt.1.d-5) then
                    if(c(mm,j).lt.0.) c(mm,j)=-1.d-5
                    if(c(mm,j).gt.0.) c(mm,j)=1.d-5
                 endif
                 if(dabs(c(mm,j)).gt.1.d-8) then
                 noconvg=noconvg+1
    endif
              else
                 if(jcount.lt.10 .or. jtime.le.1) then
                 if(c(mm,j).lt.-1.d-5) c(mm,j)=-1.d-5
                 if(c(mm,j).gt.1.d-5) c(mm,j)=1.d-5
                 endif
                 if(dabs(c(mm,j)).gt.dabs(1.d-10*cc(mm,j))) then
                    noconvg=noconvg+1
                 endif
              endif
              c(mm,j)=cc(mm,j)+c(mm,j)
 18        continue
104 format (4e15.8)
103 format (3i4,' vell=',e15.7,' velsav=',e15.7)
    if(noconvg.eq.0) goto 20
893 format (7(e15.8,1x))
891 format (10(e15.8,1x))
    if(jcount.lt.400) goto 1
    print *,'Did not converge'
 20 print *, 'jcount=',jcount
    jcosav=jcount
    if(dabs(vell-velsav).gt.1.d-10*dabs(vell)) then
       jco=0
       if(jcount.gt.399) return
       if(velhi.eq.0.d0) then
          velhi=velsav
          velhil=vell
          velsav=vell
       else
          vellow=velhi
          vellol=velhil
```

```
            velhi=velsav
            velhil=vell
            velsav=(velhil*vellow-vellol*velhi)
     &              /(vellow-velhi-vellol+velhil)
         endif
         go to 1
       endif
   31 return
       end
c ------------------------------------------------------------
       Subroutine eqn(j,eq,jp,k,dc,m,njmsum)
       implicit real*8 (a-h,o-z)
       dimension eq(25)
       common /ablk/a(25,25),b(25,25),c(25,401),d(25,51),g(25),
     & x(25,25),y(25,25),n,nj
       common /bblk/ njm(5),nmb(5),ipu(5),ivu(5),cc(25,401)
     & ,pot(5,401),z(5,25)
       common /cblk/ nph,nsp(5),mb(5,15),ivar(5,25)
       common /fblk/ vtot,mvset,moset,lrvset,lroset,pm(5,15,15),
     & qm(5,15,15),sm(5,15,15),infm(5,15)
       common /iblk/ aj,u(5,15),dif(5,15),frt,co
       common /nblk/ rate1,rate2,rate3,time,ji(6)
       common /test/ err(5,2),jcount,jco,jcosav
       csave=c(k,jp)
       c(k,jp)=c(k,jp)+dc
       mm=m
    5  do 6 ii=1,nsp(mm)
            if(mb(mm,ii).eq.0) goto 6
            if(k.ne.ivar(mm,ii)) goto 6
            csave=cc(k,jp)
            cc(k,jp)=cc(k,jp)+dc
            goto 7
    6       continue
    7  if(ipu(mm).eq.0) po=pot(mm,jp)
       if(ipu(mm).eq.1) po=c(ivar(mm,nmb(mm)+1),jp)
       do 8 ii=1,nsp(mm)
            if(mb(mm,ii).eq.0) goto 8
            i=ivar(mm,ii)
            c(i,jp)=cc(i,jp)*dexp(-z(mm,ii)*frt*po)
            if(mm.eq.2 .and. i.eq.5) c(i,jp)=(cc(i,jp)+co)
     &                               *dexp(-z(mm,ii)*frt*po)
    8       continue
       if(j.ne.njmsum) goto 9
       if(mm.eq.m+1) goto 9
       mm=m+1
       goto 5
    9  if(j.ne.1) goto 1
       call eqnlnj(j,eq,m,njmsum)
       goto 4
    1  if(j.ne.nj) goto 2
       call eqnlnj(j,eq,m,njmsum)
```

```
      goto 4
    2 if(j.ne.njmsum) goto 3
      call eqni(j,eq,m,njmsum)
      goto 4
    3 call eqnj(j,eq,m,njmsum)
    4 continue
      c(k,jp)=csave
      mm=m
   10 do 11 ii=1,nsp(mm)
           if(mb(mm,ii).eq.0) goto 11
           if(k.ne.ivar(mm,ii)) goto 11
           cc(k,jp)=csave
           goto 12
   11      continue
   12 if(ipu(mm).eq.0) po=pot(mm,jp)
      if(ipu(mm).eq.1) po=c(ivar(mm,nmb(mm)+1),jp)
      do 13 ii=1,nsp(mm)
           if(mb(mm,ii).eq.0) goto 13
           i=ivar(mm,ii)
           c(i,jp)=cc(i,jp)*dexp(-z(mm,ii)*frt*po)
           if(mm.eq.2 .and. i.eq.5) c(i,jp)=(cc(i,jp)+co)
     &                              *dexp(-z(mm,ii)*frt*po)
   13      continue
      if(j.ne.njmsum) goto 14
      if(mm.eq.m+1) goto 14
      mm=m+1
      goto 10
   14 return
      end
c -----------------------------------------------------------------
      Subroutine eqnlnj(j,eq,m,njmsum)
      implicit real*8(a-h,o-z)
      dimension eq(25),ic(25),ih(25)
      common /ablk/a(25,25),b(25,25),c(25,401),d(25,51),g(25),
     & x(25,25),y(25,25),n,njt
      common /bblk/ nj(5),nmb(5),ipu(5),ivu(5),cc(25,401)
     & ,pot(5,401),z(5,25)
      common /cblk/ nph,nsp(5),mb(5,15),ivar(5,25)
      common /fblk/ vtot,mvset,moset,lrvset,lroset,pm(5,15,15),
     & qm(5,15,15),sm(5,15,15),infm(5,15)
      common /hblk/ mvi,nhmr(5),cin(5,15),equilm(5,15),
     & v(5,401),vl(5,401)
      common /mblk/ zmn(25,25),zmv(25,25),ie(25),p(25,25),
     & q(25,25),s(25,25),dum(5,2,25)
c
c     Boundary condition at the far left and right.
c
      do 1 ml=1,nph
           do 1 i=1,n
                dum(ml,1,i)=1.
                ih(i)=0
```

```
                ic(i)=0
                do 1 k=1,n
                     p(i,k)=0.
                     q(i,k)=0.
                     s(i,k)=0.
                     zmn(i,k)=0.
    1                zmv(i,k)=0.
      do 2 ii=1,nsp(m)
           if(mb(m,ii).eq.0) goto 2
           i=ivar(m,ii)
           zmn(i,i)=1.
           ic(i)=0
           do 20 l=1,nhmr(m)
                p(i,l)=pm(m,ii,l)
                q(i,l)=qm(m,ii,l)
                s(i,l)=p(i,l)-q(i,l)
                zmv(i,l)=s(i,l)
   20           continue
    2      continue
      do 3 l=1,nhmr(m)
    3      ih(l)=infm(m,l)
      call eqnprod(zmv,zmn,ih,ie,n,nhmr(m))
c
c     Equilibrium conditions
c
      do 4 ll=1,nhmr(m)
           l=ie(ll)
           call eqlbr(eq,ic,zmv,m,s,l,dum,l,j,j,equilm,l)
    4      continue
c
c     Electroneutrality
c
      do 8 iii=1,nsp(m)
           if(mb(m,iii).ne.0) goto 8
           do 7 l=1,nhmr(m)
                if(sm(m,iii,l).eq.0.) goto 7
                do 6 ii=1,nsp(m)
                     if(mb(m,ii).eq.0) goto 6
                     if(sm(m,ii,l).eq.0.) goto 6
                     i=ivar(m,ii)
                     if(ic(i).eq.1) goto 6
                     if(z(m,ii).eq.0.) goto 6
                     eq(i)=0.
                     do 5 kk=1,nsp(m)
                          k=ivar(m,kk)
                          if(mb(m,kk).eq.1) then
                             eq(i)=eq(i)+z(m,kk)*c(k,j)
                          else
                             eq(i)=eq(i)+z(m,kk)*cin(m,kk)
                          endif
    5                     continue
```

```
                    ic(i)=1
                    goto 9
    6               continue
    7           continue
    8       continue
    9 continue
c
c     Mole conservation
c
      do 11 ii=1,nsp(m)
           if(mb(m,ii).eq.0) goto 11
           i=ivar(m,ii)
           if(ic(i).eq.1) goto 11
           eq(i)=0.
           do 10 kk=1,nsp(m)
                if(mb(m,kk).eq.0) goto 10
                k=ivar(m,kk)
                eq(i)=eq(i)+zmn(i,k)*(c(k,j)-cin(m,kk))
   10           continue
           ic(i)=1
   11      continue
c
c     Set potential
c
      if(ipu(m).eq.0) then
         if(m.eq.mvset) then
            pot(m,j)=vtot
         else
            pot(m,j)=0.
         endif
      else
         i=ivar(m,nmb(m)+ipu(m))
         if(m.eq.mvset) then
            eq(i)=c(i,j)-vtot
         else
            eq(i)=c(i,j)
         endif
      endif
c
c     Set velocity
c
      if(j.eq.1) then
         if(mvi.eq.1) then
            if(ivu(m).eq.1) then
               i=ivar(m,nmb(m)+ipu(m)+1)
               eq(i)=c(i,j)
            endif
            do 15 mm=1,nph
   15            eq(mm)=c(mm,j)-c(mm,j+1)
         else
            if(ivu(m).eq.1) then
```

```
            i=ivar(m,nmb(m)+ipu(m)+1)
            eq(i)=c(i,j)-c(i,j+1)
         endif
         if(mvi.eq.2) then
            eq(m)=c(m,j)
         else
            eq(m)=c(m,j)-c(m+1,j)
         endif
         do 16 mm=2,nph
16             eq(mm)=c(mm,j)-c(mm,j+1)
      endif
   else
      if(mvi.eq.nph+1) then
         if(ivu(m).eq.1) then
            i=ivar(m,nmb(m)+ipu(m)+1)
            eq(i)=c(i,j)
         endif
         do 17 mm=1,nph
17             eq(mm)=c(mm,j)-c(mm,j-1)
      else
         if(ivu(m).eq.1) then
            i=ivar(m,nmb(m)+ipu(m)+1)
            eq(i)=c(i,j)-c(i,j-1)
         endif
         if(mvi.eq.nph) then
            eq(m)=c(m,j)
         else
            eq(m)=c(m,j)-c(m-1,j)
         endif
         do 18 mm=1,nph-1
18             eq(mm)=c(mm,j)-c(mm,j-1)
      endif
   endif
   return
   end
c ------------------------------------------------------------
   Subroutine eqni(j,eq,m,njmsum)
   implicit real*8(a-h,o-z)
   dimension eq(25),ic(25),pi(25,25),qi(25,25),si(25,25),
  & zmvi(25,25),zmni(25,25),
  & ih(25),rflx(25),
  & ihi(25),iei(25),pti(5,15,15),qti(5,15,15),
  & sti(5,15,15),ptii(5,15,15),qtii(5,15,15),stii(5,15,15),vi(6)
   common /ablk/a(25,25),b(25,25),c(25,401),d(25,51),g(25),
  & x(25,25),y(25,25),n,njt
   common /bblk/ nj(5),nmb(5),ipu(5),ivu(5),cc(25,401)
  & ,pot(5,401),z(5,25)
   common /cblk/ nph,nsp(5),mb(5,15),ivar(5,25)
   common /dblk/ kontrol,cr0,mcro,lrcro,idlr(5),den(5),zmw(5),
  & blen(6),ltcs(5,15)
   common /eblk/ nhtr(5,2),pt(5,2,15,15),qt(5,2,15,15),
```

```
     & st(5,2,15,15),inft(6,15),rkba(6,15),equilt(6,15),
     & be(6,15),zks(5,2,25),curl(6),curr(6)
      common /fblk/ vtot,mvset,moset,lrvset,lroset,pm(5,15,15),
     & qm(5,15,15),sm(5,15,15),infm(5,15)
      common /gblk/ zlen(5),ninfm(5),rkbv(5,15),h(5,401),perm(5),f
     & ,ccsav(25,401),csav(25,401),yy(5,401)
      common /hblk/ mvi,nhmr(5),cin(5,15),equilm(5,15),
     & v(5,401),vl(5,401)
      common /iblk/ aj,u(5,15),dif(5,15),frt,co
      common /mblk/ zmn(25,25),zmv(25,25),ie(25),p(25,25),
     & q(25,25),s(25,25),dum(5,2,25)
      common /test/ err(5,2),jcount,jco,jcosav
      common/rate/velsav,vel,vell,rrxn(25),cur(401),cursav(401),jtime
     & ,flxs(401,15),flxsav(401,15),chd(401),chdsav(401),currsav(6)
c
c     Equations at an interior boundary.
c
      mp1=m+1
      if(m.gt.mvi) vi(m)=c(m-1,j)
      if(m.lt.mvi) vi(m)=c(m,j)
      if(m.eq.mvi) vi(m)=0.
      if(m+1.gt.mvi) vi(m+1)=c(m,j)
      if(m+1.lt.mvi) vi(m+1)=c(m+1,j)
      if(m+1.eq.mvi) vi(m+1)=0.
      if(m+2.gt.mvi) vi(m+2)=c(m+1,j)
      if(m+2.lt.mvi) vi(m+2)=c(m+2,j)
      if(m+2.eq.mvi) vi(m+2)=0.
      do 1 i=1,n
           ihi(i)=0
           iei(i)=0
           do 1 k=1,n
                pi(i,k)=0.
                qi(i,k)=0.
                si(i,k)=0.
                zmvi(i,k)=0.
                zmni(i,k)=0.
                zmv(i,k)=0.
1               zmn(i,k)=0.
      do 3 ii=1,nsp(m)
           do 2 l=1,nhtr(m,2)
                pti(m,ii,l)=pt(m,2,ii,l)
                qti(m,ii,l)=qt(m,2,ii,l)
2               sti(m,ii,l)=st(m,2,ii,l)
           if(mb(m,ii).eq.0) goto 3
           i=ivar(m,ii)
           zmni(i,i)=1.
           ic(i)=0
           do 31 l=1,nhtr(m,2)
                pi(i,l)=pt(m,2,ii,l)
                qi(i,l)=qt(m,2,ii,l)
                si(i,l)=pi(i,l)-qi(i,l)
```

```
                zmvi(i,l)=si(i,l)
 31             continue
  3        continue
     do 6 ii=1,nsp(mpl)
          do 5 l=1,nhtr(m,2)
               ptii(mpl,ii,l)=pt(mpl,l,ii,l)
               qtii(mpl,ii,l)=qt(mpl,l,ii,l)
  5            stii(mpl,ii,l)=st(mpl,l,ii,l)
          if(mb(mpl,ii).eq.0) goto 6
          i=ivar(mpl,ii)
          zmni(i,i)=1.
          ic(i)=0
          do 32 l=1,nhtr(m,2)
               pi(i,l)=pt(mpl,l,ii,l)
               qi(i,l)=qt(mpl,l,ii,l)
               si(i,l)=pi(i,l)-qi(i,l)
               zmvi(i,l)=si(i,l)
 32            continue
  6       continue
     do 7 l=1,nhtr(m,2)
  7       ihi(l)=inft(mpl,l)
     call eqnprod(zmvi,zmni,ihi,iei,n,nhtr(m,2))
     do 9 ii=1,nsp(mpl)
          if(mb(mpl,ii).eq.0) goto 9
          i=ivar(mpl,ii)
          zmn(i,i)=1.
          do 8 l=1,nhmr(mpl)
                p(i,l)=pm(mpl,ii,l)
                q(i,l)=qm(mpl,ii,l)
                s(i,l)=p(i,l)-q(i,l)
  8             zmv(i,l)=s(i,l)
  9 continue
     do 10 l=1,nhmr(mpl)
 10        ih(l)=infm(mpl,l)
     call eqnprod(zmv,zmn,ih,ie,n,nhmr(mpl))
c
c    Limiting reaction boundary condition.
c
     if(kontrol.eq.1) then
        if(m.eq.mcro) then
           if(lrcro.eq.1) then
              i=ivar(m,idlr(m))
              eq(i)=c(i,j)-cr0
              ic(i)=1
           endif
        endif
        if(mpl.eq.mcro) then
           if(lrcro.eq.-1) then
              i=ivar(mpl,idlr(mpl))
              eq(i)=c(i,j)-cr0
              ic(i)=1
```

```
            endif
         endif
      endif
c
c     Equilibrium of interfacial reactions.
c
      if(ipu(m).eq.0) then
         pom=pot(m,j)
         pmn=pot(m,j-1)
         p0=pom
         pb=pmn
      else
         i=ivar(m,nmb(m)+ipu(m))
         pom=c(i,j)
         pmn=c(i,j-1)
         p0=csav(i,j)
         pb=csav(i,j-1)
      endif
      if(ivu(m).eq.0) then
         vlom=vl(m,j)
         vlm=vl(m,j-1)
      else
         i=ivar(m,nmb(m)+ipu(m)+ivu(m))
         vlom=c(i,j)
         vlm=c(i,j-1)
      endif
      if(ipu(mp1).eq.0) then
         pp=pot(mp1,j+1)
         pom1=pot(mp1,j)
         pf=pp
         p00=pom1
      else
         i=ivar(mp1,nmb(mp1)+ipu(mp1))
         pp=c(i,j+1)
         pom1=c(i,j)
         pf=csav(i,j+1)
         p00=csav(i,j)
      endif
      if(ivu(mp1).eq.0) then
         vlp=vl(mp1,j+1)
         vlom1=vl(mp1,j)
      else
         i=ivar(mp1,nmb(mp1)+ipu(mp1)+ivu(mp1))
         vlp=c(i,j+1)
         vlom1=c(i,j)
      endif
      zh=zlen(m)*h(m,j)
      zh1=zlen(mp1)*h(mp1,j+1)
      fac=1.d0
      do 11 ii=1,nsp(m)
            if(mb(m,ii).eq.0) goto 11
```

```
          i=ivar(m,ii)
          ccf=cc(i,j)
          ccb=cc(i,j-1)
          cf=c(i,j)
          cb=c(i,j-1)
          rflx(i)=-(yy(m,j)*(vi(m+1)-vi(m))+vi(m))*cf
  &       +((yy(m,j)+yy(m,j-1))/2.*(vi(m+1)-vi(m))+vi(m))*(cf+cb)/2.
  &       +(3.*cf+cb)/4.*(vi(m+1)-vi(m))*h(m,j)/2.
  &       -flxhfpt(cc(i,j),cc(i,j-1),pom,pmn,m,ii,zh,z(m,ii))
  &       -(vlom+vlm)/2.*(cf+cb)/2.-(3.*cf+cb)/4.*(vlom-vlm)/2.
  &       +cf*vi(m+1)
 11 continue
    do 12 ii=1,nsp(mp1)
          if(mb(mp1,ii).eq.0) goto 12
          i=ivar(mp1,ii)
          ccf=cc(i,j+1)
          ccb=cc(i,j)
          cf=c(i,j+1)
          cb=c(i,j)
          rflx(i)=-(h(m+1,j+1)/2.*(vi(m+2)-vi(m+1))+vi(m+1))*(cf
  &       +cb)/2.+vi(m+1)*cb+(3.*cb+cf)/4.*(vi(m+2)-vi(m+1))/2.
  &       *h(m+1,j+1)/2.
  &       +flxhfpt(cc(i,j+1),cc(i,j),pp,pom1,mp1,ii,zh1,z(mp1,ii))
  &       +(vlp+vlom1)/2.*(cf+cb)/2.-(3.*cb+cf)/4.*(vlp-vlom1)/2.
  &       -cb*vi(m+1)
 12 continue
    do 13 l=1,nhtr(m,2)
          rrxn(l)=0.
          if(inft(mp1,l).eq.1) goto 13
          uo=0.
          cpd=2400.
          if(m.eq.2 .and. l.eq.1) uo=dlog(2./(((cpd*(7.5d-8
  &          /zlen(m)-1.)+2.)**2+4*(cpd-1))**.5+cpd
  &          *(7.5d-8/zlen(m)
  &          -1.)+2))/frt
          rlb=1.
          rlf=1.
          call rfb(rlb,rlf,m,l,j,j,zks,2,pi,qi,si,pti,qti,sti,cin)
          call rfb(rlb,rlf,mp1,l,j,j,zks,1,pi,qi,si,ptii,qtii,stii
  &            ,cin)
          ft=fnrt(nsp(mp1),mp1,st,l,l,z)
          rrxn(l)=rkba(mp1,l)*(rlf*equilt(mp1,l)
  &           *dexp((1.-be(mp1,l))*ft*(pom-pom1-uo))
  &           -rlb*dexp(-be(mp1,l)*ft*(pom-pom1-uo)))
 13 continue
    do 17 ii=1,nsp(m)
          if(mb(m,ii).eq.0) goto 17
          i=ivar(m,ii)
          if(ic(i).eq.1) goto 17
          ic(i)=1
          eq(i)=0.
```

```
          infrxn=0
          do 14 l=1,nhtr(m,2)
                if(zmvi(i,l).eq.0) goto 14
                if(inft(mpl,l).eq.1) then
                   infrxn=1
                   goto 15
                else
                   eq(i)=eq(i)+zmvi(i,l)*rrxn(l)
                endif
14        continue
15        do 16 kk=1,nsp(m)
                if(mb(m,kk).eq.0) goto 16
                k=ivar(m,kk)
                if(zmni(i,k).eq.0) goto 16
                if(infrxn.eq.1) then
                   rrxn(l)=rrxn(l)-zmni(i,k)/zmvi(i,l)*rflx(k)
                else
                   eq(i)=eq(i)+zmni(i,k)*rflx(k)
                endif
16        continue
          do 40 kk=1,nsp(mpl)
                if(mb(mpl,kk).eq.0) goto 40
                k=ivar(mpl,kk)
                if(zmni(i,k).eq.0) goto 40
                if(infrxn.eq.1) then
                   rrxn(l)=rrxn(l)-zmni(i,k)/zmvi(i,l)*rflx(k)
                else
                   eq(i)=eq(i)+zmni(i,k)*rflx(k)
                endif
40        continue
          if(infrxn.eq.0) goto 17
          eq(i)=0.
          call smslnc(eq(i),m,si,l,zks,2,j,j)
          call smslnc(eq(i),mpl,si,l,zks,1,j,j)
          ft=fnrt(nsp(m),m,st,2,l,z)
          uo=0.
          cpd=2400.
          if(m.eq.2 .and. l.eq.1) uo=dlog(2./(((cpd*(7.5d-8
  &          /zlen(m)-1.)+2.)**2+4*(cpd-1))**.5+cpd
  &          *(7.5d-8/zlen(m)
  &          -1.)+2))/frt
          eq(i)=eq(i)+dlog(equilt(mpl,l))+ft*(pom-poml-uo)
17 continue
   do 23 ii=1,nsp(mpl)
          if(mb(mpl,ii).eq.0) goto 23
          i=ivar(mpl,ii)
          if(ic(i).eq.1) goto 23
          ic(i)=1
          eq(i)=0.
          infrxn=0
          do 20 l=1,nhtr(m,2)
```

```
                if(zmvi(i,l).eq.0) goto 20
                if(inft(mpl,l).eq.l) then
                   infrxn=l
                   goto 21
                else
                   eq(i)=eq(i)+zmvi(i,l)*rrxn(l)
                endif
20        continue
21        do 41 kk=l,nsp(m)
                if(mb(m,kk).eq.0) goto 41
                k=ivar(m,kk)
                if(zmni(i,k).eq.0) goto 41
                if(infrxn.eq.l) then
                   rrxn(l)=rrxn(l)-zmni(i,k)/zmvi(i,l)*rflx(k)
                else
                   eq(i)=eq(i)+zmni(i,k)*rflx(k)
                endif
41        continue
          do 22 kk=l,nsp(mpl)
                if(mb(mpl,kk).eq.0) goto 22
                k=ivar(mpl,kk)
                if(zmni(i,k).eq.0) goto 22
                if(infrxn.eq.l) then
                   rrxn(l)=rrxn(l)-zmni(i,k)/zmvi(i,l)*rflx(k)
                else
                   eq(i)=eq(i)+zmni(i,k)*rflx(k)
                endif
22        continue
          if(infrxn.eq.0) goto 23
          eq(i)=0.
          call smslnc(eq(i),m,si,l,zks,2,j,j)
          call smslnc(eq(i),mpl,si,l,zks,l,j,j)
          ft=fnrt(nsp(mpl),mpl,st,l,l,z)
          uo=0.
          cpd=2400.
          if(m.eq.2 .and. l.eq.l) uo=dlog(2./(((cpd*(7.5d-8
  &          /zlen(m)-l.)+2.)**2+4*(cpd-l))**.5+cpd
  &          *(7.5d-8/zlen(m)
  &          -l.)+2))/frt
          eq(i)=eq(i)+dlog(equilt(mpl,l))+ft*(pom-poml-uo)
23 continue
   rtfml=0.
   curl(mpl)=0.
   do 19 l=l,nhtr(m,2)
          sil=0.
          zisil=0.
          do 18 ii=l,nsp(m)
                if(sti(m,ii,l).eq.0.) goto 18
                zisil=zisil+z(m,ii)*sti(m,ii,l)
                if(ltcs(m,ii).eq.0) goto 18
                sil=sil+sti(m,ii,l)
```

```
18        continue
          curl(mpl)=curl(mpl)+f*zisil*rrxn(l)
          rtfml=rtfml+sil*rrxn(l)
19 continue
   rtfmr=0.
   curr(mpl)=0.
   do 25 l=1,nhtr(m,2)
          sil=0.
          zisil=0
          do 24 ii=1,nsp(mpl)
                if(stii(mpl,ii,l).eq.0.) goto 24
                zisil=zisil+z(mpl,ii)*stii(mpl,ii,l)
                if(ltcs(mpl,ii).eq.0) goto 24
                sil=sil+stii(mpl,ii,l)
24        continue
          rtfmr=rtfmr+sil*rrxn(l)
          curr(mpl)=curr(mpl)-f*zisil*rrxn(l)
25 continue
c
c     Gauss's equation.
c
      if(ipu(m).eq.0) goto 27
      i=ivar(m,nmb(m)+ipu(m))
      if(m.eq.mvset) then
         if(lrvset.eq.1) then
            eq(i)=c(i,j)-vtot
            goto 27
         endif
      endif
      if(m.eq.moset) then
         if(lroset.eq.1) then
            eq(i)=c(i,j)
            goto 27
         endif
      endif
      smc=0.
      smkc=0.
      smce=0.
      do 26 kk=1,nsp(m)
           if(z(m,kk).eq.0.) goto 26
           if(mb(m,kk).eq.0) then
              smc=smc+z(m,kk)*cin(m,kk)
              smkc=smkc+z(m,kk)*zks(m,2,kk)*cin(m,kk)
              smce=smce+z(m,kk)*cin(m,kk)
           else
              k=ivar(m,kk)
              smc=smc+z(m,kk)*(3.*c(k,j)+c(k,j-1))/4.
              smkc=smkc+z(m,kk)*zks(m,2,kk)*c(k,j)
              smce=smce+z(m,kk)*c(k,j)
           endif
26         continue
```

```
      smkc=0.
      permo=(perm(m)+perm(m+1))/2./perm(m)
      eq(i)=zh/2.*smc+smkc+perm(m)/f*(permo*(poml-pom)/blen(mpl)
     &      -(pom-pmn)/zh)
c     eq(i)=(poml-pom)/blen(mpl)*permo
c    &      -(pom-pmn)/zh
c     eq(i)=smce
   27 if(ipu(mpl).eq.0) goto 29
      i=ivar(mpl,nmb(mpl)+ipu(mpl))
      if(mpl.eq.mvset) then
         if(lrvset.eq.-1) then
            eq(i)=c(i,j)-vtot
            goto 29
         endif
      endif
      if(mpl.eq.moset) then
         if(lroset.eq.-1) then
            eq(i)=c(i,j)
            goto 29
         endif
      endif
      smc=0.
      smkc=0.
      smce=0.
      do 28 kk=1,nsp(mpl)
           if(z(mpl,kk).eq.0.) goto 28
           if(mb(mpl,kk).eq.0) then
              smc=smc+z(mpl,kk)*cin(mpl,kk)
              smkc=smkc+z(mpl,kk)*zks(mpl,1,kk)*cin(mpl,kk)
              smce=smce+z(mpl,kk)*cin(mpl,kk)
           else
              k=ivar(mpl,kk)
              smc=smc+z(mpl,kk)*(3.*c(k,j)+c(k,j+1))/4.
              smkc=smkc+z(mpl,kk)*zks(mpl,1,kk)*c(k,j)
              smce=smce+z(mpl,kk)*c(k,j)
           endif
   28      continue
      smkc=0.
      perml=(perm(m)+perm(m+1))/2./perm(mpl)
      eq(i)=zhl/2.*smc+smkc+perm(mpl)/f*((pp-poml)/zhl
     &      -(poml-pom)*perml/blen(mpl))
c     eq(i)=(pp-poml)/zhl*2.
c    &      -(poml-pom)*perml/blen(mpl)
c     eq(i)=smce
   29 continue
c
c     Velocity
c
      rtfml=rtfml/1000./den(m)*zmw(m)
      rtfmr=rtfmr/1000./den(mpl)*zmw(mpl)
      vel=rtfml
```

```
c       velsav=rtfml
        rtfml=velsav
        if(ivu(m).eq.0) then
           if(m.ge.mvi) then
              eq(m)=c(m,j)-vi(m)+rtfml
c             eq(m)=c(m,j)-vl(m,j)+rtfml
           else
              eq(m)=c(m,j)-c(m,j-1)
           endif
        else
           i=ivar(m,nmb(m)+ipu(m)+ivu(m))
           if(m.ge.mvi) then
              eq(m)=c(m,j)-c(i,j)+rtfml
              eq(i)=c(i,j)-c(i,j-1)
           else
              eq(m)=c(m,j)-c(m,j-1)
              eq(i)=vi(mpl)-c(i,j)+rtfml
           endif
        endif
        if(ivu(mpl).eq.0) then
           if(mpl.ge.mvi) then
              eq(mpl)=c(mpl,j)-c(mpl,j+1)
           else
              eq(mpl)=c(mpl,j)-vi(m+2)-rtfmr
           endif
        else
           i=ivar(mpl,nmb(mpl)+ipu(mpl)+ivu(mpl))
           if(mpl.ge.mvi) then
              eq(mpl)=c(mpl,j)-c(mpl,j+1)
              eq(i)=c(i,j)-vi(mpl)+rtfmr
           else
              eq(mpl)=c(mpl,j)-c(i,j)-rtfmr
              eq(i)=c(i,j)-c(i,j+1)
           endif
        endif
        do 30 ml=1,nph
             if(ml.lt.m) eq(ml)=c(ml,j)-c(ml,j-1)
             if(ml.gt.mpl) eq(ml)=c(ml,j)-c(ml,j+1)
   30        continue
        if(m.eq.1) then
c       eq(4)=cc(4,j)-8.2*dexp(3.*frt*(-351.2))
c       eq(5)=cc(5,j)-3.*8.2*dexp(-frt*(-351.2))
c       eq(4)=cc(4,j)-8.2*dexp(3.*frt*(-351.2))
c       eq(5)=cc(5,j)
c  &&&&&&&&
c       eq(6)=c(6,j)+351.2
        endif
        if(m.eq.2) then
c       eq(4)=cc(4,j)-.3937*dexp(-3.*frt*325)
c       eq(5)=cc(5,j)-67.684*dexp(frt*325.)
c       eq(6)=c(6,j)+217.
```

```
c     eq(8)=cc(8,j)-.54366
c     eq(9)=cc(9,j)-0.0067667
c     eq(10)=cc(10,j)-0.036790
c     eq(11)=cc(11,j)+0.0
      endif
      return
      end
c ------------------------------------------------------------
      Subroutine eqnj(j,eq,m,njmsum)
      implicit real*8(a-h,o-z)
      dimension eq(25),ic(25),vi(6)
      common /ablk/a(25,25),b(25,25),c(25,401),d(25,51),g(25),
     & x(25,25),y(25,25),n,njt
      common /bblk/ nj(5),nmb(5),ipu(5),ivu(5),cc(25,401)
     & ,pot(5,401),z(5,25)
      common /cblk/ nph,nsp(5),mb(5,15),ivar(5,25)
      common /fblk/ vtot,mvset,moset,lrvset,lroset,pm(5,15,15),
     & qm(5,15,15),sm(5,15,15),infm(5,15)
      common /gblk/ zlen(5),ninfm(5),rkbv(5,15),h(5,401),perm(5),f
     & ,ccsav(25,401),csav(25,401),yy(5,401)
      common /hblk/ mvi,nhmr(5),cin(5,15),equilm(5,15),
     & v(5,401),vl(5,401)
      common /iblk/ aj,u(5,15),dif(5,15),frt,co
      common /mblk/ zmn(25,25),zmv(25,25),ie(25),p(25,25),
     & q(25,25),s(25,25),dum(5,2,25)
      common/rate/velsav,vel,vell,rrxn(25),cur(401),cursav(401),jtime
     & ,flxs(401,15),flxsav(401,15),chd(401),chdsav(401),currsav(6)
      common /test/ err(5,2),jcount,jco,jcosav
c
c     Material balance at an interior point
c
c     Equilibrium conditions
c
      if(m.gt.mvi) vi(m)=c(m-1,j)
      if(m.lt.mvi) vi(m)=c(m,j)
      if(m.eq.mvi) vi(m)=0.
      if(m+1.gt.mvi) vi(m+1)=c(m,j)
      if(m+1.lt.mvi) vi(m+1)=c(m+1,j)
      if(m+1.eq.mvi) vi(m+1)=0.
      do 1 ii=1,nsp(m)
           if(mb(m,ii).eq.0) goto 1
           i=ivar(m,ii)
           ic(i)=0
    1      continue
      do 2 ll=1,ninfm(m)
           l=ie(ll)
           call eqlbr(eq,ic,zmv,m,s,l,dum,1,j,j,equilm,l)
    2      continue
c
c     Mole flux balance
c
```

```
if(ipu(m).eq.0) then
   pp=pot(m,j+1)
   po=pot(m,j)
   pmn=pot(m,j-1)
   pf=pp
   p0=po
   pb=pmn
else
   i=ivar(m,nmb(m)+ipu(m))
   pp=c(i,j+1)
   po=c(i,j)
   pmn=c(i,j-1)
   pf=csav(i,j+1)
   p0=csav(i,j)
   pb=csav(i,j-1)
endif
if(ivu(m).eq.0) then
   vlp=vl(m,j+1)
   vlo=vl(m,j)
   vlm=vl(m,j-1)
else
   i=ivar(m,nmb(m)+ipu(m)+ivu(m))
   vlp=c(i,j+1)
   vlo=c(i,j)
   vlm=c(i,j-1)
endif
njsum=njmsum-nj(m)+1
yd=yy(m,j)
hlf=.5/dfloat(nj(m)-1)
zh1=zlen(m)*h(m,j)
zh2=zlen(m)*h(m,j+1)
fac=1.d0
do 10 ii=1,nsp(m)
      if(mb(m,ii).eq.0) goto 10
      i=ivar(m,ii)
      if(ic(i).eq.1) goto 10
      eq(i)=0.
      do 4 kk=1,nsp(m)
           if(mb(m,kk).eq.0) goto 4
           k=ivar(m,kk)
           if(zmn(i,k).eq.0.) go to 4
           zk=z(m,kk)
           ccf=cc(k,j+1)
           cco=cc(k,j)
           ccb=cc(k,j-1)
           cf=c(k,j+1)
           c0=c(k,j)
           cb=c(k,j-1)
           eq(i)=eq(i)+zmn(i,k)*(-((yy(m,j+1)+yy(m,j))/2.*(vi(m+1)
&          -vi(m))+vi(m))*(cf+c0)/2.+((yy(m,j)+yy(m,j-1))/2.
&          *(vi(m+1)-vi(m))+vi(m))*(c0+cb)/2.
```

```
     &          +(3./8.*c0*(h(m,j+1)+h(m,j))+1./8.*(cf*h(m,j+1)+cb
     &          *h(m,j)))*(vi(m+1)-vi(m))
     &          +flxhfpt(cc(k,j+1),cc(k,j),pp,po,m,kk,zh2,zk)
     &          -flxhfpt(cc(k,j),cc(k,j-1),po,pmn,m,kk,zh1,zk))
                conv=(vlp+vlo)/2.*(cf+c0)/2.-(vlo+vlm)/2.*(c0+cb)/2.
     &          -(3.*c0+cf)/4.*(vlp-vlo)/2.-(3.*c0+cb)/4.*(vlo-vlm)/2.
                eq(i)=eq(i)+zmn(i,k)*conv
    4           continue
c     Find the maximum rkbv.
            rkbmax=0.
            le=0
            do 7 l=1,nhmr(m)
                 if(zmv(i,l).eq.0.) goto 7
                 if(rkbmax.lt.rkbv(m,l)) then
                    rkbmax=rkbv(m,l)
                    lmax=l
                 endif
    7            continue
            if(rkbmax.eq.0.) goto 10
            if(rkbmax.ge.1.d6) le=lmax
            do 8 l=1,nhmr(m)
                 if(l.eq.le) goto 8
                 if(zmv(i,l).eq.0.) go to 8
                 rlb=1.
                 rlf=1.
                 call rfb(rlb,rlf,m,l,j,j,dum,l,p,q,s,pm,qm,sm,cin)
                 eq(i)=eq(i)+zmv(i,l)*rkbv(m,l)*(rlf*equilm(m,l)-rlb)
    8            continue
            if(le.eq.0) goto 10
            zkbmax=1.
            sumlnc=0.
            do 9 kk=1,nsp(m)
                 if(mb(m,kk).eq.0) goto 9
                 k=ivar(m,kk)
                 if(s(k,le).eq.0.) goto 9
                 zkbmax=zkbmax*c(k,j)**q(k,le)
                 sumlnc=sumlnc+s(k,le)*dlog(c(k,j))
    9            continue
            zkbmax=zkbmax*zmv(i,le)*rkbv(m,le)
            eq(i)=dlog(equilm(m,le))+sumlnc-dlog(1.-eq(i)/zkbmax)
   10       continue
c
c     Poisson's equation.
c
      if(ipu(m).eq.0) goto 12
      i=ivar(m,nmb(m)+ipu(m))
      eq(i)=0.
      do 11 kk=1,nsp(m)
           k=ivar(m,kk)
           if(mb(m,kk).eq.0) then
              eq(i)=eq(i)+z(m,kk)*cin(m,kk)*(zh1+zh2)/2.
```

```
            else
               eq(i)=eq(i)+z(m,kk)*(3./8.*c(k,j)*(zh2+zh1)+
     &         +1./8.*(c(k,j+1)*zh2+c(k,j-1)*zh1))
            endif
   11       continue
      eq(i)=eq(i)+perm(m)/f*((pp-po)/zh2-(po-pmn)/zh1)
   12 if(ivu(m).eq.1) then
         i=ivar(m,nmb(m)+ipu(m)+ivu(m))
         if(m.ge.mvi) then
            eq(i)=c(i,j)-c(i,j-1)
         else
            eq(i)=c(i,j+1)-c(i,j)
         endif
      endif
      do 13 ml=1,nph
            if(ml.ne.m) then
               if(ml.gt.m) eq(ml)=c(ml,j)-c(ml,j+1)
               if(ml.lt.m) eq(ml)=c(ml,j)-c(ml,j-1)
            else
               if(ml.ge.mvi) eq(ml)=c(ml,j)-c(ml,j+1)
               if(ml.lt.mvi) eq(ml)=c(ml,j)-c(ml,j-1)
            endif
   13       continue
      cur(j)=0.
      chd(j)=0.
      do 14 ii=1,nsp(m)
             if(z(m,ii).eq.0.) goto 14
             if(mb(m,ii).eq.0) goto 14
             i=ivar(m,ii)
c            cur(j)=(flxhfpt(cc(i,j+1),cc(i,j-1),
c    &               pp,pmn,m,ii,2.*zh1,z(m,ii))
c    &               +vlo*c(i,j))*z(m,ii)+cur(j)
      zi=z(m,ii)
      flxs(j,ii)=flxhfpt(cc(i,j+1),cc(i,j),pp,po,m,ii,zh2,zi)
     &+vlo*(c(i,j)+c(i,j+1))/2.d0
      cur(j)=cur(j)+zi*flxhfpt(cc(i,j+1),cc(i,j),pp,po,m,ii,zh2,zi)
     &+vlo*(c(i,j)+c(i,j+1))/2.d0*zi
             chd(j)=chd(j)+zi*c(i,j)
   14        continue
      cur(j)=cur(j)*f
      chd(j)=chd(j)*f
      return
      end
c ------------------------------------------------------------
      Subroutine eqnprod(zmv,zmn,ih,ie,n,nrs)
      implicit real*8(a-h,o-z)
      integer ih(25),ic(25),ie(25)
      dimension ns(25),id(25),zmv(25,25),zmn(25,25)
c
c     Determine which equations are at finite rates and
c     which are infinite, putting those that are infinite
```

```
c     at the front of an identifying vector, ie, and the
c     others at the back.
c     This will allow me to set up the equations such that
c     the equilibrium equations are defined first.
c
      do 1 l=1,nrs
    1      ie(l)=0
      j=0
      k=-1
      do 3 l=1,nrs
           if(ih(l).ne.1) goto 2
              j=j+1
              ie(j)=1
           goto 3
    2         k=k+1
              ie(nrs-k)=1
    3 continue
c     Define an identifying vector, ic, so that I know which equations
c     have been used as the pivot and that they are not repeated.
      do 4 i=1,n
    4      ic(i)=0
      do 19 l=1,nrs
            ie(l)=1
            m=ie(l)
c     Define a vector, ns, which tells me how many different reactions
c     each species is involved in.
            do 7 i=1,n
                 ns(i)=0
                 do 7 ll=1,nrs
                      if(zmv(i,ll).ne.0.) ns(i)=ns(i)+1
    7       continue
c     Determine the pivot point by picking a species which hasn't
c     been chosen before (ic(*)=0), and is involved in the fewest
c     reactions (but greater than zero.)
            j=0
            do 10 i=1,n
                 if(ic(i)) 8,8,10
    8            if(zmv(i,m)) 9,10,9
    9               j=j+1
                    id(j)=i
   10       continue
            if (j.eq.0) goto 19
            nsmin=ns(id(1))
            iz=id(1)
            do 11 k=2,j
                 if(nsmin.gt.ns(id(k))) then
                     nsmin=ns(id(k))
                     iz=id(k)
                 endif
   11       continue
c     (iz,m) is the pivot point.
```

```
c     Don't want to pivot around this point again so we set
c     ic(iz)=1.
            ic(iz)=1
            do 18 k=1,n
                  if(k-iz) 12,15,12
   12                fctr=zmv(k,m)/zmv(iz,m)
                     do 13 ll=1,nrs
   13                      zmv(k,ll)=zmv(k,ll)-fctr*zmv(iz,ll)
                     do 14 ll=1,n
   14                      zmn(k,ll)=zmn(k,ll)-fctr*zmn(iz,ll)
                  goto 18
   15                dvsr=zmv(k,m)
                     do 16 ll=1,nrs
   16                      zmv(k,ll)=zmv(k,ll)/dvsr
                     do 17 ll=1,n
   17                      zmn(k,ll)=zmn(k,ll)/dvsr
   18       continue
   19 continue
      return
      end
c ------------------------------------------------------------
      Subroutine band(j)
      implicit real*8(a-h,o-z)
      dimension e(25,26,401)
      common /ablk/a(25,25),b(25,25),c(25,401),d(25,51),g(25),
     1 x(25,25),y(25,25),n,nj
      save e,npl
  101 format (15h determ=0 at j=,i4)
      if (j-2) 1,6,8
    1 npl=n+1
      do 2 i=1,n
           d(i,2*n+1)= g(i)
      do 2 l=1,n
                lpn=l+n
    2           d(i,lpn)=x(i,l)
      call matinv(n,2*n+1,determ)
      if (determ) 4,3,4
    3     print 101, j
      stop
    4     do 5 k=1,n
                e(k,npl,1)=d(k,2*n+1)
          do 5 l=1,n
                     e(k,l,1)= -d(k,l)
                     lpn=l+n
    5                x(k,l)= -d(k,lpn)
      return
    6     do 7 i=1,n
          do 7 k=1,n
          do 7 l=1,n
    7                     d(i,k)= d(i,k)+a(i,l)*x(l,k)
    8 if (j-nj) 11,9,9
```

```
 9      do 10 i=1,n
        do 10 l=1,n
                  g(i)= g(i) - y(i,l)*e(l,npl,j-2)
        do 10 m=1,n
10                     a(i,l)= a(i,l) + y(i,m)*e(m,l,j-2)
11      do 12 i=1,n
              d(i,npl)= - g(i)
        do 12 l=1,n
                  d(i,npl)= d(i,npl) + a(i,l)*e(l,npl,j-1)
        do 12 k=1,n
12                     b(i,k)= b(i,k) + a(i,l)*e(l,k,j-1)
    call matinv(n,npl,determ)
    if (determ) 14,13,14
13      print 101, j
    stop
14      do 15 k=1,n
        do 15 m=1,npl
15            e(k,m,j)= - d(k,m)
    if (j-nj) 20,16,16
16      do 17 k=1,n
17            c(k,j)= e(k,npl,j)
        do 18 jj=2,nj
              m= nj - jj + 1
        do 18 k=1,n
                  c(k,m)= e(k,npl,m)
        do 18 l=1,n
18                     c(k,m)= c(k,m) + e(k,l,m)*c(l,m+1)
    do 19 l=1,n
    do 19 k=1,n
19            c(k,l)= c(k,l) + x(k,l)*c(l,3)
20  return
    end
c ------------------------------------------------------------
    subroutine matinv (n,m,determ)
    implicit real*8(a-h,o-z)
    common /ablk/a(25,25),b(25,25),c(25,401),d(25,51),g(25),
   1 x(25,25),y(25,25),neqt,njt
    dimension id(26)
    determ=1.0
    do 1 i=1,n
 1      id(i)=0
    do 18 nn=1,n
          bmax=1.1
          do 6 i=1,n
                if(id(i).ne.0) go to 6
                bnext=0.0
                btry=0.0
                do 5 j=1,n
                      if(id(j).ne.0) go to 5
                      if(dabs(b(i,j)).le.bnext) go to 5
                      bnext=dabs(b(i,j))
```

```
                    if(bnext.le.btry) go to 5
                    bnext=btry
                    btry=dabs(b(i,j))
                    jc=j
 5            continue
              if(bnext.ge.bmax*btry) go to 6
              bmax=bnext/btry
              irow=i
              jcol=jc
 6       continue
         if(id(jc).eq.0) go to 8
         determ=0.0
   return
 8       id(jcol)=1
         if(jcol.eq.irow) go to 12
         do 10 j=1,n
               save=b(irow,j)
               b(irow,j)=b(jcol,j)
10             b(jcol,j)=save
         do 11 k=1,m
               save=d(irow,k)
               d(irow,k)=d(jcol,k)
11             d(jcol,k)=save
12       f=1.0/b(jcol,jcol)
         do 13 j=1,n
13             b(jcol,j)=b(jcol,j)*f
         do 14 k=1,m
14             d(jcol,k)=d(jcol,k)*f
   do 18 i=1,n
                    if(i.eq.jcol) go to 18
                    f=b(i,jcol)
                    do 16 j=1,n
16                        b(i,j)=b(i,j)-f*b(jcol,j)
                    do 17 k=1,m
17                        d(i,k)=d(i,k)-f*d(jcol,k)
18 continue
   return
   end
c -----------------------------------------------------------
   Subroutine matmul(a,m,l,b,n,c)
   implicit real*8(a-h,o-z)
   dimension a(25,25),b(25,25),c(25,25)
   do 10 i=1,m
         do 10 j=1,n
10             c(i,j)=0.
   do 20 i=1,m
         do 20 j=1,n
               do 20 k=1,l
20                   c(i,j)=c(i,j)+a(i,k)*b(k,j)
   return
   end
```

```
c -------------------------------------------------------
      Subroutine eqlbr(eq,ic,zmv,m,s,l,zks,lr,j,jp,equilm,ll)
      implicit real*8(a-h,o-z)
      dimension eq(25),ic(25),zmv(25,25),s(25,25),zks(5,2,25),
     & equilm(5,25)
      common /ablk/a(25,25),b(25,25),c(25,401),d(25,51),g(25),
     & x(25,25),y(25,25),n,njt
      common /cblk/ nph,nsp(5),mb(5,15),ivar(5,25)
      do 1 ii=1,nsp(m)
           if(mb(m,ii).eq.0) goto 1
           i=ivar(m,ii)
           if(ic(i).eq.1) goto 1
           if(zmv(i,1).eq.0.) goto 1
           eq(i)=0.
           call smslnc(eq(i),m,s,l,zks,lr,j,jp)
           eq(i)=eq(i)+dlog(equilm(m,ll))
           ic(i)=1
           goto 2
    1      continue
    2 return
      end
c ---------------------------------------------------------------
      Subroutine smslnc(sum,m,s,l,zks,lr,j,jp)
      implicit real*8(a-h,o-z)
      dimension s(25,25),zks(5,2,15)
      common /ablk/a(25,25),b(25,25),c(25,401),d(25,51),g(25),
     & x(25,25),y(25,25),n,nj
      common /bblk/ njm(5),nmb(5),ipu(5),ivu(5),cc(25,401)
     & ,pot(5,401),z(5,25)
      common /iblk/ aj,u(5,15),dif(5,15),frt,co
      common /cblk/ nph,nsp(5),mb(5,15),ivar(5,25)
      if(ipu(m).eq.0) p1=pot(m,j)
      if(ipu(m).eq.0) p2=pot(m,jp)
      if(ipu(m).eq.1) p1=c(ivar(m,nmb(m)+1),j)
      if(ipu(m).eq.1) p2=c(ivar(m,nmb(m)+1),jp)
      do 1 kk=1,nsp(m)
           if(mb(m,kk).eq.0) goto 1
           k=ivar(m,kk)
           if(c(k,j).le.0.) goto 1
c             sum=sum+s(k,l)*dlog(zks(m,lr,kk)*(3.*c(k,j)+c(k,jp))/4.)
           if(k.eq.5) then
              if(3.*cc(k,j)+cc(k,jp)+4.*co.le.0.) goto 1
              sum=sum+s(k,l)*(dlog(zks(m,lr,kk)*
     &        (3.*cc(k,j)+cc(k,jp))/4.+co)
     &        -z(m,kk)*frt*(3.*p1+p2)/4.)
           else
              if(3.*cc(k,j)+cc(k,jp).le.0.) goto 1
              sum=sum+s(k,l)*(dlog(zks(m,lr,kk)*
     &        (3.*cc(k,j)+cc(k,jp))/4.)
     &        -z(m,kk)*frt*(3.*p1+p2)/4.)
           endif
```

```
    1       continue
      return
      end
c ------------------------------------------------------------------
      Subroutine rfb(rlb,rlf,m,l,j,jp,zks,lr,p,q,s,pr,qr,sr,cin)
      implicit real*8(a-h,o-z)
      dimension zks(5,2,15),p(25,25),q(25,25),s(25,25),
     & pr(5,15,15),qr(5,15,15),sr(5,15,15),cin(5,15)
      common /ablk/a(25,25),b(25,25),c(25,401),d(25,51),g(25),
     & x(25,25),y(25,25),neqt,njt
      common /cblk/ nph,nsp(5),mb(5,15),ivar(5,25)
      do 9 kk=1,nsp(m)
           if(mb(m,kk).eq.1) then
              k=ivar(m,kk)
              if(s(k,l)) 1,9,3
    1            if(c(k,j).gt.0.0) goto 2
                 rlb=0.0
              go to 9
    2            rlb=rlb*(zks(m,lr,kk)*(3.*c(k,j)+c(k,jp))/4.)
     &           **(q(k,l))
              go to 9
    3            if(c(k,j).gt.0.0) go to 4
                 rlf=0.0
              go to 9
    4            rlf=rlf*(zks(m,lr,kk)*(3.*c(k,j)+c(k,jp))/4.)
     &           **p(k,l)
           else
              if(sr(m,kk,l)) 5,9,7
    5            if(cin(m,kk).gt.0.0) goto 6
                 rlb=0.0
              go to 9
    6            rlb=rlb*(zks(m,lr,kk)*cin(m,kk))**qr(m,kk,l)
              go to 9
    7            if(cin(m,kk).gt.0.0) go to 8
                 rlf=0.0
              go to 9
    8            rlf=rlf*(zks(m,lr,kk)*cin(m,kk))**pr(m,kk,l)
           endif
    9      continue
      return
      end
c ------------------------------------------------------------------
      Function fnrt(nsp,m,st,lr,l,z)
      implicit real*8(a-h,o-z)
      dimension st(5,2,15,15),z(5,15)
      common /iblk/ aj,u(5,15),dif(5,15),frt,co
      fnrt=0.
      do 1 k=1,nsp
    1      fnrt=fnrt+(2.*lr-3.)*st(m,lr,k,l)*z(m,k)
           fnrt=frt*fnrt
  800 format (i2,1x,i2,1x,i2,1x,i2,1x,f4.1,1x,f4.1)
```

```
      return
      end
c ------------------------------------------------------------
      Function flxhfpt(cp,cm,pp,pm,m,k,h,z)
      implicit real*8(a-h,o-z)
      common /iblk/ aj,u(5,15),dif(5,15),frt,co
      common/rate/velsav,vel,vell,rrxn(25),cur(401),cursav(401),jtime
     & ,flxs(401,15),flxsav(401,15),chd(401),chdsav(401),currsav(6)
      common /test/ err(5,2),jcount,jco,jcosav
      d=dif(m,k)
      zuf=2.*d/aj
      if(jtime.lt.1 .or. m.eq.3 .or. m.eq.2) then
         flxhfpt=-d*(cp-cm)/h*dexp(-z*frt*(pp+pm)/2.)
      else
         if(k.eq.2) then
            flxhfpt=zuf*(cp+cm+2.*co)/2.*dexp(-z*frt*(pp+pm)/2.)
     &              *dsinh(-aj/2./h*dlog((cp+co)/(cm+co)))
c           flxhfpt=-d*(cp-cm)/h*dexp(-z*frt*(pp+pm)/2.)
c           flxhfpt=zuf*(cp+cm+2.*co)/2.*dexp(-z*frt*(pp+pm)/2.)
c    &              *(((cp+co)/(cm+co))**(-aj/2./h)-((cp+co)/(cm+co))
c    &              **(aj/2./h))
         else
            flxhfpt=zuf*(cp+cm)/2.*dexp(-z*frt*(pp+pm)/2.)
     &              *dsinh(-aj/2./h*dlog(cp/cm))
c           flxhfpt=-d*(cp-cm)/h*dexp(-z*frt*(pp+pm)/2.)
c           flxhfpt=zuf*(cp+cm)/2.*dexp(-z*frt*(pp+pm)/2.)
c    &              *((cp/cm)**(-aj/(2.*h))-(cp/cm)**(aj/2./h))
         endif
      endif
      return
      end
c ------------------------------------------------------
      Function accum(c,x,vip,vim)
      implicit real*8(a-h,o-z)
      accum=c*(x*(vip-vim)+vim)
      return
      end
```

Data File

iren.dat

```
3 2 0.0 .382
-253.20 10.0
2
1 -1
3 1
2 0 1 3
1 0 +0.0000e+00 +1.0000e-05 +00.0 Fe
0 0 -9.6800e+06 +2.5500e+05 -01.0 e-
1.0 0.0
1.0 1.0
0
2
0. 0. 1. 0.
0. 1. 0. 3.
1 1.e0 4.065e-2 .5
1 1.e0 8.20 .5
1. 1.
1. 1.
0 0
1 0.
4 0 1 121
3.0e-09 5.24 159.69 9.
0 1 +4.5064e-09 +4.0000e-11 +03.0 Ife3+
0 1 -3.7554e+08 +1.0000e+07 -01.0 e-
1 0 +0.0000e+00 +0.0000e+00 +00.0 Fe
1 0 +0.0000e+00 +0.0000e+00 +00.0 O
8.20 0.
24.6 0.
1. 0.
1. 0.
2
0. 0. 0. 1.
1. 0. 0. 0.
0. 0. 0. 0.
0. 0. 0. 0.
3
0.3333333 0. 1. 0. 1. 0.
0. 0. 0. 0. 1. 0.
0. 0.3333333 0. 0. 0. 0.
0. 0.5 0. 0. 0. 0.
1 1.0e-11 8.57272e+05 .5
1 1.0e-10 4.07739e-01 .5
1 1.0e-11 1.44466e+04 .5
1. 1.
1. 1.
1. 1.
```

```
1. 1.
1 1
6 0 4 181
3. 1. 18.0 78.
0 1 +5.0110e+01 +1.3340e+00 +01.0 Na+
0 1 +5.4000e+01 +0.7200e+00 +02.0 Fe2+
0 1 +3.7554e+01 +1.0000e+00 +01.0 FeOH2
0 1 -7.5108e+01 +1.0000e+00 -02.0 B4O7
0 1 -3.7554e+01 +1.0000e+00 -01.0 HB4O7
0 0 +0.0000e+00 +4.0000e+00 +00.0 H2O
0.20 0.
1.0e-11 0.
1.3e-18 0.
0.05000000001 0.
0.10 0.
1.0 1.0
3
0. 0. 0. 0. 0. 0.
0. 0. 0. 0. 0. 1.
0. 0. 0. 1. 0. 0.
1. 0. 2. 0. 0. 0.
0. 1. 0. 2. 0. 0.
0.5 0. 2. 0. 0. 0.
0
1. 1.
1. 1.
1. 1.
1. 1.
1. 1.
1. 1.
1 0
4 -1.
```

Chapter 4

The Oxidation of Thiosulfate on Copper for Electroless Deposition

Foreword

An investigation of sodium thiosulfate as a possible reducing agent for electroless copper deposition at 25°C using a copper rotating disk electrode was carried out. The polarization curves of solutions containing copper sulfate and EDTA were obtained, as were the polarization curves of solutions of thiosulfate and EDTA. It was determined that the optimum potential range for copper deposition in the presence of EDTA is −1.3 to −1.1 V relative to a Hg/HgO/1 M NaOH reference electrode. It was also found that the oxidation currents of solutions of thiosulfate with EDTA are roughly linearly dependent on the amount of thiosulfate present and are dependent on the concentration of EDTA to the one-fifth power. Ultimately, it appears that thiosulfate forms a stable intermediate with cuprous ions, thereby precluding electroless deposition of cupric ions.

Introduction

Thiosulfate is investigated as a possible reducing agent for the electroless deposition of copper by means of polarization data derived with a copper rotating disk electrode. This work involves the experimental determination of the oxidation kinetics of sodium thiosulfate on a copper surface and the reduction kinetics of cupric/EDTA solutions as functions of various chemical environments

and additive concentrations. No chemical analyses of the solutions or surface analyses of the electrodes were performed. All results are based strictly on the polarization data and knowledge of possible reactions and their theoretical open-circuit potentials. Following the presentation of the results will be a discussion of why we think electroless deposition did not occur. First off, a summary of electroless deposition and some reasons for trying thiosulfate are provided.

Electroless deposition (from the words electrodeless deposition[1] and previously described by Paunovic[2]) is a process for plating metals without the application of an outside agency (potential or current). In this process the reduction of a plating cationic species occurs simultaneously with the oxidation of a redox species. These reactions are to occur only through a catalytic surface and not homogeneously. An example is depicted by the following system which is currently used in industry.

$$Cu^{2+} + 2\,e^{-} \longrightarrow Cu,$$

$$HCHO + 2\,OH^{-} \longrightarrow HCOOH + H_2O + 2\,e^{-}.$$

A further understanding can be derived from the hypothetical polarization curves presented in figure 1.

Polarization curves are a measure of the kinetics of a particular system in terms of the current produced as a function of the potential applied to an electrode. Curves that rise sharply imply faster rates of reaction than those that rise more slowly. The solid

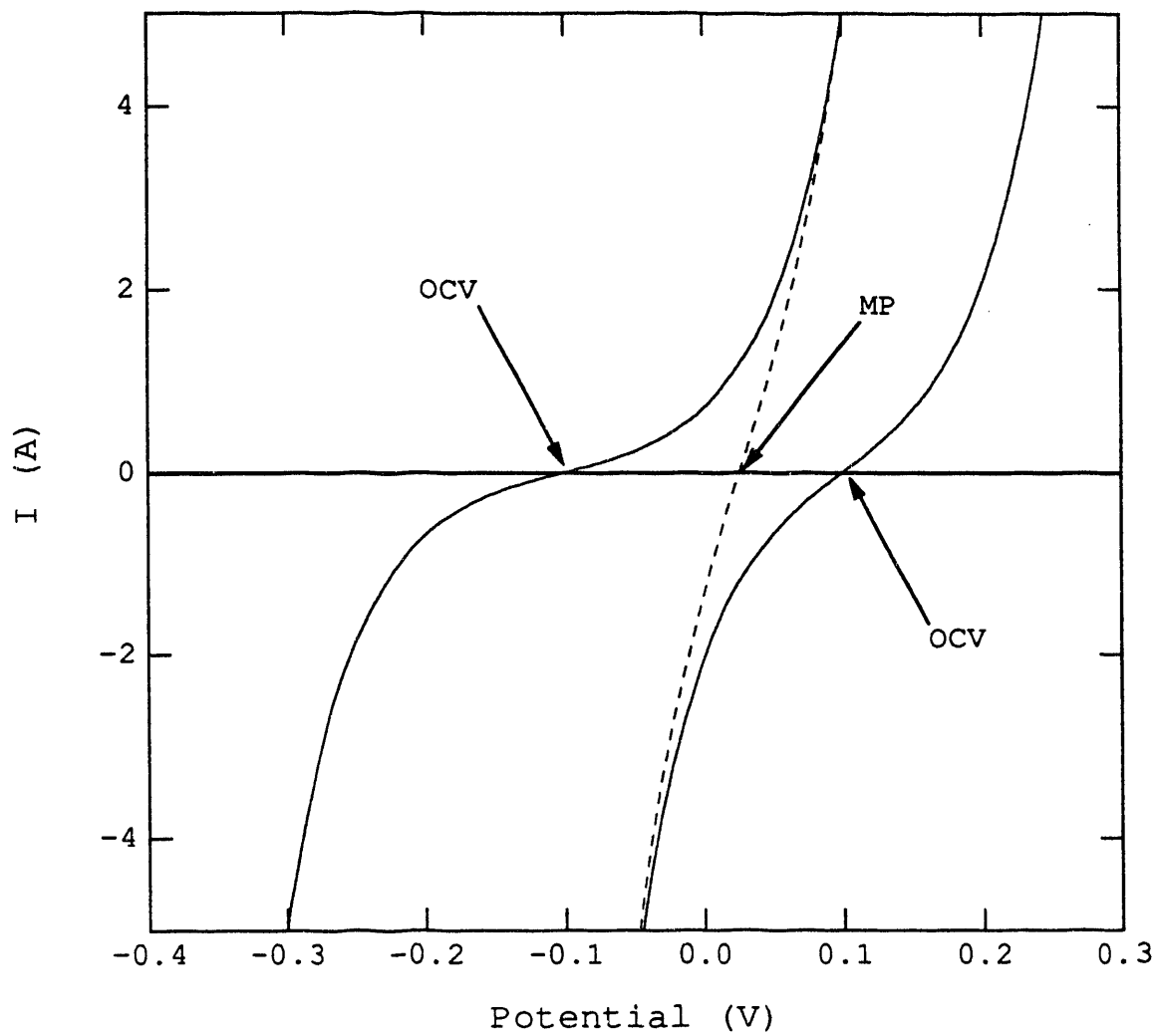

Figure 1. Solid curves are hypothetical polarization curves. The dashed curve is the sum of the two curves.

curve on the right of figure 1 exhibits faster kinetic properties than the solid curve on the left. Positive currents are considered anodic, while negative currents are considered cathodic. The points where the solid curves cross the abscissa are the open-circuit voltages of the respective reactions.

The solid curve on the right can be thought of as the polarization curve of copper in the absence of a reducing agent. A positive current suggests copper dissolution while a negative current suggests copper deposition. The solid curve on the left can be viewed as the polarization of formaldehyde in the absence of copper ions. The positive current suggests oxidation to formic acid while the negative current suggests the reverse reaction. The dashed line is the summation of the two curves. It is inherently steeper than both curves and approaches one or the other for potentials between the open circuit potentials depending upon whether the current is positive or negative. This feature is due to the typically exponential dependence of the current on potential at currents higher than the exchange current but less than the limiting current (see Newman[3] chapter 8 for details on these concepts). The point at which the dashed curve crosses the abscissa is aptly named the mixed potential, and by its nature it must fall between the open-circuit potentials of the two reacting species. It is at this potential that electroless deposition would take place. That is the potential at which the oxidative current exactly balances the reductive current. Deviations from this potential may be due to the presence of another reactive

species or to an interaction of the kinetics of the two primary reacting species.

The objectives of this research are to replace the formaldehyde with a more innocuous substance and then to characterize completely the kinetics of the system to determine the optimum plating conditions.

When choosing a reducing agent, it is a proviso that the species is oxidized at a lower potential than that at which the cation is reduced. The larger the difference between these two potentials, the larger the driving force for each reaction when the species are combined. But keep in mind, the driving force may be too large. Specifically, if the oxidation potential of the reducing agent is below the reduction potential of hydrogen ions, hydrogen gas is evolved. Not only does this result in poor reducing-agent utilization, it can lead to bubbles and nonuniform plating. Consequently, there is a window of oxidation potentials to which one is limited. The reducing agent and the oxidized products must also be soluble. These criteria eliminate a number of elements. Inspection of Pourbaix's table of electrochemical potentials[4] reveals that only the sulfur, phosphorous, and carbon containing compounds meet these criteria. As has been stated, it is our intention to remove formaldehyde from the system; the focus of this research is on the sulfur compounds.

Because sulfate and sulfite are oxidized at relatively high potentials compared to copper reduction, they are eliminated as

possibilities. Sulfide reacts readily with cuprous ions to form copper sulfide which precipitates from the solution. Thiosulfate, with its fairly low oxidation potential, is investigated.

Thiosulfate oxidizes to sulfite by the reaction[5]

$$S_2O_3^{2-} + 6\,OH^- \rightleftarrows 2\,SO_3^{2-} + 3\,H_2O + 4\,e^-$$

with an open-circuit potential of

$$U^\theta = 0.705 - \frac{RT}{F}2.303\left(\frac{6}{4}pH + \frac{1}{4}\log\frac{[S_2O_3^{2-}]}{[SO_3^{2-}]^2}\right)$$

versus a SHE (standard hydrogen electrode). It is unstable at low pH, decomposing to form sulfur and sulfite,[6]

$$S_2O_3^{2-}(aq) \rightleftarrows S + SO_3^{2-}(aq).$$

This demands that the solution be maintained at a moderate to high pH. Thiosulfate also forms a stable compound with Cu^+. As we shall show, this reaction plays a pivotal role in the explanation of our experimental results.

To reduce cupric ions to copper at a catalytic surface with thiosulfate and yet prevent cupric ions from reacting homogeneously at high pH to form cupric oxide, a chelating agent must be added to the solution. A chelating agent forms soluble ligands with copper ions and eliminates the reaction to an oxide. A number of chelating agents have been investigated in the literature;[7,8,9,10] the most pervasive and the one used in this research is ethylenediamine tetraacetic acid (EDTA). This homogeneous reaction can be portrayed by the mechanism

$$Cu^{2+} + [EDTA]^{4-} \longrightarrow Cu[EDTA]^{2-}$$

and has an equilibrium constant of 6.31×10^{18} kg/mol.[11] Such a large equilibrium constant suggests interpreting the copper species as existing exclusively as $Cu[EDTA]^{2-}$ in solution.

Polarization curves for the oxidation of thiosulfate and the reduction of $Cu[EDTA]^{2-}$ on a copper rotating disk electrode were obtained as described by the following experimental section.

Experimental

To obtain the polarization data for this system, a copper rotating disk, serial number 5144 of the Pine Instruments Company, with an active area of 0.382 cm^2 is used as the working electrode for both the copper reduction and the thiosulfate oxidation. Before each experiment, the electrode is polished with emery paper, then 6 μm diamond paste, 1 μm diamond paste, and finally 1/4 μm diamond paste. The disk is then rinsed with deionized water. The paste is Metaldi Diamond Compound by Buehler Ltd. catalog No.s 40-6162, 40-6122, and 40-6102, respectively, and is spread on *Microcloth* with adhesive backing by Buehler Ltd. catalog No. 40-7218 attached to an Ecomet III by Buehler Ltd. polishing wheel. The electrode is screwed into a Pine Instruments Analytical Rotator model ASR2 before being immersed into the solution. All experiments are performed at 1000 rpm.

Solutions are made to 100 ml and poured into the main body of an H-cell and one its arms, which is to hold the counterelectrode. The counterelectrode is a coiled piece of 0.2 cm diameter copper wire

with an exposed surface area greater than twenty times that of the working electrode. The reference-electrode compartment of the H-cell is filled with 1 M NaOH. pH measurements are made with a Beckman Φ 32 pH Meter.

The reference electrode is a Hg/HgO/1 M NaOH electrode constructed with a piece of platinum wire encased in a glass tube with one end of the wire sticking out of the tube for electrical connection and the other end of the wire is fixed two centimeters from the other end of the tube. This end of the wire is encased in one centimeter of liquid mercury, which is then covered with 0.5 cm of red mercuric oxide. The remaining end of the tube is plugged with glass wool.

The H-cell is set in a stainless steel tub of water and thermostated to the desired temperature to within 0.1 degrees by a Thermomix 1441 heater by B. Braun Melsungen AG.

Most of the experiments are performed potentiostatically. The reference electrode is set at a potential relative to the grounded working electrode, and current is supplied through the counterelectrode to maintain that potential. The device used for setting the potential is a Potentiostat BC1200 by Stonehart Associates Inc. The potential of the reference electrode versus the working electrode is read from a digital display. The current in the system is also displayed as a potential and is interpreted as a current by dividing the potential by a set resistance. These data are also fed through a bus into a Macintosh II through a LabVIEW NB-MIO-16X-Multifunction

16-Bit A/D Board and displayed as graphs of potentials versus time with LabVIEW 2 software by National Instruments. After the potential is set to the desired potential and the system reaches steady state, the potential and current are recorded; the potential is then stepped to a new value. This technique was followed throughout the next section in deriving the polarization curves.

Results

Reduction of Copper Sulfate in the Presence of EDTA

Figure 2 presents five curves of the polarization data for copper deposition at 25°C for various concentrations of copper sulfate. The composition of the base-case solution is provided in table 1. The concentration of EDTA used in each experiment was equal to twice the concentration of the copper sulfate except for the experimental data listed as the first two curves in figure 2 where the copper concentration is zero and the EDTA is three times the copper concentration, respectively. The open-circuit potentials of the five

Table 1

species	conc.(mol/dm^3)
$CuSO_4$	0.005
EDTA	0.015
NaOH*	0.075
Na_2SO_4	0.1

* (adjusted to pH = 11 to 12)

curves are recorded in table 2 in the same order as listed in the figure.

No trend was established between the open-circuit potential and the quantity of copper sulfate in solution. The average value of the open-circuit potential is approximately −0.16 V. Inspection of the curves from the open-circuit potential to a potential of −1.1 V reveals that the current remains very low (<2 mA) and is independent of the concentration of the copper sulfate species. This leads us to believe that there is a film on the electrode at these higher potentials — possibly an oxide. This is significant, for it indicates that in order to deposit copper electrolessly at 25°C, the redox couple must have an open-circuit potential much less than the open-circuit potential of −0.16 V (at least as low as −1.1 V.)

From −1.1 V to −1.3 V, the current is roughly linearly dependent on the amount of copper in the solution: as the amount of copper doubles, so does the current. This behavior is expected for the deposi-

Table 2

curve	open-circuit potential (V)
1	-0.150
2*	
3	-0.216
4	-0.115
5	-0.150

* (not recorded)

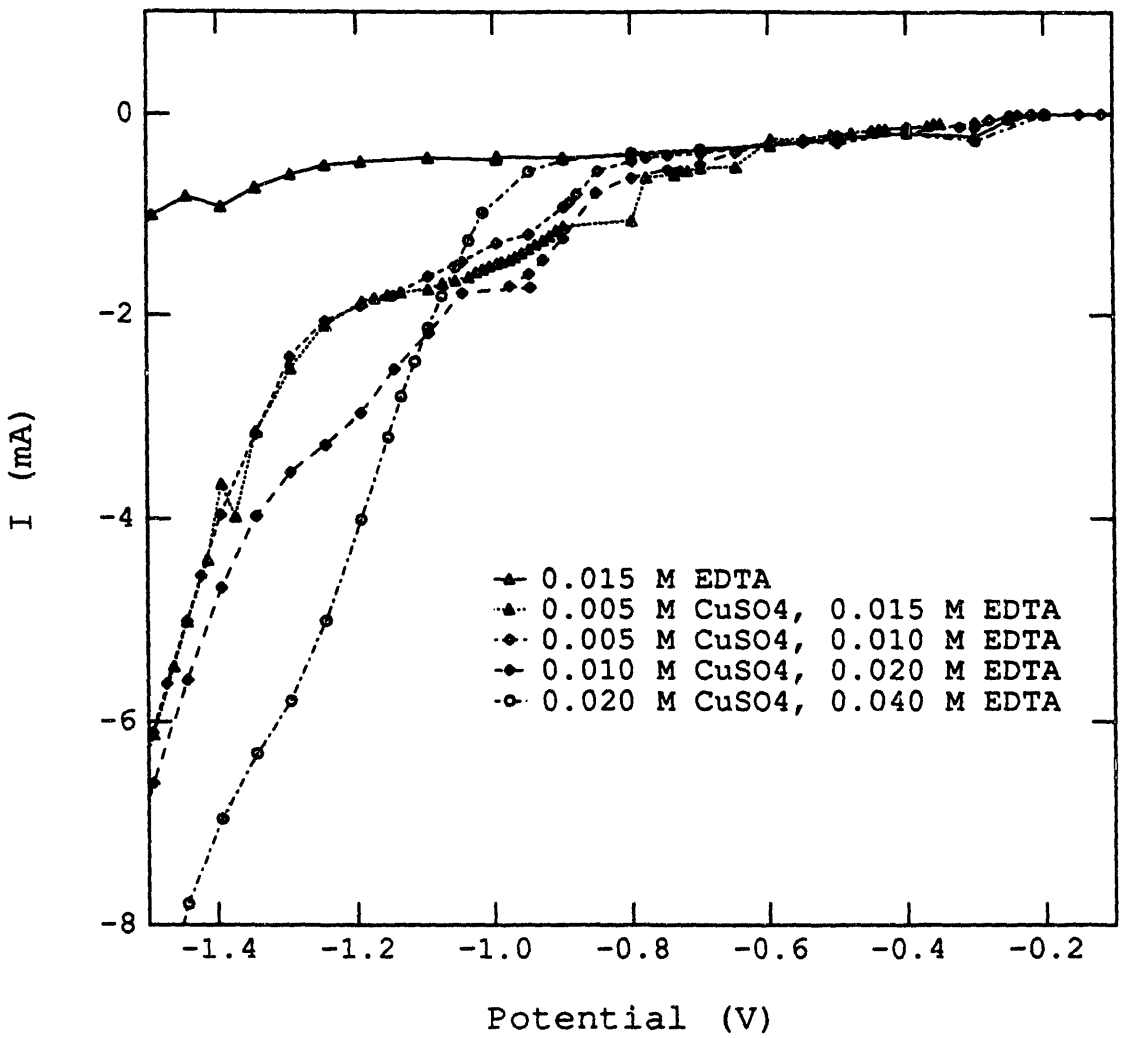

Figure 2. Cathodic current *verses* potential curves for solutions at a pH between 11 and 12 with 0.1 M Na_2SO_4 and the concentrations listed on the figure.

tion of copper. At potentials lower than −1.3 V, the curves once again move toward each other losing their dependence on copper concentration and suggesting the formation of another type of film or changes in the surface morphology. The deposits at these low potentials are also powdery, a property that is normally undesirable. This information leads us to believe that the optimum potential for electroless copper plating at 25°C is between −1.1 and −1.3 V.

The second and third curves of figure 2 are representative of two experiments with the same amount of copper sulfate but different amounts of EDTA. The lines virtually fall on top of each other, which agrees with experiments by Molenaar *et al.*[12] and Kondo *et al.*,[9] who found that the rate of electroless deposition of copper is independent of the ratio of EDTA to copper in the solution as long as it is greater than one.

Oxidation of Sodium Thiosulfate

Polarization curves for the oxidation of thiosulfate for different concentrations of thiosulfate, supporting electrolyte (Na_2SO_4), and OH^- ions are presented in figure 3. The base-case concentrations are provided in table 3. The curves were derived by stepping the potential in 10 mV intervals from the open-circuit potential to a potential beyond which the current drops significantly. This drop in current is indicative of the formation of an oxide film on the electrode surface which maintains poor catalytic properties for thiosulfate oxidation. The potential at which this drop off occurred was between −0.18 and −0.16 V.

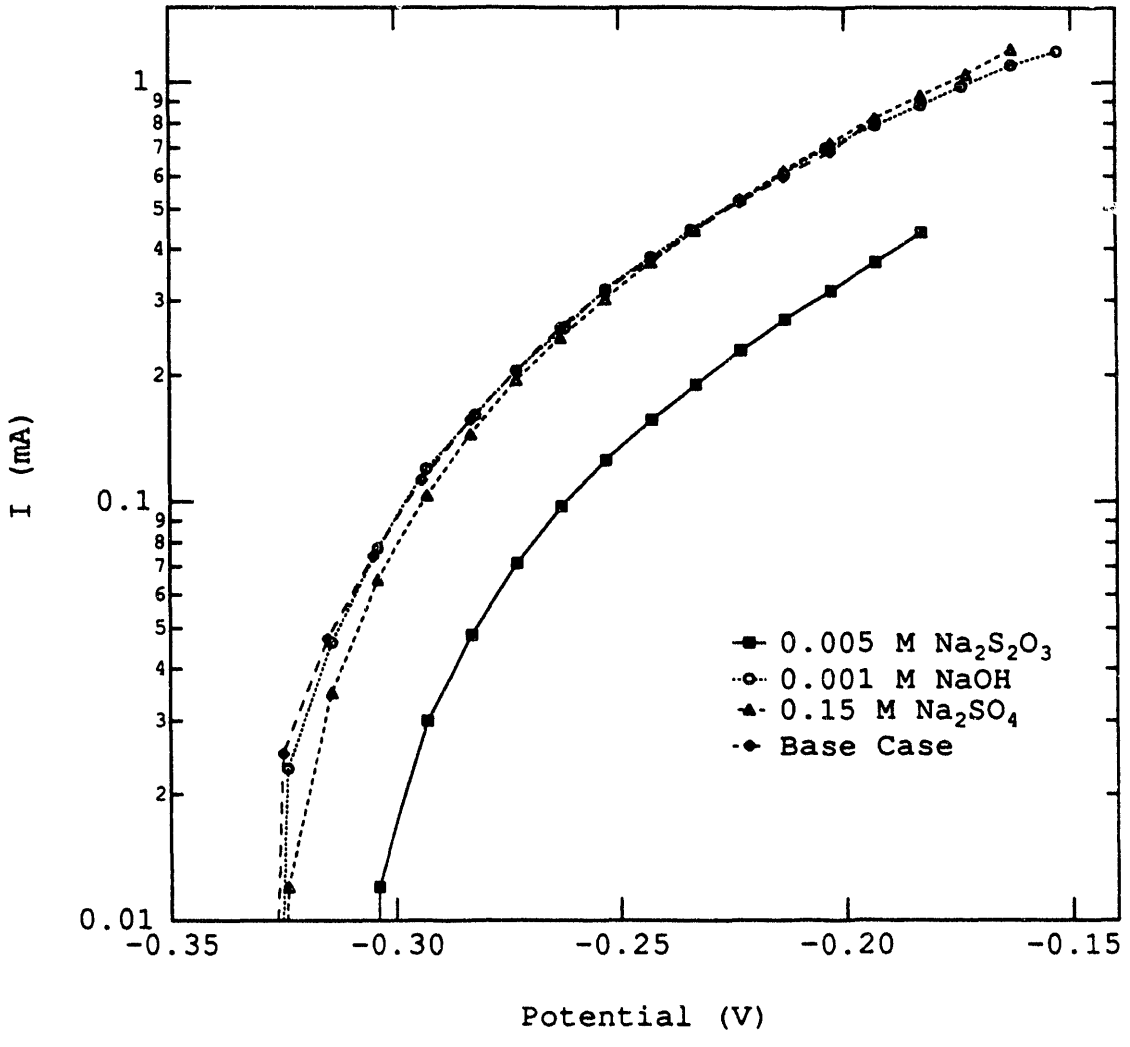

Figure 3. Anodic current-*versus*-potential curves of thiosulphate solutions containing species concentrations as given in table 3 with the differences listed on the figure.

Table 3

species	conc.(mol/dm^3)
$Na_2S_2O_3$	0.010
NaOH	0.001
Na_2SO_4	0.1

The open-circuit potential, for solutions with 0.010 M $Na_2S_2O_3$, was measured at approximately −0.335 V versus the Hg/HgO/1 M NaOH reference electrode, varying by ±0.004 V in any given experiment. Without prior knowledge of the copper deposition kinetics, this low open-circuit potential suggests that electroless deposition of copper is plausible.

The data in figure 3 for various concentrations of Na_2SO_4 and OH^- ions fall on top of each other. The current at a given potential for the solution with half as much thiosulfate is approximately half. Thus, the oxidation of thiosulfate is independent of the amount of supporting electrolyte and the pH and is directly proportional to the amount of thiosulfate in the solution.

The next step was the determination of the effect of EDTA on the oxidation of thiosulfate. Initial speculation suggested that the addition of EDTA should lower the current for a given potential by occupying surface sites for thiosulfate oxidation. In these experiments a solution of 0.005 M $Na_2S_2O_3$, 0.1 M Na_2SO_4, 0.005 M EDTA, and

enough NaOH to achieve a pH of 10 was prepared. The polarization data were obtained. In the following experiments the same concentrations of the species were maintained except for the EDTA, which was doubled (the pH was maintained at 10 by the addition of NaOH). The doubling of the amount of EDTA continued until a concentration of 0.08 M EDTA was realized. These curves are provided in figure 4. Contrary to our hypothesis, the current increased with the addition of EDTA. The rate of increase was proportional to the concentration of EDTA to the one-fifth power. Also, subsequent inspection of the disk revealed a slight amount of etching. The surface took on a more crystalline than polished appearance.

Now that we had the polarization curves for both the copper and the thiosulfate and their dependence on all the other species present in the solution, we combined the components into a single vessel.

Results of Combining Thiosulfate and Copper Ions in the Presence of Copper

In order to increase the likelihood of electrolessly plating copper, the concentrations of the active species were increased by at least an order of magnitude, see table 4. 100 ml of this solution were poured into the H-cell and placed in the water bath, which was maintained at a temperature of 25°C. The copper electrode was lowered into the solution, and the open-circuit potential versus the Hg/HgO/1 M NaOH reference electrode was monitored for the next three hours. The potential remained at approximately −0.34 V. Upon removal of the electrode, no electrolessly plated copper was found. On

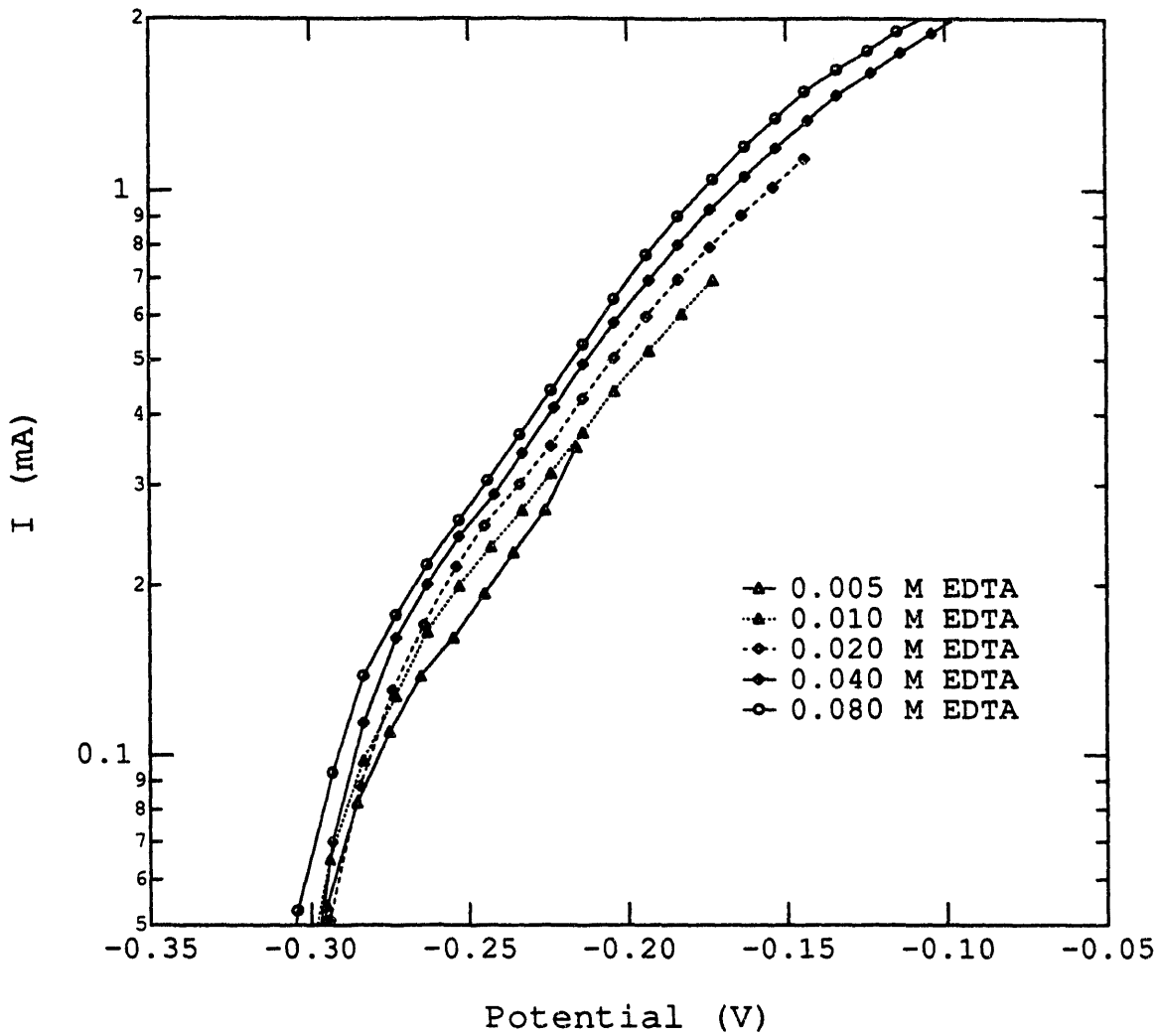

Figure 4. Anodic current *vs.* potential ofsolutions containing 0.005 M $Na_2S_2O_3$, 0.01 M Na_2SO_4, at a pH of 10 with the concentrations of EDTA as listed on the figure.

Table 4

species	conc.(mol/dm^3)
$CuSO_4$	0.040
EDTA	0.080
$Na_2S_2O_3$	0.5
NaOH*	0.370
Na_2SO_4	0.1
pH	11.92

* (pH = 11.92)

the contrary, the electrode had partially dissolved. This led to the following investigation of possible reactions of Cu(s) with $S_2O_3^{2-}$.

According to Kimura and Ishibashi,[13] the reaction

$$Cu^+(aq) + S_2O_3^{2-}(aq) \rightleftarrows [Cu(S_2O_3)]^-(aq)$$

takes place with an equilibrium constant of 2.24×10^{10} kg/mol. In an aqueous phase, in the absence of complexing species, where the reactive species possibly present are Cu, Cu^+, and Cu^{2+}, only Cu or Cu^{2+}, depending on the concentration and potential, is present at equilibrium. Cu^+ is unstable. This is evident from the values of the standard potentials of the following reactions:

$$Cu \rightleftarrows Cu^+(aq) + e^-;$$

$$U^\theta = 0.521\ V + \frac{RT}{F}\ln[Cu^+].$$

$$Cu \rightleftarrows Cu^{2+}(aq) + e^-;$$

$$U^\theta = 0.337\ V + \frac{RT}{2F}\ln[Cu^{2+}].$$

$$Cu^+(aq) \rightleftarrows Cu^{2+}(aq) + e^-;$$

$$U^\theta = 0.153\ V + \frac{RT}{F}\ln\frac{[Cu^{2+}]}{[Cu^+]}.$$

(All potentials are vs. SHE.) Assuming concentrations of 1 M, Cu is the stable phase below 0.337 V, and $Cu^{2+}(aq)$ is the stable phase above 0.337 V.

In the presence of thiosulfate, the following additional reactions with standard potentials must be considered.

$$Cu + S_2O_3^{2-}(aq) \rightleftarrows Cu(S_2O_3)^-(aq) + e^-;$$

$$U^\theta = -0.091\ V + \frac{RT}{F}\ln\frac{[Cu(S_2O_3)^-]}{[S_2O_3^{2-}]}.$$

$$Cu(S_2O_3)^-(aq) \rightleftarrows Cu^{2+}(aq) + S_2O_3^{2-}(aq) + e^-;$$

$$U^\theta = 0.765\ V + \frac{RT}{F}\ln\frac{[Cu^{2+}][S_2O_3^-]}{[Cu(S_2O_3)^-]}.$$

(Both potentials are vs. SHE.) (Note: The potentials listed above are not applicable for solutions containing EDTA.) Again assuming concentrations of 1 M, Cu is the stable phase below −0.091 V, $Cu^{2+}(aq)$ is the stable phase above 0.765 V, and $Cu(S_2O_3)^-(aq)$ is the stable phase between these two voltages. Hence, the presence of thiosulfate stabilizes the cuprous ion. The significance of this finding in rela-

tion to the experiments is discussed.

Discussion

When a copper electrode is placed in a basic solution consisting solely of supporting electrolyte and an appropriate amount of sodium hydroxide to achieve a particular pH (no copper ions present), it is difficult to predict the open-circuit potential. However, if there is dissolved oxygen present, it is likely that a passive layer of Cu_2O will form on the surface. When we perform this experiment, an open-circuit potential of −0.056 V is measured, and little current is produced (<5 μA) when the potential is swept ±0.100 V. This indicates that copper does not readily dissolve at potentials as high as 0.05 V and is further evidence that an oxide film exists.

Addition of sodium thiosulfate to the solution results in a drop of the open-circuit potential: a consequence of the thiosulfate to sulfite reaction. Furthermore, inspection of the electrode indicates that the copper surface does not retain its polished condition. This is perhaps due to the dissolution of the oxide layer and/or to the simultaneous dissolution of the Cu(s) to form $Cu[S_2O_3]^-$. This may then explain the effects of EDTA on the polarization data obtained for solutions with thiosulfate. The curves of figure 4 are most likely a combination of thiosulfate oxidation and copper oxidation to cuprous thiosulfate. The EDTA may act as a catalyst in the latter reaction in removing the copper atoms from the surface or by promoting some stability of the copper ions.

When thiosulfate is added to a solution of copper sulfate and EDTA at a pH of 10 to 12 and a copper electrode is then immersed into the solution, the copper dissolves. The open-circuit potential ($\approx$-0.34V) is lower than the open-circuit potential of the copper in a copper sulfate/EDTA solution. This potential is not low enough for copper deposition (figure 2.) However, this potential is lower than that necessary to transform cupric ions to cuprous thiosulfate.

From this information it appears that when copper sulfate is added to a solution of sodium thiosulfate in the presence of copper, cupric ions are reduced to cuprous thiosulfate at a rate that is equal to the sum of the rates of the thiosulfate oxidation and of the copper oxidation to cuprous thiosulfate. This makes the use of thiosulfate as a possible reducing agent in electroless copper deposition unlikely.

Conclusions

The open-circuit potential of a copper electrode in a copper sulfate solution with EDTA at 25°C versus a Hg/HgO/1 M NaOH reference electrode is approximately -0.16 V. This value is independent of the amount of copper sulfate in the solution and, for the reasons discussed, indicates that there is probably an oxide on the electrode. The cathodic current does not become dependent on the concentration of copper sulfate until the potential is reduced to -1.1 V. The dependence of the current on concentration of copper sulfate is roughly linear to a potential of -1.3 V, where the dependence is lost. This potential window is considered the optimum potential

range for plating copper at 25 °C in an alkaline solution containing EDTA.

The open-circuit potential of a copper electrode in a solution containing 0.010 M $Na_2S_2O_3$ is −0.337 V. The application of an anodic potential produced polarization curves which were independent of the pH and dependent on the amount of EDTA to the one-fifth power and linearly dependent on the amount of thiosulfate present. These curves represent a combination of copper oxidation to cuprous thiosulfate and thiosulfate oxidation.

Finally, thiosulfate forms a stable soluble complex with Cu^+. This complex allows for Cu^{2+} to be reduced to Cu^+ and copper to be oxidized to Cu^+ and thus negates the possibility of electroless copper deposition.

References

1. A. Brenner and G. Riddell, "Nickel Plating on Steel by Chemical Reduction," *J. Research Nat. Bur. Standards*, 37, July, 1946, and the *A. E. S. Annual Proceedings* p. 23 (1946).

2. M. Paunovic, "Electrochemical Aspects of Electroless Deposition of Metals," *Plating*, 55, 1161 (1968).

3. J. Newman, *Electrochemical Systems*, 2nd Edition, Prentice-Hall, Englewood Cliffs, N. J. (1991).

4. M. Pourbaix, *Atlas of Electrochemical Equilibria in Aqueous Solutions*, Second English Edition, National Association of Corrosion Engineers, Houston, Texas (1974).

5. J. V. Quagliano and L. M. Vallarino, *Chemistry*, 3rd Edition, Prentice-Hall, Inc., Englewood Cliffs, N.J. (1969).

6. B. H. Mahan, *University Chemistry*, 3rd Edition, Addison-Wesley Publishing Company, Menlo Park, Ca., p. 664 (1975).

7. A. Hung and K.-M. Chen, "Mechanism of Hypophosphite-Reduced Electroless Copper Plating," *J. Electrochem. Soc.*, **136**, 72 (1989).

8. R. Schumacher, J. J. Pesek, and O. R. Melroy, "Kinetic Analysis of Electroless Deposition of Copper," J. Phys. Chem., **89**, 4338 (1985).

9. K. Kondo, J. Ishikawa, O. Takenaka, T. Matsubara, and M. Irie, "Acceleration of Electroless Copper Deposition in the Presence of Excess Triethanolamine," *J. Electrochem. Soc.*, **138**, 3629 (1991).

10. A. M. Mance, R. A. Waldo, and A. A. Dow, "Interactions of Electroless Catalysts with Plasma-Oxidized Surfaces of Polystyrene-Based Resins," *J. Electrochem. Soc.*, **136**, 1667 (1989).

11. C. F. Bell, *Principles and Applications of Metal Chelation*, Clarendon Press, Oxford, p. 78 (1977).

12. A. Molenaar, M. F. E. Holdrinet, and L. K. H. van Beek, "Kinetics of Electroless Copper Plating with EDTA as the Complexing

Agent for Cupric Ions," *Plating*, **61**, 238 (1974).

13. M. Kimura and M. Ishibashi, "Kinetics of the Reaction of the Tris(oxalato)cobalt(III) Ion Induced by the Reaction between Copper(II) and Thiosulfate in Aqueous Solution," *Inorganic Chimica Acta*, **129**, 69 (1987).

Chapter 5

Electroless Deposition of Copper by Hypophosphite and Nickel Solutions

Foreword

Mixed-potential-versus-time curves are presented for various solutions consisting of copper and nickel ions. The data reveal that the addition of small amounts of copper ions to nickel solutions reduces the rate of electroless nickel deposition; whereas, there is a maximum concentration of nickel ions that can be added to a primarily copper sulfate solution to maximize electroless copper deposition.

Introduction

Formaldehyde is the most widely used and investigated reducing agent for the electroless deposition of copper.[1,2,3,4,5] (A review of plating including electroless copper plating is provided by Yung, *et al.*[6]) Formaldehyde is very volatile (normal boiling point is −40°C) and hazardous to one's health, but is used because it works. Hypophosphite is a widely used reducing agent for electroless nickel deposition,[7,8,9,10,11,12] and is an ion in solution. It would be preferable to use hypophosphite for copper deposition as well; unfortunately, hypophosphite is not readily oxidized on copper surfaces.[13] This research is an extension of previous attempts by other researchers[14,15] to use hypophosphite as a possible reducing agent for elec-

troless copper deposition while in the presence of nickel ions. Dubin[16 has shown that hypophosphite can be used as a reducing agent for nickel in the presence of a small amount of copper; this was also reinvestigated.

The combination of reactants — Ni^{2+}, Cu^{2+}, and $H_2PO_2^-$ — in the presence of a palladium chloride activated surface initiates the deposition of nickel, which then promotes the simultaneous deposition of copper. This work presents the mixed potentials versus time for solutions of various concentrations of copper sulfate, hypophosphite, and nickel solutions. It was found that copper poisons the nickel deposition and that there is an optimum amount of nickel sulfate that can be added to a copper solution to maximize the duration of copper deposition.

Experimental

The equipment used in this research is identical to that used in the previous study of thiosulfate oxidation on copper (Chapter 4), and, hence, shall not be repeated here. The one major equipment difference is the electrode, which is a palladium ring-disk electrode of the Pine Instruments Company, serial number 297, having a total surface area of 0.382 cm^2. The electrode is prepared by polishing, as described in the previous chapter, and activating. Activation is achieved by dipping the electrode into an activating solution, as described in table 1, for two minutes, prior to each experiment.

Table 1

species	amount
$PdCl_2$	0.1 g
Glacial acetic acid	50 ml
HCl (37%)	0.5 ml
Deionized H_2O	to 100 ml

The experimental technique differs substantially from the work in the previous chapter. Here, the circuit is left open, and the potential of the palladium disk versus a Hg/HgO/1 M NaOH reference electrode is monitored as a function of time. These data are relayed from the potentiostat directly to a Macintosh II through coaxial cables and a LabVIEW NB-MIO-16X multifunction 16-bit A-D board. The data are stored on a disk and displayed on the terminal using LabVIEW 2 software by National Instruments.

Results and Discussion

Nickel Chloride Solutions with Sparing Amounts of Copper Sulfate

As mentioned, hypophosphite is used as a reducing agent for electroless nickel deposition (due primarily to its favorable kinetic properties on nickel surfaces), but is a poor agent for electroless copper (for the inverse reason). The purpose of these experiments is to determine the extent to which copper sulfate can be added to nickel/hypophosphite solutions to maximize copper deposition yet

still achieve a moderate rate of codeposition. Thus, solutions with relatively large amounts of nickel chloride and hypophosphite are prepared with various amounts of copper sulfate. The concentrations of the species used in each experiment are taken from the work of Dubin[16] and are either listed on figure 1 or are provided below.

The experiment with no copper sulfate also contains 0.37 M citric acid. The experiments with copper sulfate also contain 0.33 M glycine and 0.037 M sodium acetate. Each of the solutions is adjusted to the pH listed on the figure with the appropriate amount of sodium hydroxide.

In the experiment in which no copper sulfate is present, the open-circuit potential starts at −0.65 V and quickly decreases (within the next 200 seconds) to −0.97 V. Inspection of the electrode after an hour of being immersed reveals a nickel covered surface with bubbles vigorously evolving from portions of the electrode still covered with solution.

The mixed potential diagrams of solutions which contain increasing amounts of copper sulfate are also provided in figure 1. One sees that as the concentration of copper ions increases, so does the potential. Inspection of the electrodes after each experiment reveals less deposit as the copper content of the solution is increased. These data lead to the following discussion.

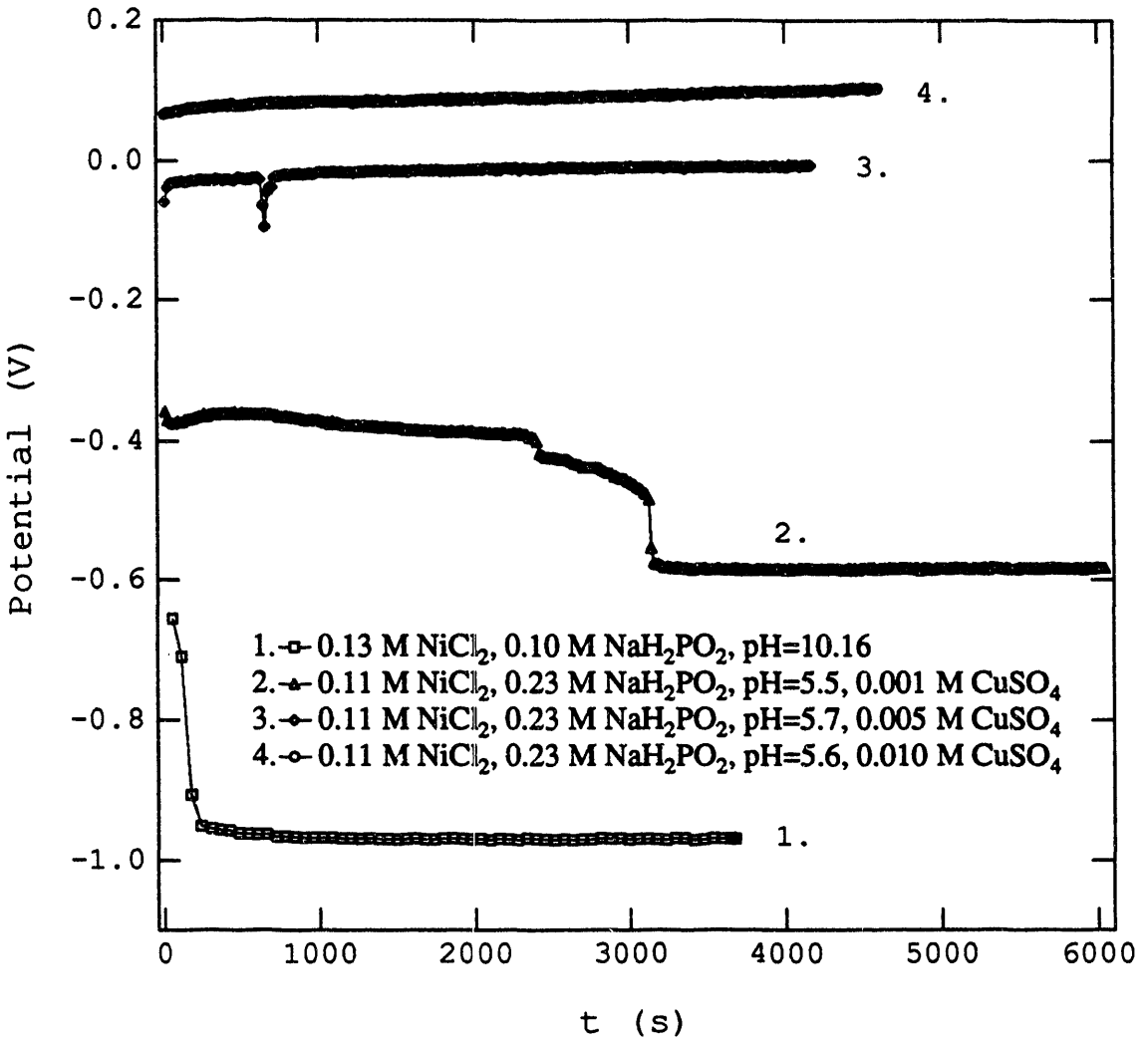

Figure 1. Mixed potential curves of nickel predominant solutions. Concentrations of additives are listed in the text.

Discussion

According to data found in Vetter,[17] palladium is a slightly better catalyst for hydrogen evolution than is nickel, which is better still than copper. The hydrogen to hydrogen ion and hypophosphite to phosphite open-circuit potentials are functions of solution composition and are independent of the surface present. However, the surface does play a large role in the kinetic properties. The nickel deposition open-circuit potential is a strong function of the surface since this reaction consists of a dissolved species reduced to a solid species. This information leads to the following arguments. For the solution without copper ions, nickel is initially deposited on the electrode, which brings about the immediate decrease in potential (curve 1, figure 1.) This new surface must then be either more kinetically favorable for hypophosphite reduction, or less kinetically favorable for nickel deposition or hydrogen evolution, or a combination of the three. Since hydrogen evolution on the nickel surface is prevalent, it is unlikely that reduction of the hydrogen reaction overpotential is responsible for the large change of potential (over 300 mV.)

However, the drop in potential combined with the vigorous bubble evolution and the obvious presence of nickel does suggest a shift to a much more kinetically favorable state of hypophosphite oxidation. Therefore, we conclude that this change in potential is due mainly to an increase of the hypophosphite kinetics on nickel relative to palladium.

In discussing the data it is important to consider that the palladium electrode was "activated;" that is it was dipped in the activating solution before each experiment. And that the electrode was relatively inactive without this step. It thus appears that the activator is creating a finite number of activation sites. These sites are probably utilized by all four components, hypophosphite, protons, and copper and nickel ions. For the solution with no copper present, it appears that the nickel and hypophosphite compete for these sites, but as the nickel is deposited, it creates more active sites for hypophosphite oxidation. The potential drops.

For solutions with copper ions, it appears that the copper deposition also competes for these activation sites. However, the copper does not catalyze the hypophosphite; and, therefore, as the experiment proceeds, the copper ions consume the activation sites and little deposition is seen. In the case of the solution with the smallest copper composition (curve 2, figure 1), the nickel can compete with the copper in consuming sites; and once all the sites are occupied (after 3000 s, see figure 1), the nickel can still act as a catalytic site for both the nickel deposition and the hypophosphite oxidation. Thus the potential abruptly drops nearly 100 mV after 3000 seconds, and nickel deposition and hydrogen evolution proceed simultaneously with an increased rate of hypophosphite oxidation. (This provides further support that nickel is an excellent catalyst for hypophosphite oxidation and that copper is a poor one).

Copper Sulfate Solutions with Sparing Amounts of Nickel Sulfate

Solutions which primarily consist of copper sulfate, hypophosphite, and boric acid were prepared with various sparing amounts of nickel chloride. The purpose of these experiments is to deposit copper with hypophosphite and to elucidate the effect that nickel plays in the process. The base-case concentration of components, as duplicated from Hung *et al.*,[14] is provided in table 2. The open-circuit-versus-time data for various solutions containing primarily copper ions and hypophosphite as a reducing agent are provided in figure 2.

For the base-case solution composition, the open-circuit potential starts at a low potential, −0.7 V, which is conducive to high rates of deposition. However, the potential steadily rises, and after the first 900 seconds the potential has essentially reached a steady value of −0.1 V. Inspection of the electrode after approxi-

Table 2

species	conc. (mol/dm^3)
$CuSO_4$	0.024
$NiSO_4$	0.002
H_3BO_3	0.5
Citric Acid	0.056
NaH_2PO_2	0.27

(solutions adjusted to a pH of 9.2 w/NaOH)

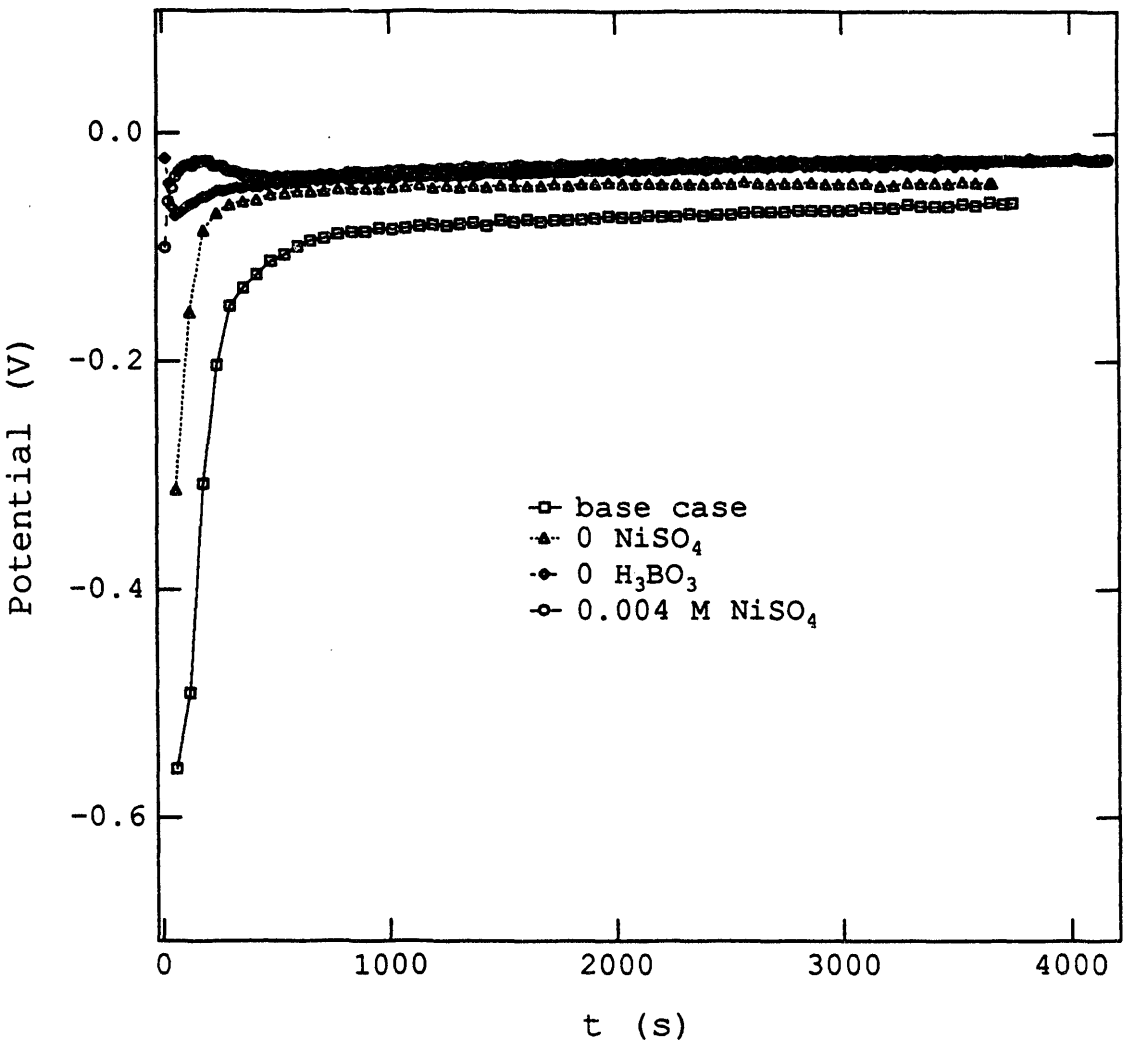

Figure 2. Mixed potential versus time for prodomiantly copper solutions. Base Case concentrations: 0.024 M $CuSO_4$; 0.002 M $NiSO_4$; 0.5 M H_3BO_3; 0.056 M Citric Acid; 0.27 M NaH_2PO_2; NaOH to a pH=9.2. Adjustments from these concentrations are listed on the figure.

mately one hour reveals a faint copper surface.

For the solution with no nickel present, the potential again starts at a low potential, −0.7 V, and rises quickly, within 200 seconds, to a steady potential of −0.07 V.

The solution with twice as much nickel starts at a potential of −.8 V (observed but not stored or displayed in figure 2), but rose very rapidly (within 10 seconds) to a potential of −0.06 V.

Lastly, the solution with no boric acid does very little, hovering around −0.06 V.

Discussion

Again it appears that there is competition for the activation sites. For the base case, the copper competes for the sites with the nickel, and codeposition continues for approximately 900 seconds. In the experiment where the nickel concentration has been doubled, nickel ions consume most of the sites but there is not much nickel present in solution to create an appreciable amount of current. For the case where no nickel is present, the copper consumes all the sites, and the current stops because the kinetics for hypophosphite oxidation on copper are poor. The last curve mentioned is the mixed potential of a solution of copper and nickel but with no boric acid present. According to Ohno *et al.*,[13] boric acid is needed for the nickel deposition and the hypophosphite oxidation. These data agree with his argument to the extent that nothing occurs without the presence of boric acid.

Further Discussions

The transient experiments presented here showed little reproducibility. This is most likely due to the problems faced in reproducing the surface prior to each experiment. The surface was polished and dipped in 100 ml of activating solution, which was therefore depleted of some Pd ions each time it was used. The solution was never replenished. The number of activation sites was poorly controlled by this technique. The electrode was then exposed to air as it was transferred to the rotating-disk apparatus. Oxygen in the atmosphere could have a significant effect on the activated palladium surface by chemical reaction or adsorption. This too would obviously affect the ability of reproducing the same surface of the electrode for each run.

Experimental results provided in this manuscript are those for which the lowest potential was observed immediately after the electrode was immersed in the solution. For some experiments, the potential started at a relatively high potential (-0.1 V) and remained there. In those cases, the electrode was removed from the electroless solution and redipped in the activating solution. As a consequence of this experimental artifact of poor reproducibility, we are not overly confident of the arguments that have been presented.

Conclusions

Open-circuit potentials versus time of various solutions containing copper and nickel are presented. It was demonstrated for

solutions consisting primarily of nickel ions, that as the copper concentration is increased, the mixed potential increases and is accompanied by a decrease in nickel deposition. This was attributed to the simultaneous deposition of copper, which is a poor catalytic surface for hypophosphite oxidation.

For solutions consisting primarily of copper sulfate, a maximum in copper deposition is observed as nickel sulfate is added. This effect was attributed to nickel consumption of most the activation sites which prohibits further deposition of copper. Surface preparation plays an important role in the system performance.

References

1. R. Schumacher, J. J. Pesek, and O. R. Melroy, "Kinetic Analysis of Electroless Deposition of Copper," *J. Phys. Chem.*, **89**, 4338-42 (1985).

2. M. Paunovic, "Potentiostatic High Overpotential Studies of Copper Deposition from Electroless Copper Solutions," *J. Electrochem. Soc.*, **132**, 1155-57 (1985).

3. B. J. Feldman and O. R Melroy, "The Mechanism of Electroless Cu Deposition: Extraction of the Oxidative and Reductive Electrochemical Half-Cell Currents from a Complete Bath," *J. Electrochem. Soc.*, **136**, 640-43 (1989).

4. M. Matsuoka, K. Iwamoto, and T. Hayashi, "Deposition Rate of Electroless Copper Monitored by a Computer-aided Coulostatic Method,"

Plating and Surface Finishing, **78**, 64-68 (1991).

5. T. Ogura, "Mechanism of Copper Deposition in Electroless Plating," *Langmuir*, **6**, 1709-10 (1990).

6. E. K. Yung, L. T Romankiw, and R. C. Alkire, "Plating of Copper into Through-Holes and Vias," *J. Electrochem. Soc.*, **136**, 206-15 (1989).

7. F. M. Donahue, "Interactions in Mixed Potential Systems," *J. Electrochem. Soc.*, **119**, 72-73 (1972).

8. P.-L. Pai and C. H. Ting, "Selectively Deposited Nickel Film for Via Filling," *IEEE Electron Dev. Lett.*, **10**, 257-59 (1989).

9. C. H. Ting and M. Paunovic, "Selective Electroless Metal Deposition for Integrated Circuit Fabrication," *J. Electrochem. Soc.*, **136**, 456-62 (1989).

10. T. Osaka, I. Koiwa, M. Usuda, K. Arai, and I. Saito, "Behavior of the Electroless Composite Films Plated from a Ni-P Bath with Metallic Dispersion of Zr and Nb Powders," *J. Electrochem. Soc.*, **136**, 1124-28 (1989).

11. K.-L Lin and P.-J. Lai, "The Crystalization of an Electroless Ni-P Deposit," *J. Electrochem. Soc.*, **136**, 3803-09 (1989).

12. V. Dubin, "Electroless Ni-P Deposition on Silicon with Pd Activation," *J. Electrochem. Soc.*, **139**, 1289-94 (1992).

13. I. Ohno, O. Wakabayashi, and S. Haruyama, "Anodic Oxidation of Reductants in Electroless Plating," *J. Electrochem. Soc.*, **132**, 2323-2330 (1985).

14. A. Hung and I. Ohno, "Electrochemical Study of Hypophosphite-Reduced Electroless Copper Deposition," *J. Electrochem. Soc.*, **137**, 918-921 (1990).

15. A. Hung and K.-M. Chen, "Mechanism of Hypophosphite-Reduced Electroless Copper Plating," *J. Electrochem. Soc.*, **136**, 72-75 (1989).

16. V. Dubin, "Selective Electroless Ni-Cu(P) Deposition for Via Hole Filling and Conductor Pattern Clodding in a VLSI Multilevel Interconnection Structures," *J. Electrochem. Soc.*, **139**, 633-638 (1992).

17. K. J. Vetter, *Electrochemical Kinetics: Theoretical and Experimental Aspects*, Academic Press Inc., New York, pp. 576-77 (1967).

END

DATE FILMED

10/13/93